INTRAGENIC COMPLEMENTATION IN METHYLMALONYL CoA MUTASE

RITA S. FARAH
Department of Biology
McGill University, Montreal

August, 1994

A thesis submitted to the Faculty of Graduate Studies and Research in partial fulfilment of the requirements for the Masters degree in Sciences

ABSTRACT

Methylmalonic aciduria (MMA) is an autosomal recessive metabolic disorder with an incidence of 1 in 48,000, which may be due to a defect in the mitochondrial homodimeric enzyme methylmalonyl CoA mutase (*mut* MMA). *mut* MMA is subdivided into *mut*^{0} and *mut*$^-$ subclasses on the basis of complementation analysis; *mut*^{0} cell lines have very low incorporation of [^{14}C] from propionate into acid precipitable material while incorporation in *mut*$^-$ cells is increased when cells are incubated in cobalamin. Intragenic complementation was first observed with WG 1130, a *mut*^{0} fibroblast line with a homozygous R93H mutation, that is capable of complementing MCM activity when fused with some *mut*^{0} and some *mut*$^-$ cells (1). Extensive intragenic complementation in *mut*$^-$ MMA was subsequently observed. Fibroblasts cultured from thirteen unrelated patients (6 *mut*$^-$, 7 *mut*^{0}) were fused in all possible pairwise combination and MCM activity was assayed in the heterokaryons by measuring the incorporation of [^{14}C] from propionate into acid precipitable material. Intragenic complementation, indicated by stimulation of [^{14}C]-propionate incorporation following cell fusion with polyethylene glycol, was observed in fusions involving twelve of the thirteen strains. Of these thirteen strains, mutations have been identified in six; four have a homozygous mutation [WG 1130 (R93H), WG 1511 (H678R), WG 1610 (G717V), WG 1609 (G630E)], and two cell lines are compound heterozygous [WG 1681 (G623R and G703R), WG 1607 (W105R and A377E)]; the remainders are yet to be determined. These intragenic complementations will provide information for grouping the mutations in defined domains in order to correlate structure and function of MCM.

SOMMAIRE

L'acidurie méthylmalonique (AMM) est un désordre métabolique autosomal récessif qui peut être causé par une activité déficiente de l'apoenzyme méthylmalonyl CoA mutase (*mut* AMM). La mutation *mut*^{0} est charactérisée par un manque de stimulation d'incorporation d'acide propionique 1-^{14}C en culture en presence d'hydroxycobalamine (OH-Cbl), et la mutation *mut*$^-$ est charactérisée par une élevation dans l'incorporation de propionate 1-^{14}C en presence d'OH-Cbl. La complementation intragenique dans *mut* AMM a été premièrement démontrée avec WG 1130, une lignée cellulaire *mut*^{0} avec la mutation homozygote R93H, qui a été capable de complementer d'autres lignées cellulaires *mut*^{0} et *mut*$^-$ (1). Par la suite, on a identifié une considerable complementation intragenique dans *mut* AMM. Des fibroblastes cutanées provenant de 13 *mut* patients (6 *mut*$^-$, 7 *mut*^{0}) ont été fusionnées en paires dans toutes les combinaisons possibles. La complementation est indiquée par une élevation dans l'incorporation de propionate 1-^{14}C, en culture en presence de polyéthylene glycole (PEG), dans les protéines precipitables des cellules par comparision à ce que l'on observe en absence de PEG. La complementation intragenique a été observée dans les fusions de 12 des 13 lignées cellulaires. Les mutations ont été déjà identifiées dans 6 de ces 13 lignées cellulaires. Quatres ont une mutation homozygote [WG 1130 (R93H), WG 1511 (H678R), WG 1609 (G630E), WG 1610 (G717V)]; deux ont des mutations hétérozygotes [WG 1681 (G623R and G703R), WG 1607 (W105R and A377E)]. Le groupement des mutations selon la complementation intragenique dans des domaines definés aidera a trouvé une relation entre la structure et la fonction du mutase.

ACKNOWLEDGEMENTS

I would like to thank God for everything.

I would like to thank Dr. David S. Rosenblatt for accepting me as his Masters graduate student, and for introducing me to the research in genetics. I would especially like to thank him for his constant guidance, encouragement, support, and great sense of humour all of which made work a pleasure.

I would like to thank Brian Hershenfield, Adrian Chan, Sophie Sun, and Stacy Evans for their very helpfull assistance in the mutation detection analysis.

I would like to thank Robby Chan and Iliaj Kovac for their help with the statistics, and Eric Campeau for his helpfull suggestions.

I would like to thank Alfonso Lion del Rio and Monica Naujokas for their assistance with the PC Gene program.

I would like to thank Dr. Roy Gravel for his eagerness to help, his guidance, and very helpfull suggestions.

I would like to thank my supervisory committee of Dr. L. Pinsky, Dr. P. Hechtman, Dr. R. Gravel, and Dr. D.S. Rosenblatt for their support and suggestions.

I would like to thank Dr. David Watkins for all his suggestions and support.

I would like to thank Dr. Fred Ledley for his insight.

I would like to thank Gail Dunbar for teaching me tissue culture techniques.

I would like to thank Nora Matiaszuk for introducing me to the complementation analysis. I would like to especially thank her for her motherly love and support.

I would like to thank Estelle Lamothe and Angie Hosack for all their encouragement and assistance.

I would like to thank Yasmin Karim for her help and support.

I would like to thank Sally Lue-Shing, May Boothe, and Maria Galvez for their support and delightful conversations.

I would like to thank Ramani, Takis, Caroline, Sharon, and Jehangir for their support, encouragement, and very entertaining and stress-relieving conversations.

I would especially like to thank my family, especially my mother, and Souhail Hakim for their constant help, encouragement, and support during times of depression and frustration.

This work was supported by funds from Fonds pour la Formation de chercheurs et l'Aide à la Recherche (FCAR), from the Medical Research Council of Canada--Genetics Group, and from the Hess B. Finestone Laboratory.

ABBREVIATIONS

Cbl	cobalamin, vitamin B_{12}
$Cbl^{+3,+2,+1}$	cobalamin in +3,+2,+1 oxidation states
cbl	cobalamin complementation group
AdoCbl	5'deoxyadenosylcobalamin
AdoMet	S-adenosylmethionine
CN-Cbl	cyanocobalamin
OH-Cbl	hydroxocobalamin
GS-Cbl	gluthathionylcobalamin
IF	intrinsic factor
TCI,II,III	transcobalamin I,II,III
MeTHF	methyltetrahydrofolate
MeCbl	methylcobalamin
MCM	methylmalonyl CoA mutase
MMA	methylmalonic aciduria
MUT	methylmalonyl CoA mutase locus
mut	defect in mutase apoenzyme
Mut A	bacterial MCM gene encoding small subunit
Mut B	bacterial MCM gene encoding large subunit
MS	methionine synthase
CRM	cross reactive material
PEG	polyethylene glycol
PBS	phosphate buffered saline
TAE	tris acetate
TBE	tris borate
PCR	polymerase chain reaction
bp	base pair
aa	amino acid

TABLE OF CONTENTS

CHAPTER 1
STRUCTURE, DISTRIBUTION, AND REQUIREMENTS OF COBALAMIN

CHAPTER 2
TRANSPORT OF COBALAMIN

CHAPTER 3
COBALAMIN-DEPENDENT ENZYMES

CHAPTER 4
INHERITED DEFECTS OF CBL TRANSPORT AND METABOLISM

CHAPTER 5
METHYLMALONYL CoA MUTASE (MCM)

CHAPTER 6
MATERIALS AND METHODS

CHAPTER 7
RESULTS

CHAPTER 8

LIST OF FIGURES AND TABLES

CHAPTER 1

STRUCTURE, DISTRIBUTION, AND REQUIREMENTS OF COBALAMIN

1.1 STRUCTURE OF COBALAMIN

Vitamin B_{12}, also known as cobalamin (Cbl), is a water-soluble organometallic molecule, that is a crucial cofactor for many organisms (2). Following its crystallization in 1947 by Folkers and coworkers, its three-dimensional structure was first determined in 1956 by Hodgkin using X-ray crystallographic techniques (3). Cobalamin's main skeleton consists of a planar corrin ring surrounding a central cobalt atom which may be found in any of three oxidation states: cobalt 3+, cobalt 2+, or cobalt 1+. The corrin nucleus is the central structure of all corrinoids, of which Cbl is a specific class with the lower axial ligand as phosphoribo-5,6-dimethylbenzimidazolyl (Fig.1). The ligand at the upper coordination site determines the type of Cbl compound. In naturally occurring vitamin B_{12}, the upper ligand may be a hydroxy group (hydroxocobalamin (OH-Cbl)), a glutathione group (glutathionylcobalamin (GS-Cbl))(4), or a sulfito group (sulfitocobalamin (HSO_3)). This ligand may also be methyl or adenosyl groups, comprising the two coenzyme forms of cobalamin which have been isolated from mammalian tissues: methylcobalamin (MeCbl), and 5'-deoxyadenosylcobalamin (AdoCbl) respectively (5). These two coenzymes are unique in that they contain a covalent carbon-metal bond between the ligand and the central cobalt atom which plays a major role in the enzymatic reactions (2). Cyanocobalamin (CN-Cbl) is the most common commercial form, and does not occur naturally in plants, microorganisms, and animal tissues.

FIG. 1 **THE STRUCTURE OF COBALAMIN.** R= $-CH_2CONH_2$; R'= $-CH_2CH_2CONH_2$; X= -OH (hydroxocobalamin), -CN (cyanocobalamin), $-CH_3$ (methylcobalamin), or 5'-deoxy 5'-adenosyl (adenosylcobalamin). Reprinted from Fenton and Rosenberg (6).

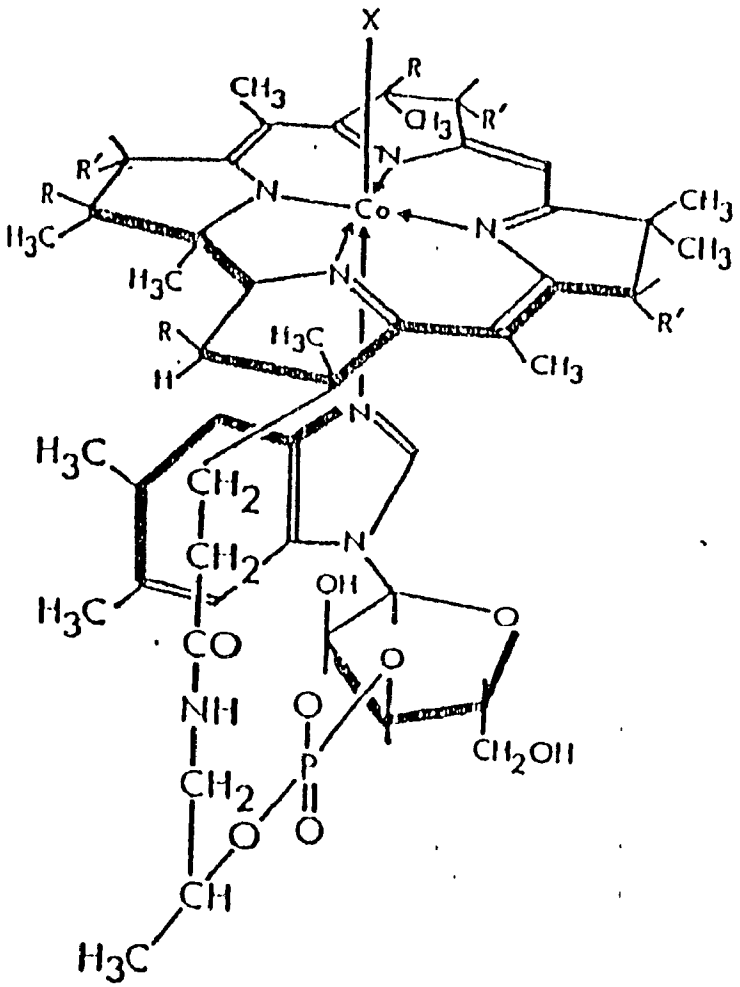
X
R
CH3
CH3
R'
N
R'
R
N
Co
N
CH3
CH3
H3C
H3C
N
R'
R
H3C
H
CH3
N
H3C
CH2
CH2
N
H3C
OH
O
CO
O
NH
O
P
CH2OH
CH2
O
O
CH
H3C

1.2 DISTRIBUTION AND DIETARY SOURCES

Cobalamin serves as a cofactor for many organisms, ranging from prokaryotes to mammals, although its synthesis is achieved only by microorganisms such as certain fungi (*Streptomyces griseus*, *Streptomyces aureofaciens*), and certain bacteria (*Propionibacterium shermanii, Clostridium tetanomorphum, Rhizobium meliloti*) (7). Recently, the entire biosynthetic pathway of vitamin B_{12} showing the structures of essentially all of its intermediates has been elucidated (8). Humans are wholly dependant on dietary Cbl (9). Even though it is synthesized by the colonic flora, Cbl cannot be absorbed in the colon. Vitamin B_{12} is found ubiquitously in animal products and somewhat rarely in plants, but it is all derived from bacteria (9). AdoCbl and OH-Cbl are most prevalent in meat, whereas dairy products contain mostly MeCbl and OH-Cbl (9).

1.3 REQUIREMENTS FOR COBALAMIN

The total body content of cobalamin in the adult male is 2-5mg, with high concentrations of AdoCbl in the liver, kidney, and pituitary, and MeCbl in the plasma and spleen (10). The established daily dietary requirement of cobalamin for adults is 2-5μg, and the estimated daily rate of loss is approximately 0.1% of the total body pool (10). This implies that a deficiency state will not arise for several years after total cessation of vitamin B_{12} intake (11). Cbl in human serum, as measured either by microbiological methods or by isotope dilution assays, is present in concentrations of around 300×10^{-12} mol/l all bound to transport proteins (12).

CHAPTER 2

TRANSPORT OF COBALAMIN

2.1 COBALAMIN TRANSPORT IN MICROORGANISMS

Since the de novo synthesis of the corrin ring of cobalamin is restricted to bacteria, microorganisms are essential components in the production of vitamin B_{12} (13). They are used commercially to produce of cobalamin (7). *Escherichia coli* has been used as the subject of most of the work done on bacterial cobalamin metabolism. Although *E. coli* cannot synthesize the corrin ring of vitamin B_{12}, it is able to take it up from the environment (13). Since cobalamin is too large to pass through the porin channels of the outer membrane of *E. coli*, the bacterium has developed a complex and efficient biphasic system, involving proteins coded by several genes, to take up cobalamin which is usually present in the environment at low concentrations (10fM-1nM) (13). The first phase consists of a rapid, energy-independent binding to cell surface. The second phase is a slower, energy-dependent transfer into the cell. Five components have been identified in the uptake process: proton motive force, Btu B, Btu C, Btu D, and Ton B (14). The Btu B product is the outer membrane receptor for Cbl. Btu B mutants are either deficient in the energy-dependent transport across the outer membrane or lack Cbl binding ability. The proton motive force and Ton B mutants are also unable to internalize Cbl due to their inability to stimulate the release of cbl from the receptor into the periplasmic space. The Btu C and Btu D mutants fail to transport Cbl across the inner membrane.

2.2 COBALAMIN ABSORPTION AND TRANSPORT IN MAMMALS

After ingestion, dietary cobalamin is released from proteins by the action of acid and pepsin in the stomach (15). Cbl is then transported by a complex system consisting of carrier-receptor interactions. In the absence of such a mechanism, only 0.1-1% of vitamin B_{12} will cross the cell membrane (10).

2.2.1 R Binders

R proteins, named such for their rapid motility during electrophoresis, are ubiquitous glycoproteins with high affinity for Cbl (16). They are present in the plasma, secretions (eg. bile, saliva), and the cytoplasm of many cells (eg. platelets, erythrocytes, granulocytes) (10). Transcobalamin I (TCI), transcobalamin III (TCIII), cobalophylin, and haptocorrin are examples of R binders. They are the products of a single genetic locus, differing in the amount of glycosylation (16). Johnston et al (17) have recently isolated the full length human TCI cDNA. The mRNA transcript is 1.5kb encoding 433 amino acids with 9 glycosylation sites. It has been shown that TCI and TCIII bind 75% of total endogenous Cbl (18). While the physiological significance of R proteins is still unclear, it has been suggested that they play a role in maximizing Cbl utilization through the removal of potentially harmful Cbl analogues from the circulation (15). Moreover, R binders are thought to play a bacteriostatic role by denying availability of Cbl and Cbl analogues to bacteria which may require them for growth (15).

When ingested Cbl binds to salivary and gastric R binders, it cannot be absorbed or reabsorbed (9). In the small intestine, pancreatic enzymes digest this complex,

and Cbl then binds to intrinsic factor (IF) (16). Pancreatic insufficiency could cause Cbl malabsorption due to the lack of tryptic digestion of the R binders and the subsequent release of Cbl to allow binding to IF (10).

2.2.2 Intrinsic Factor (IF)

Intrinsic factor (IF), a 48 KDa glycoprotein synthesized in the parietal cells of the gastric mucosa, mediates Cbl uptake from R binders in the gastrointestinal tract (5). The rat gastric IF cDNA clone has been isolated by Dieckgraefe (19); the deduced protein contains 421 amino acids. IF production and release are stimulated by hormones and food. IF binds Cbl very stringently and is unable to biad corrinoids other than Cbl (15). Cbl mediated uptake is thus selective and ensures that only Cbl enters the circulation (20). The Cbl-IF complex then binds to specific receptors present on the luminal side of enterocytes located in the brush border of the distal ileum (20). This binding requires the presence of calcium ions and a pH between 5 and 7.5 (20). The complex is taken up into the enterocytes through an energy-dependent endocytotic mechanism. Cbl is then released from IF at a pH of 5, consistent with localization to lysosomes or endosomes (21). It has been shown that there is no substantial recycling of IF to the brush border membrane (21). Cbl binds to transcobalamin II within the enterocytes before the complex appears in the portal circulation after traversing the basal membrane (5).

2.2.3 Transcobalamin II (TCII)

Transcobalamin II (TCII) is a serum protein carrier which transports newly

absorbed Cbl into tissues (10). Human TCII has been localized to chromosome 22q (22). The cDNA, comprised of 1866 nucleotides, is deduced to encode an 18 aa leader sequence and a 409 aa mature protein (23). This protein has a molecular weight of 38,000. The amino acids alignment of TCII with that of other Cbl binding proteins (rat IF, human TCI, and porcine haptocorrin) revealed 33% overall homology (24). However, there were 6 regions of high homology (60%-80%). The Cbl-binding functional domain is predicted to reside within these regions of high homology (24). Variant forms of human TCII have been isolated recently (24). The two identified cDNA clones differed at codons 259 and 376 from the previous isolated TCII sequence, and differed from each other at codon 198 and 219 and in the length of the 5' and 3' non-coding regions. TCII is present in plasma, spinal fluid, semen, and extracellular fluid (10). It is synthesized by a variety of cells including amniocytes, fibroblasts, and enterocytes (10). TCII accounts for only a small percent of total Cbl binding, but it represents the only physiologically active Cbl source, which can promote the entry of vitamin B_{12} into cells (20,25). Finkler and Hall showed that HeLa cells accumulated CN-Cbl bound to TCII much more rapidly than free CN-Cbl or CN-Cbl bound to TCI, IF or other binding proteins (26). TCII binds all newly absorbed Cbl in the plasma. The binding depends on the presence of calcium ions (20). When TCII complexes with Cbl, it undergoes conformational change which increases its affinity for specific receptors on the plasma membrane of all tissues (20). The complex binds the receptors in the presence of calcium ions and is internalized into lysosomes or endosomes via adsorptive endocytosis (25). Another mechanism has been described whereby a small amount of TCII-Cbl is taken up via non-specific pinocytosis (27).

2.2.4 Alternative Cobalamin Transport

Although the process just described is surely the most widely distributed physiologic means by which mammalian cells obtain Cbl, in vivo and in vitro findings indicate that human cells are capable of taking up Cbl by some mechanism not bound to TCII. Cultured human skin fibroblasts have been shown to have the ability to take up free Cbl via a specific, saturable, low capacity component which is calcium-independent, cycloheximide-sensitive, and requires free sulfhydryl groups and an intact electron transport chain (28). This process helps to explain the improvement of patients with congenital TCII deficiency treated with high doses of OH-Cbl or CN-Cbl. The existence of another mechanism has been demonstrated whereby the asialoglycoprotein membrane receptors of hepatocytes are recognized by R proteins and can clear bound Cbl from plasma (15). Upon internalization, Cbl is digested free in the lysosome, and is released intracellularly.

2.2.5 Intracellular Cobalamin Metabolism

After the internalization of TCII-Cbl complex into the cell, lysosomal proteases digest Cbl free, and TCII fragments leave the cell (Fig.2) (27). Cbl may now efflux across the lysosomal membrane into the cytosol (27). The mechanism of Cbl efflux is unclear. There is evidence that chloroquine, an inhibitor of lysosomal proteolysis, inhibits the processing of TCII-Cbl complex, which accumulates in lysosomes (25). Once released intracellularly, Cbl can be converted into its coenzyme forms: methyl-Cbl (Me-Cbl) and adenosyl-Cbl (Ado-Cbl) (5). Pezacka and Rosenblatt (29) suggested that the intracellularly released cob(III)alamin must first undergo a ß-ligand exchange reaction with

FIG. 2 **INTRACELLULAR Cbl METABOLISM.** General pathway of the intracellular metabolism of Cbl. Reprinted from Pezacka and Rosenblatt (29).

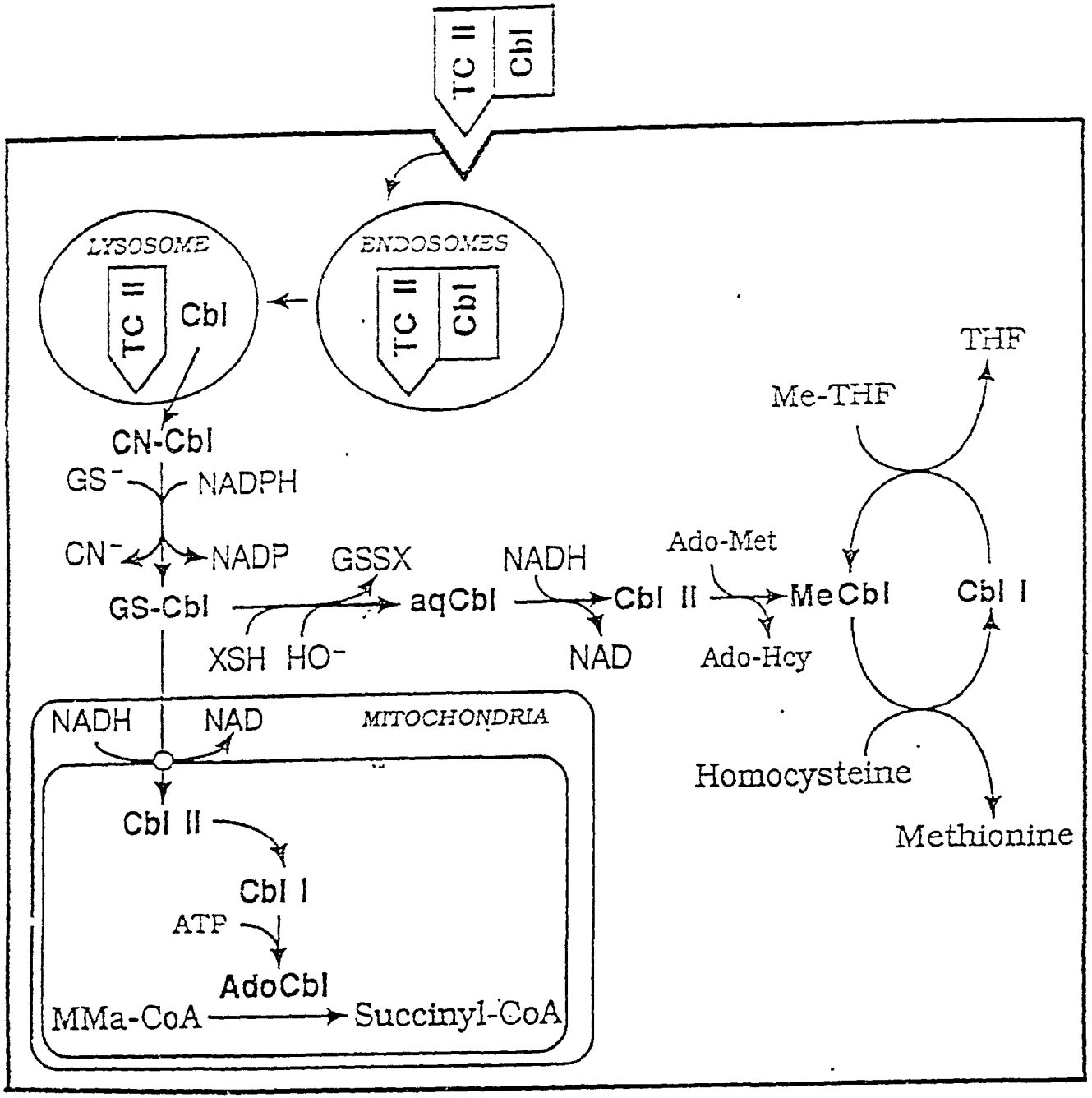
TC II
Cbl
LYSOSOME
ENDOSOMES
CN-Cbl
GS⁻
NADPH
CN⁻
NADP
GSSX
GS-Cbl
aqCbl
XSH
HO⁻
NADH
Cbl II
NAD
Ado-Met
MeCbl
Ado-Hcy
Cbl I
THF
Me-THF
Homocysteine
Methionine
NADH
NAD
MITOCHONDRIA
Cbl II
Cbl I
ATP
AdoCbl
MMa-CoA
Succinyl-CoA

the formation of GS-Cbl. In the cytoplasm, GS-Cbl is converted to aquocobalamin (H_2O-Cbl or aqCbl) by mix-disulfide formation, after which cob(III)alamin is reduced to cob(II)alamin. Cob(II)alamin then binds to methionine synthase (MS) which is activated by coupled reductive methylation with adenosylmethionine as a primary methyl donor. Me-Cbl serves as a cofactor for MS in methylating homocysteine to methionine. Alternatively, GS-Cbl can be transported through the outer mitochondrial membrane to an intermembranous space where it is reduced to cob(II)alamin by mitochondrial Cbl reductase. Cbl is then further transported into the matrix where cob(II)alamin is reduced to cob(I)alamin (29). After its adenosylation to Ado-Cbl by adenosyltransferase, it assists methylmalonyl CoA mutase (MCM) in the isomerization of methylmalonyl CoA to succinyl CoA. It has been shown that 95% of intracellular Cbl is associated with either MS or MCM (30).

2.2.6 Mitochondrial Cobalamin Uptake

There is evidence that lysosome-free preparations of rat liver mitochondria take up OH-Cbl by a process dependent on mitochondrial swelling (31). It is assumed that the permeability of mitochondria to OH-Cbl is increased by the swelling (31). The mechanism, which is specific for OH-Cbl, is saturable, concentrative, and does not require ion transport or energy metabolism (31). OH-Cbl binds with high affinity to an intramitochondrial protein that comigrates with MCM (30). Although no specific Cbl mitochondrial transport system has been described, this evidence suggests that Cbl is taken up into the mitochondria by passive diffusion followed by binding to MCM (6).

CHAPTER 3

COBALAMIN-DEPENDENT ENZYMES

3.1 CBL-DEPENDENT ENZYMES IN MICROORGANISMS

The *Escherichia coli* Cbl metabolism system has been studied intensively. *E.coli* cannot synthesize the corrin ring of vitamin B_{12}, but it is able to convert cyano-Cbl or aquo-Cbl into their coenzymes forms. It possesses two Cbl-dependent enzymes, an adenosylCbl dependent ethanolamine-ammonia lyase (EC 4.3.1.7), and a methylCbl dependent methylfolate-homocysteine methyltransferase (EC 2.1.1.13) (32). The bacteria requires the former enzyme only when ethanolamine is the sole nitrogen source. The Cbl-dependent methyltransferase, which is the product of metH gene, is responsible for methionine biosynthesis (32). *E.coli* cells also possess a Cbl-independent methyltransferase (EC 2.1.1.14), product of metE gene, and can therefore grow in the absence of supplied methionine and Cbl. However, the cells prefer to use the Cbl-dependent enzyme, and when Cbl is available the metH holoenzyme represses the synthesis of the metE gene product (13). The metH gene product is a monomeric enzyme, and contains one mole of Cbl per mole of enzyme (32). It also contains one mole of copper per mole of enzyme-bound Cbl. However, since the enzyme from the strain K-12 of *E.coli* lacks stoichiometric copper (0.1 mol/mol Cbl), it is not believed to play a crucial catalytic role. A reducing system required for Cbl-dependent methyltransferase activity has been identified (32). This system involves two flavoprotein called R and F components. FAD and FMN are noncovalently bound to each component, respectively, and operate as intermediates in electron transport from NADPH to

methyltransferase. The metH gene has been cloned using methionine-requiring nutritional auxotrophs of *E.coli* that were deficient in metH or metE gene products (32).

3.2 CBL-DEPENDENT ENZYMES IN MAMMALS

3.2.1 Methylmalonyl CoA Mutase (MCM)

Methylmalonyl CoA mutase (MCM) (EC 5.4.99.2) is a Cbl-dependent enzyme that converts methylmalonyl CoA to succinyl CoA in mammalian cells. It was first identified in 1955 in rat liver and sheep kidney (33). It catalyses the final isomerization reaction in the propionate metabolism pathway (34). This pathway is not a quantitatively important source of succinate in mammals, but it is an intermediate step in the degradation of valine, isoleucine, threonine, methionine, thymine, odd chain fatty acids, and cholesterol to be recovered as succinyl CoA for the use in the tricarboxylic acid cycle (35) (Fig.3). MCM has different functions in lower species. Prokaryotic mutase is involved in the reverse reaction, that is the isomerization of succinyl CoA to methylmalonyl CoA, a step essential to synthesize propionate from the Krebs cycle intermediates (36). MCM in ruminants is required for gluconeogenesis from propionate (37). It has been demonstrated that the MCM-catalysed isomerization of methylmalonyl CoA to succinyl CoA occurs by an intramolecular shift of the CoA carboxy group to the methyl moiety (38,39). Studies on MCM intramolecular rearrangement from rat liver extracts showed that the transcarboxylation depends on the presence of a cofactor form of Cbl (40).

FIG. 3 **PRECURSORS OF AND THE MAJOR CATABOLIC PATHWAY FOR PROPIONATE AND METHYLMALONATE.** Broken arrows indicate the presence of several reactions. Reprinted from Rosenberg and Fenton (35).

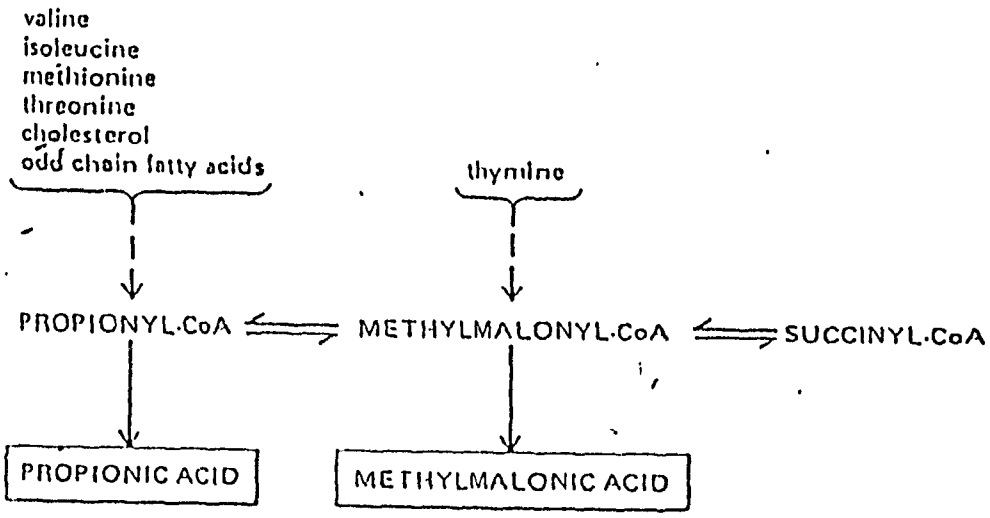
valine
isoleucine
methionine
threonine
cholesterol
odd chain fatty acids
thymine
PROPIONYL-CoA
METHYLMALONYL-CoA
SUCCINYL-CoA
PROPIONIC ACID
METHYLMALONIC ACID

3.2.1.1 Intracellular localization

MCM is found in most mammalian tissues, but it is most abundant in liver and kidney. MCM activity has been localized to the mitochondrial matrix of human and rat liver using specific enzymes markers (41). The rat liver mitochondria contained 97.5% of MCM, and Cbl deficiency did not alter this distribution (41).

3.2.1.2 MCM activity assays

MCM activity can be measured by two different methods. The first is a radioactive assay that examines the conversion of methylmalonyl CoA to succinyl CoA in mammalian cells (34). A reaction mixture is prepared with MCM, AdoCbl, buffer, and [1-^{14}C]-L-methylmalonyl CoA. Perchloric acid is used to terminate the reaction. Potassium permanganate oxidizes excess methylmalonyl CoA producing $^{14}CO_2$ which is removed. Succinate is resistant to the oxidation. MCM enzymatic activity is measured as μmol succinate formed per minute.

The second assay uses spectrophotometry to measure the consumption of NADH in the succinyl CoA -> methylmalonyl CoA reaction (11). A reaction mixture containing NADH, AdoCbl, succinyl CoA, glutathione, sodium pyruvate, oxaloacetate transcarboxylase, malate dehydrogenase, and methylmalonyl CoA racemase is incubated with MCM. MCM activity is measured by the decrease in absorbance at 340 nm as μmol succinyl CoA consumed per minute.

3.2.1.3 Requirements for adenosylcobalamin (AdoCbl)

AdenosylCbl (AdoCbl) is the form in which Cbl acts as a cofactor for MCM. It is synthesized in the mitochondrial matrix from dietary OH-Cbl. AdoCbl was isolated in 1958 by Barker et al. (42). Using spectrophotometry, they identified it as the coenzyme form of Cbl which is required for the decomposition of glutamate in *Clostridium tetanomorphum*. In 1959 and 1960, several groups reported that AdoCbl is an essential cofactor in the analogous mammalian enzymatic conversion of methylmalonyl CoA to succinyl CoA (40,43). In vitro studies on vitamin B_{12} deficient rat-liver mitochondria (40) and liver homogenates (43) established that endogenous holomutase activity increased when incubated with AdoCbl, but not with CN-Cbl. Subsequent studies deduced that the interaction of MCM from normal human fibroblasts with its substrate methylmalonyl CoA and its cofactor AdoCbl results from non-cooperative binding at independent and non-equivalent active sites (44). The exact role of AdoCbl in the isomerization reaction remains to be established. It has been suggested that the vitamin B_{12} dependent rearrangement proceeds by way of free radical intermediates of methylmalonyl CoA generated through oxidation-reduction of the cobalamin cobalt atom by hydrogen transfer between substrate and coenzyme (38). Murakami demonstrated such a process (45). An effective artificial enzyme simulating the catalytic functions of MCM was produced by combining a hydrophobic cobalamin molecule with a synthetic lipid bilayer membrane, and was capable of rearranging the carbon-skeleton of the substrate.

3.2.1.3.1 AdoCbl synthesis

Conversion of vitamin B_{12} to the coenzyme form AdoCbl has been primarily demonstrated in extracts of *Clostridium tetanomorphum*, where three enzymatic steps have been identified (46). Cob(III)alamin undergoes a reduction to cob(II)alamin by cob(III)alamin reductase (EC 1.6.99.8), and subsequently to cob(I)alamin by cob(II)alamin reductase (EC 1.6.99.9) (47). Cob(I)alamin is then converted to 5'-deoxyadenosylCbl by the enzyme 5'-adenosyltransferase (EC 2.5.1.17), with ATP supplying the 5'-deoxyadenosyl moiety (46). Bacterial Cbl reductases have been partially purified and shown to require oxidation-reduction cofactors (DPNH, FAD, FMN) (47). Adenosyltransferase, which has been purified 300 fold, was demonstrated to function at an optimum pH of 8, to utilize Cbl in a monovalent state as its substrate, and to require Mn^{+2} divalent cations for activity (46). Further evidence indicated that mammalian cellular metabolism of Cbl may proceed by a very similar set of reactions. Kerwar et al demonstrated AdoCbl synthesis in HeLa human skin fibroblasts (48). They showed that cell extracts readily converted OH-Cbl to AdoCbl in the presence of a reducing system (NADH or glutamate) and ATP, suggesting the presence of combined Cbl reductase - adenosyltransferase activities. This was confirmed subsequently by the observation that intact rat liver mitochondria, provided only with a source of reducing equivalents and a source of ATP, were also capable of making AdoCbl from OH-Cbl (49). These data localized the enzymatic conversion of vitamin B_{12} to AdoCbl to the mammalian mitochondria. There is np evidence implicating a transport system for Cbl into mitochondria.

3.2.2 Methionine Synthase (MS)

Methionine synthase (5-methyltetrahydrofolate-homocysteine methyltransferase) (EC 2.1.1.13) is a cytosolic enzyme that catalyses the methylation of homocysteine to form methionine (10). MS requires MeCbl as its cofactor. The gene encoding the mammalian enzyme has not been cloned yet, but the enzyme has been isolated from several animal sources including porcine kidney and liver, and from human placenta (50). MS has been localized to chromosome 1 by measuring [^{57}Co]-Cbl binding and MS activity in rodent-human somatic cells hybrids (51). MS purified from human placenta when run on unreduced polyacrylamide gel was demonstrated to have a molecular weight of 160,000, and appeared to be a monomer (50). On a reduced gel, human placental extracts yielded three bands of 90,000 Da, 45,000 Da, and 35,000 Da, suggesting a complex subunit structure (50). MS contains one mole of Cbl per mole of apoenzyme and two moles of iron per mole of holoenzyme (50). It has been proposed that the lower subunits may bind the iron and thus act as a reducing agent (50). MS activity has been demonstrated in human fibroblasts, and maximal activity was observed in late stationary phase fibroblasts cells (52). However, in most other cells studied (e.g. human lymphoblasts), MS activity has usually been highest during the rapid growth phase. The mammalian enzyme has not been as well characterized as its bacterial equivalent, the metH gene product in *E.coli*, but both appear very similar in their catalytic properties (32).

Homocysteine remethylation is also catalysed by an alternative enzyme, betaine homocysteine methyltransferase (EC 2.1.1.5), requiring betaine as methyl donor (53). However, this enzyme is generally confined to the liver.

3.2.2.1 Methylcobalamin (MeCbl)

MeCbl is the cytosolic coenzyme form of Cbl involved in the formation of methionine from homocysteine, a reaction catalysed by the enzyme methionine synthase (10). MeCbl is the major circulating Cbl species, accounting for 60% to 80% of total plasma Cbl; OH-Cbl and AdoCbl make up the remainder (22). The formation of MeCbl occurs once the MS-bound cob(II)alamin has been reduced to cob(I)alamin and receives a methyl group from either S-adenosylmethionine (AdoMet) or 5-methyltetrahydrofolate (MeTHF) (54).

3.2.2.1.1 S-Adenosylmethionine (AdoMet)

AdoMet is a crucial methyl group donor in a variety of biosynthesis reactions. It is required along with a reducing system to activate the catalytic activity of the enzyme MS, as is the case with the *E.coli* methyltransferase (32). AdoMet provides the initial methyl group for the methylation of cob(II)alamin bound to MS. MeCbl then transfers the methyl group to homocysteine to form methionine, and cob(I)alamin is left bound to the enzyme. Subsequent methyl groups are then provided by 5-methyltetrahydrofolate, until Cbl undergoes a spontaneous oxidation to cob(II)alamin, whereupon it once more requires AdoMet and a reducing system to regenerate MeCbl. AdoMet is involved in the negative feedback regulation of methionine synthesis, with high levels inhibiting the production of methionine. An MS-associated reducing system has not yet been demonstrated in mammals in vivo (32). However, Rosenblatt et al reported normal MS activity in cell extracts of a patient with megaloblastic anemia and homocystinuria under standard reducing conditions, but low enzyme activity at decreased concentrations of reducing agents (55). This evidence

demonstrate the existence of a defective MS-related reducing system (56). Moreover, partially purified enzyme is found to be associated with thiol oxidase activity, suggesting that thiols may function as the physiological reductants for the mammalian enzyme (57).

3.2.2.1.2 5-Methyltetrahydrofolate (MeTHF)

An important function of MS, other than the conservation of cellular methionine, is the regeneration of tetrahydrofolate which is essential for the biosynthesis of purines, pyrimidines, and serine (32). The enzyme methylene tetrahydrofolate (CH_2-THF) reductase (EC 1.5.1.20) is a flavoprotein that catalyses the irreversible NADPH-dependent reduction of CH_2-THF to MeTHF (58). MS-cob(I)alamin transfers the methyl group from MeTHF, which is the major storage form of intracellular folate, to homocysteine, generating methionine and tetrahydrofolate (THF) (58). THF is then reconverted to CH_2-THF which is necessary for thymidylate biosynthesis (32). If MS is non functional, MeTHF cannot be converted to THF, leading to the accumulation of MeTHF. This phenomenon is called the MeTHF trap, and results in a depletion of total intracellular folate levels (32).

3.2.2.2 Nitrous oxide

Long-term exposure to nitrous oxide (N_2O), a commonly used anesthetic agent, has been shown to inactivate MS irreversibly causing megaloblastic and aplastic bone marrow changes, anemia and myelopathy in humans (32). These side effects are similar to the symptoms of vitamin B_{12} deficiency. Model studies of the interaction of cob(I)alamin in aqueous solution with N_2O have established that N_2O oxidizes cob(I)alamin, and N_2 is

liberated according to the following reaction:

$$\text{cob(I)alamin} + N_2O + H^+ \rightarrow \text{cob(II)alamin} + N_2 + OH^\cdot$$

Based on these studies, it was postulated that N_2O inhibits MS activity by inactivating the transient Cbl. The irreversible loss of activity in MS may be explained by the generation of hydroxyl radicals at the active site.

CHAPTER 4

INHERITED DEFECTS OF CBL TRANSPORT AND METABOLISM

4.1 DEFECTIVE ABSORPTION AND TRANSPORT OF CBL

Inherited disorders of Cbl metabolism may be caused by inadequate ingestion, absorption, or transport of vitamin B_{12} to target cells (10). However, because of the large hepatic reserve, deficiency states may be present for years before the plasma Cbl level is decreased.

4.1.1 R Binder Deficiency

Several patients have been described with a deficiency of R binders. However, they have not shown a distinct phenotype associated with the disease. Although the patients have low serum Cbl levels, they have normal levels of TCII, and thus do not exhibit the clinical symptoms related to Cbl deficiency (10). The fact that these patients have no apparent clinical disease attributable to their lack of R binders serves to emphasize the unclear role of these proteins in normal metabolism and homeostasis.

4.1.2 Defective Intrinsic Factor (IF)

Inherited IF deficiency results in the juvenile form of pernicious anemia. A number of affected children have presented with developmental delay and megaloblastic anemia. In these patients, serum levels of Cbl are markedly deficient, but in contrast to the adult acquired form of pernicious anemia, gastric function and morphology are normal and

serum autoantibodies to IF are absent (5). Cbl absorption is abnormal in these children, but is restored when the vitamin is mixed with normal human gastric juice as a source of IF. Further investigations of the gastric secretions of these patients have shown that there are several different classes of functional IF deficiency. One class results in failure to produce or secrete any immunologically recognizable IF (59). There are also cases of patients with normal IF secretion and abnormal Cbl absorption (60). This problem has been demonstrated in some cases to be the result of an abnormal IF protein with lowered affinity for the ileal receptor (60). This may also be the result of secreting a labile IF protein with a lowered affinity for Cbl or an increased susceptibility to proteolysis (61).

4.1.3 Enterocyte Malabsorption

Many cases have been reported of patients with abnormal Cbl absorption with a normal secretion of a functional IF protein, normal TCII levels, normal intestinal and gastric morphology, and no antibodies against IF in the serum (16). In contrast to IF deficiency patients, Cbl absorption defect in these patients is not corrected by providing normal human IF with vitamin B_{12} (10). Symptoms include megaloblastic anemia, serum Cbl deficiency, and many patients also exhibit proteinuria (62). In some patients, the problem has been described as a defect in or absence of the ileal cell IF-Cbl receptor; this has been referred to as the Immerslund-Grasbeck syndrome (63). Some patients, however, have been shown to have normal receptor activity, the defect probably residing within the ileal cell itself. Because the mechanism for Cbl transport across the enterocyte is complex and not well understood, it seems likely that this syndrome encompasses defects at several points in

this overall pathway, including the receptor itself, receptor internalization, and Cbl transfer to TCII (63).

4.1.4 TCII Deficiency

Patients with this condition usually present in the first few months of life with symptoms consisting of vomiting, pallor, weakness, megaloblastic anemia, and neurological defects (64). Because TCII is required for the receptor-mediated endocytosis of Cbl, TCII-deficient patients cannot deliver Cbl to tissues (10). However, total serum Cbl levels are normal in these patients reflecting the fact that most serum Cbl is carried by R binders. Most patients have no immunologically detectable TCII in plasma, although a few have been documented with defective protein with no Cbl binding, or with physiologically inactive TCII with normal Cbl binding (5). Studies in patients with TCII deficiency suggest that TCII synthesis by enterocytes is probably required for IF-mediated transport of Cbl across the ileal cells (10).

4.2 DISORDERS OF CBL METABOLISM

4.2.1 Methylmalonic Aciduria (MMA)

In 1967, the first cases of genetically determined metabolic disease involving cellular Cbl metabolism were detected and reported (6). The patients with the disease had the unique characteristic of massive amounts of methylmalonic acid, which in normal individuals is a minor urinary metabolite (15μg/g creatinine) and is present in the plasma at low concentrations (73-271 nmol/l), accumulating in urine (100mg-2g/g creatinine) and blood

(0.22 - 2.88 mmol/l plasma levels) (65,66). These MMA patients had normal Cbl transport and serum concentrations.

MMA is an often fatal autosomal recessive disorder, with an incidence of 1 in 50,000 (67). MMA occurs as a result of a block in the conversion of L-methylmalonyl CoA to succinyl CoA. Such a deficiency arises from either a defect in MCM which catalyses the isomerization reaction or a defect in the pathway for the biosynthesis of its cofactor, AdoCbl (68).

Clinical phenotypes of MMA are caused by precursors and abnormal derivatives of methylmalonic CoA accumulating in blood, tissues, and urine causing a widespread aberration in metabolic homeostasis (69,70). The clinical spectrum ranges from fulminant recurrent perinatal metabolic acidosis, multiorgan failure and death, to chronic or intermittent aminoaciduria, to an entirely benign or asymptomatic organic aciduria without any clinical or developmental abnormalities. Conventional long term management of the disease is based mainly on dietary restriction of amino acid precursors for propionyl CoA and administration of carnitine, which may be relatively deficient secondary to accumulation of unmetabolized organic acid esters (71).

MMA is now known to be a heterogenous group of at least six genetically and biochemically distinct disorders of methylmalonyl CoA catabolism defined on the basis of somatic cell hybridization and biochemical studies (71). Cell lines with mutations in the structural gene locus (MUT) for MCM are designated *mut* and the patients are vitamin B_{12} unresponsive (68) (although in some cases response to vitamin B_{12} is seen in cells in cultures (see section 5.3.2)), while those with mutations in genes required for the biosynthesis of

AdoCbl are subdivided into *cbl*A, *cbl*B, *cbl*C, *cbl*D, and *cbl*F classes, and are vitamin B_{12} responsive (72). The latter respond to vitamin B_{12} supplementation with an improvement in their clinical course and a reduction in methylmalonate excretion. *mut* patients present with a worse prognosis then *cbl* patients because of vitamin B*12* unresponsiveness.

4.2.2 Somatic Cell Complementation Groups

Different genetic classes of defects in the intracellular utilization of Cbl have been delineated through the use of somatic cell complementation analysis of cultured human fibroblasts and biochemical studies (6). These represent errors of Cbl metabolism associated with homocystinuria and MMA either alone or in combination.

A complementation test was developed by Gravel et al. (73) using Sendai virus to fuse different mutant fibroblast lines and produce multinucleated heterokaryons. They tested for complementation by the autoradiographic detection assay of the MCM dependent conversion of [1-^{14}C] propionate via the citric acid cycle to amino acids and thence incorporation into trichloroacetic acid (TCA) precipitable proteins. Later, the method was modified in order to measure directly [^{14}C] propionate incorporation into TCA-precipitable material by liquid scintillation spectrometry (6). Another complementation test was developed to analyze the defects in the MS pathway by measuring [^{14}C] MeTHF incorporation into acid-precipitable material (16). In recent years, the fusing chemical agent used is polyethylene glycol (PEG) (74).

A complementation group is determined by examining propionate fixation in heterokaryons formed from the fusion of pairs of patient fibroblast cell lines (74). Two cell

lines from different complementation groups will have increased propionate uptake when fused because each cell line can provide the other with the factor in which it is deficient, thus negating the defect and complementing. However, two cell lines from the same complementation group will not have increased propionate uptake when fused because the genetic defect lies in the same gene.

Eight principal groups representing mutations in distinct genes for Cbl cellular metabolism have been defined based largely on complementation analysis (5) (Fig.4). These are comprised of a defect of the mutase apoenzyme (*mut*); two distinct defects of AdoCbl synthesis- one probably due to deficiency of a mitochondrial Cbl reductase (*cbl*A), the other to deficiency of mitochondrial Cbl adenosyltransferase (*cbl*B); two distinct defects of MeCbl synthesis- one (*cbl*E) lies perhaps in a reducing system associated with MS, the other (*cbl*G) has a defect involving MS activity independent of the reducing system; and finally three distinct defects of both AdoCbl and MeCbl synthesis due to abnormal cytosolic or lysosomal metabolism of Cbl (*cbl*C, *cbl*D, and *cbl*F). The defect at the molecular level has been defined only for some patients within the *mut* class (68).

4.2.3 Defects in AdoCbl Synthesis

4.2.3.1 *cbl*A and *cbl*B

*cbl*A and *cbl*B represent two different groups of Cbl-responsive MMA patients with defective gene products required for the biosynthesis of AdoCbl (16). In both disorders, there is MMA without homocystinuria, lethargy, failure to thrive, vomiting, dehydration, hypotonia and coma.

FIG. 4 **INBORN ERRORS OF VITAMIN B_{12} (Cbl) METABOLISM.** The letters refer to the presumed site of the block in the mutations that were defined by complementation analysis. Reprinted from Rosenblatt and Cooper (75).

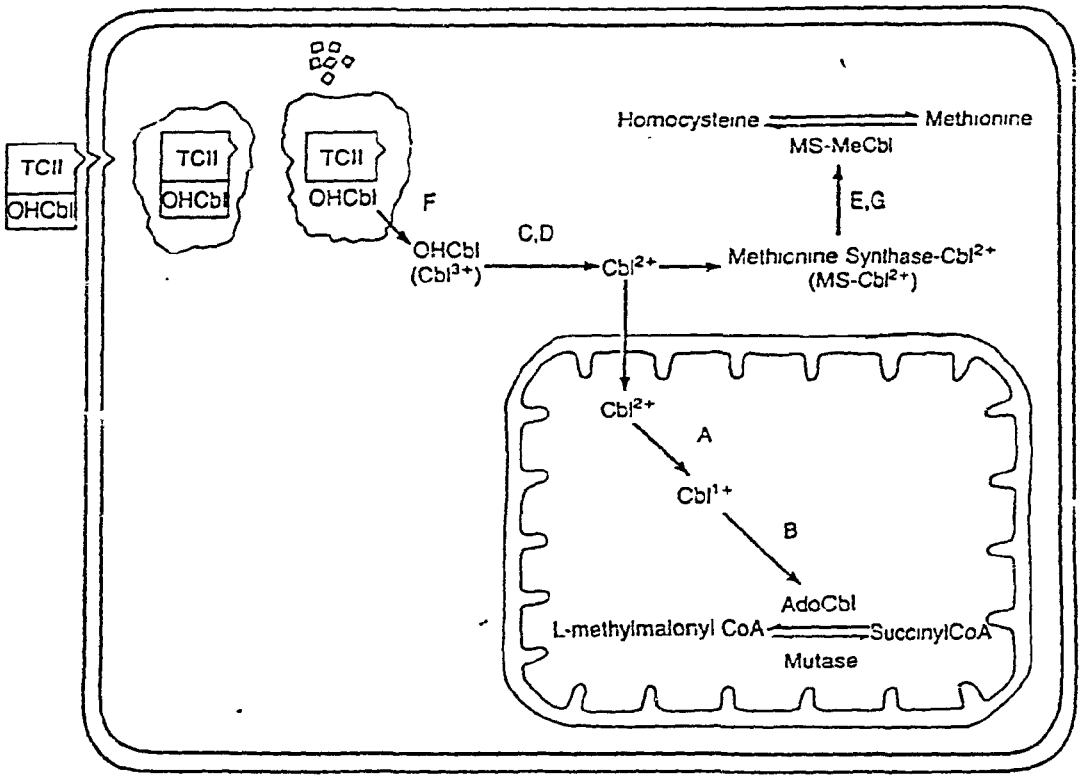
TCII
OHCbl
TCII
OHCbl
TCII
OHCbl
F
OHCbl
(Cbl3+)
C,D
Cbl2+
Homocysteine
Methionine
MS-MeCbl
E,G
Methionine Synthase-Cbl2+
(MS-Cbl2+)
Cbl2+
A
Cbl1+
B
AdoCbl
L-methylmalonyl CoA
SuccinylCoA
Mutase

cblA is characterized by onset in the first year of life and by a good response to Cbl therapy. 90% of *cblA* patients respond well to pharmacological doses of OH-Cbl or CN-Cbl with a reduction in urinary methylmalonic acid excretion and clinical improvement (76).

cblB symptoms and age of onset is similar to *cblA*, but response to therapy is relatively poor. Less than 40% of *cblB* patients demonstrate a decrease in blood or urine methylmalonate and a resolution of their clinical symptoms (76).

Both defects lead to an impaired AdoCbl synthesis and hence reduced mutase activity. Intact fibroblasts from *cblA* or *cblB* patients demonstrate low levels of AdoCbl and of propionate incorporation (77). *cblB* fibroblasts are unable to form AdoCbl either in whole cells or in cell extracts. The defect is due to a low or absent activity of ATP:Cob(I)alamin-adenosyltransferase within the mitochondria (78). In contrast, intact fibroblasts from *cblA* patients have decreased whole cell accumulation of AdoCbl, but cell extracts are able to synthesize AdoCbl when supplied with a reducing system and ATP. The defect in *cblA* patients is thought to be due to a failure to reduce cob(III)alamin or cob(II)alamin within the mitochondria (77). It is not clear if there is more than one step responsible for the reduction as a cell line from a patient has been described with all the features of *cblA* cells except that it complements other *cblA* and *cblB* lines (79). The identification of this new complementation group (*cblA'*) suggests that at least 2 gene products in addition to adenosyltransferase are required to generate AdoCbl in the mitochondria.

4.2.4 Defects in AdoCbl and MeCbl Synthesis

4.2.4.1 *cblC* and *cblD*

Patients with *cblC* and *cblD* disorders have both MMA and homocystinuria due to a combined deficiency of the synthesis of AdoCbl and MeCbl. Their total cellular content of Cbl is markedly reduced (80).

cblC disease is the most common inborn disorder of Cbl metabolism accounting for over 65 reported cases (81). The patients usually present in the first few months of life, although some have exhibited late onset, with a failure to thrive, developmental retardation, feeding difficulties, seizures, anemia, and megaloblastosis (10). Therapy with OH-Cbl and betaine often decreases blood homocysteine and methylmaloaic acid, but does not completely eliminate them. The endo-lysosomal system which mediates the specific uptake and hydrolysis of TCII-bound Cbl have shown to be normal (80). However, *cblC* cells are completely deficient in the binding of Cbl to either MS or MCM (82). Moreover, *cblC* cells have been shown to be unable to utilize CN-Cbl probably due to their inability to remove the cyanide group (82). Recently, it has been shown that the enzyme B-ligand transferase (which catalyses the replacement of the CN- group of CN-Cbl with GS-moiety) and cob(III)alamin reductase demonstrate variable decrease in their activities in *cblC* cells (29). Defective cob(III)alamin reductase has been proposed to cause *cblC* disorder. However, the observed variable decrease in the activity of both enzymes suggest that cob(III)alamin reductase is not the primary defect in *cblC* disorder, leaving the nature of the disease obscure (29).

The smaller number of patients in the *cblD* group, represented only by a single

sibship, present later in life with neurologic abnormalities (74). *cbl*D cells display a detectable, though decreased, Cbl binding activity and have some capacity to catalyse the initial removal of the cyanide group from CN-Cbl (82). Moreover, in *cbl*D cells, the specific activities of B-ligand transferase and cbl(III)alamin reductase were 33% and 55% respectively (29). Byck and Rosenblatt observed that cocultivation of *cbl*C and *cbl*F fibroblasts in the absence of PEG resulted in a partial increase of propionate and MeTHF uptake suggesting metabolic cooperation (83). However, *cbl*D fibroblasts do not exhibit such a cooperation when mixed with *cbl*F cells. The specific defect in *cbl*D is not known, although both clinical and cellular phenotypes suggest that *cbl*D is a "leaky" or less severe form of *cbl*C (80) However, *cbl*D may also have a separate defect in a metabolic step proceeding or following the *cbl*C defect (83).

4.2.4.2 *cblF*

As with cells from *cbl*C and *cbl*D patients, both MCM and MS activities are impaired in *cbl*F cells, and AdoCbl and MeCbl contents are reduced. Five Patients have been described with *cbl*F disease with a variation in the age of onset (84). One patient presented with Cbl responsive MMA without homocystinuria. The four other patients reported had Cbl responsive MMA in addition to homocystinuria. The *cbl*F cells have been shown to accumulate unmetabolized, nonprotein-bound CN-Cbl in lysosomes (85). Subcellular fractionation demonstrated that Cbl was in lysosomal fraction of the cell. Moreover, EM-radioautography with [^{57}Co] CN-Cbl showed the presence of Cbl in lysosomes of *cbl*F patients. These findings indicate that the defect in *cbl*F lies in the transfer

of Cbl from lysosomes to the cytoplasm, specifically in a lysosomal membrane-specific transport system for Cbl. The inability of *cblF* patients to absorb oral Cbl suggests that a similar mechanism may be operating at the level of the enterocytes at the distal ilium, and that IF-Cbl has to pass through a lysosomal mechanism before Cbl is released (84).

4.2.5 Defects in MeCbl Synthesis

4.2.5.1 *cblE* and *cblG*

cblE and *cblG* classes are generally characterized by megaloblastic anemia, homocystinuria, and hypomethioninemia in the absence of MMA (5). The cells exhibit functional deficiency of MS due to decreased formation of MeCbl. Patients usually present in the first few months of life with vomiting, poor feeding, lethargy, and hypotonia (10). At least one patient had adult onset (86). Although patients with *cblG* appear to respond to therapy with OH-Cbl, MeCbl, and betaine, they seem to be more resistant to treatment than *cblE* patients (16). If untreated, these diseases could lead to developmental delay and neurological manifestation, possibly on the basis of methionine deficiency (87). In fact, it has been suggested that the deficiency of MeCbl and AdoMet impairs methylation reactions essential for myelination and neurotransmitter synthesis, leading to the development of myelopathy (64). Upon long term treatment with Cbl, a slow and incomplete improvement of the psychomotor system is observed (88).

In both *cblE* and *cblG*, there is normal binding of Cbl to MS enzyme, but a decrease in MeTHF incorporation is observed (5). *cblE* fibroblasts show specific activity of MS under standard conditions equivalent to those of control fibroblasts (55). However, when

the assay is performed under suboptimal reducing conditions, the activity of MS is decreased (55). This suggests that *cblE* class has a putative defect in a MS-associated reducing system. In contrast to control cells, activity of MS in *cblE* fibroblasts is not decreased following N_2O preincubation, indicating that MS is not turning over in *cblE* cells, since a functioning enzyme is required for inactivation by N_2O (55). In contrast to *cblE*, MS activity in *cblG* is reduced even under optimal assay conditions, implying that *cblG* patients have a defect in the MS apoenzyme itself (89). This is further supported by the fact that in *cblG* cells, N_2O induces a moderate inactivation of MS, probably related to a slow catalytic turnover of the enzyme (89). However, Hall et al have shown that in a *cblG* cell line, AdoMet was not able to methylate Cbl (90). High concentrations of AdoMet relieved this impairment suggesting a defect related to the process by which AdoMet primes the enzyme system. Further heterogeneity is observed within the *cblG* class (91). In most *cblG* fibroblasts, there is significant Cbl bound to MS following incubation in labelled Cbl. However, in 3 of 10 cell lines no Cbl binding was found. Moreover, MeTHF incorporation was decreased but not as much as in the other 7 *cblG* where Cbl was associated to MS. The defect in the 3 variant lines is suggested to affect the ability of MS to retain Cbl.

CHAPTER 5

METHYLMALONYL CoA MUTASE (MCM)

5.1 PURIFICATION AND PROPERTIES OF MCM

MCM has been purified to homogeneity using a variety of purification schemes, including column affinity chromatography on DEAE-cellulose, AGMP-1, AdoCbl sepharose, Matrex-gel blue A, hydroxylapatite, and sephadex G-150 or 200 (34,92,93). Isolation of MCM has been reported from the gram-positive bacterium *Propionibacterium shermanii* (94), the actinomycete *Streptomyces cinnamonensis* (95), the intestinal worm *Ascaris lumbricoides* (93), sheep liver (34), human liver (96), and human placenta (92).

5.1.1 Isolation of Mammalian MCM

When human placental purified mammalian MCM was subjected to sodium dodecyl sulfate-polyacrylamide gel electrophoresis, a single band was obtained. Compared to the mobility of standard proteins, the reduced enzyme had a molecular weight of 72 KDa, while the MW of the native MCM was found to be 145 KDa (92). Both X ray fluorescence (92), and spectrophotometry (96) determined that MCM had 2 moles of Cbl bound per mole enzyme. These studies suggest that MCM is a dimer of identical subunits, each of which binds one AdoCbl molecule. The properties of the purified MCM are similar in all the mammalian systems reported (34,92,96).

5.1.2 Isolation of Bacterial MCM

MCM was isolated from *P. shermanii* and its properties were shown to be different from those of previously reported mammalian MCM. Its purified native MCM exhibited a single band of 165 KDa in non-denaturing polyacrylamide-gel electrophoresis, and 2 bands (79 KDa and 67 KDa) of equal intensity in SDS/polyacrylamide-gel electrophoresis (97). The molar ratio of the subunits was constantly 1:1, suggesting that the smaller subunit (beta ß) is not a proteolytic fragment of the larger one (alpha α). Moreover, using sedimentation velocity and low-speed equilibrium ultracentrifugation measurements, the bacterial enzyme was shown to dissociate progressively into its 2 dissimilar subunits (α and ß) with increasing ionic strength (98). MCM from *P. shermanii* thus contains 2 different types of subunits in contrast with mammalian MCM which exists as a dimer of identical subunits.

5.2 CLONING, MAPPING, AND STRUCTURAL CHARACTERIZATION OF MCM

5.2.1 Bacterial MCM

MCM from *P. shermanii* has been obtained in a crystalline form suitable for high resolution X ray diffraction (99), and the structural genes coding for its 2 subunits (α and ß) have been cloned and sequenced using synthetic oligonucleotides as primary hybridization probes (100). The ß subunit (69 KDa) is the product of the upstream gene (Mut A) and consists of 638 aa residues (1914 nucleotides). Mut B gene encodes the α subunit (80 KDa) and is 728 codons in length (2184 nucleotides residues). These 2 genes are

closely linked and their open reading frames lie very close together, with the last G of the C-terminal lysine codon of the Mut A gene being the first base of the Mut B gene, suggesting that the genes are probably transcribed as an operon. Moreover, Mut A and Mut B are transcribed in the same direction. There is very close structural homology and 22% identity between the 2 subunits reflecting the possible duplication of a common ancestral gene.

Similarly to *P. shermanii*, MCM cloned from the actinomycete *Streptomyces cinnamonensis* (95) is comprised of 2 polypeptides encoded by 2 structural genes. The mut A gene consists of 1848 nucleotide residues and encode a 616 aa protein of MW 65 KDa. The mut B gene comprises 733 codons (2199 bp) and encodes a protein of MW 79 KDa. The 2 genes share 29% identity.

5.2.2 Mammalian MCM

To clone the human MCM cDNA, chicken antibodies raised against human placental MCM and ^{125}I-labelled goat anti-chicken IgG were used to screen a human liver cDNA library in lambda gt11 (101). EcoR1 fragments from each clone identified were hybridized to total human liver RNA, and an mRNA species large enough to encode a protein of 72-77 KDa was identified. The authenticity of the corresponding MCM clone was established by gene transfer of the recombinant clone into cultured COS cells. The transformed cells were found to have 3 to 5-fold higher levels of MCM enzymatic activity than did controls. In addition, RNA blot analysis of cells genetically deficient in MCM indicated that several deficient cell lines had a specific decrease in the amount of

hybridizable mRNA to the cDNA probe MCM26b as compared to hybridizable mRNA from control Cbl cell lines. Later, Jansen et al reported the cloning and sequencing of full-length human MCM cDNA (102). The amino acid sequence predicted from the cDNA corresponded to the authentic amino acid sequence of peptide fragments from purified human liver MCM.

The human MCM cDNA comprises 2798 bases, including a 28 base poly A tail (102). The sequence contains a single long open reading frame beginning with a kozak consensus AUG sequence (CCAUG). The MCM gene is transcribed as a 2.8 Kb mRNA which is translated on ribosomes as 750 aa propeptide with a predicted MW of 83 KDa. Sequencing data predicts that human MCM has a mitochondrial leader sequence of 32 aa. Its aa composition is characteristic of mitochondrial matrix leader sequences, namely it is rich in arginine, serine, and leucine, though there is no discernable primary sequence homology. The mature protein of 718 aa is predicted to have a molecular weight of 78 KDa.

The MCM clone has been used as a probe to determine the chromosomal location of the human MCM gene (the MUT locus) (103). DNA from human-Chinese hamster somatic cell hybrids were digested with EcoR1, BamH1, or HindIII and analyzed by southern blot analysis. There was uniform concordance between the presence of restriction fragments representing the human MCM gene and the presence of human chromosome 6 in 5 different hybrid panels. EcoR1 restriction fragments of the humar. MCM locus were identified in cell lines containing portions of chromosome 6. These analyses assigned the locus to region q12-p23 of chromosome 6. In situ hybridization using the MCM26b fragment further localized the locus to the region 6p12-21.1. A highly informative

restriction fragment length polymorphism (HindIII) was identified at the MCM gene locus. This RFLP was used to study the MUT locus linkage relationship to HLA and D6S4 loci on the short arm of chromosome 6 (104). Strong evidence for tight linkage was demonstrated with D6S4 with maximum LOD score (z=22.93) at a recombination fraction of 0.01, and less tight linkage with HLA with Z_{max}= 3.04 at recombination fraction of 0.28.

A single chromosomal locus was suggested for MUT based on the observation that the restriction fragments from somatic cell hybrids could independently be assigned to position 6p12-21.1 (103). Further restriction digest analysis and Southern blots confirmed this and indicated the absence of pseudogenes or homologous genes elsewhere in the genome (105). Ledley et al characterized the structure of the human MCM locus (MUT) which comprises 13 exons spanning 40 Kb of the genome (Fig.5). It exhibits consensus sequences for transcription, splicing, and polyadenylation. The putative promoter region is localized in a GC island 5' to exon I, and was shown to direct expression of a beta-galactosidase reporter gene in cultured cells. It is observed that the first intron occurs within the 5' untranslated region. Moreover, the mitochondrial leader sequence does not represent an independently encoded exon, which is consistent with the genomic structure of other mitochondrial matrix proteins. Exon II encodes the mitochondrial leader sequence and the amino terminus of the mature apoenzyme.

The murine homolog of MUT (Mut) has been localized to mouse chromosome 17E-F by in situ hybridization and linkage studies, where it is syntenic with other loci from human chromosome 6 (HLA and glyoxalase) (106). The murine cDNA comprises 3245 bases, and a single long open reading frame which codes for a protein of 748 aa with a MW

FIG. 5 SCHEMATIC STRUCTURE OF THE HUMAN MUT LOCUS AND MCM cDNA. Reprinted from Ledley (71).

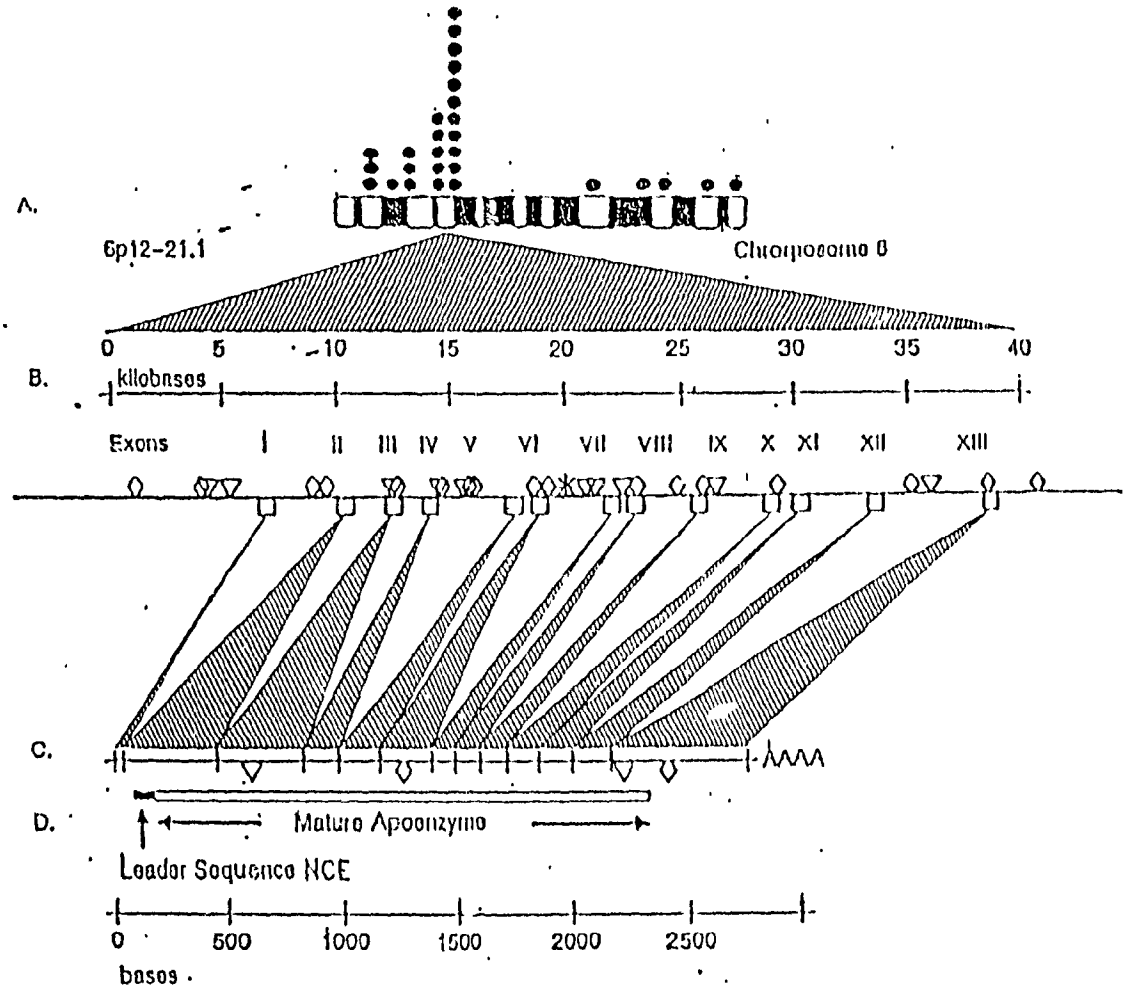
A.
6p12-21.1
Chromosome 6
0
5
10
15
20
25
30
35
40
B.
kilobases
Exons
I
II
III
IV
V
VI
VII
VIII
IX
X
XI
XII
XIII
C.
D.
Mature Apoenzyme
Leader Sequence NCE
0
500
1000
1500
2000
2500
bases

of 82 KDa (107). Transfection of the mouse cDNA into human cultured cells constitutes an active apoenzyme, and can complement genetic deficiency of the apoenzyme in cells from patients with mut MMA.

5.2.2.1 Processing of MCM precursor

In 1983, using cell-free translation system programmed with rat liver RNA, and immunoprecipitation procedures, Fenton et al demonstrated that MCM is synthesized as a precursor peptide 3-4 KDa larger than the mature MCM apoenzyme (108). When the precursor was incubated with intact rat liver mitochondria, it was taken up and processed to yield the mature subunit of 78 KDa localized to the matrix subfraction. This indicates that the MCM precursor is post-translationally processed concomitant with its translocation into the mitochondrial matrix. Moreover, the overall reaction was inhibited by compounds such as dinitrophenol, which disrupt mitochondrial energy metabolism, suggesting that the processing and transport events are energy-dependent. It is assumed that after the translation of the precursor peptide on cytoplasmic ribosomes, it is transported into the mitochondria actively via a receptor-complex present on the mitochondrial membrane, where the leader sequence is cleaved by the mitochondrial processing peptidase and the mature protein is constituted within the mitochondrial matrix (109). The mitochondrial processing peptidase recognizes an octapeptide sequence in the amino terminus of the protein. It has been postulated that the octapeptide functions to supply structural requirements for cleavage between the leader residues and the mature amino terminus.

Mitochondrial matrix proteins are presumed to have been introduced into

eukaryotes during the evolution of endosymbiotic prokaryotes into modern mitochondria. In the process, genes for many proteins, such as MCM were translocated into the nucleus (110). Expression of the nuclear encoded gene in mitochondria evolved by development of sequences for mitochondria targeting. The amino terminus of the mature processed *Homo sapiens* MCM corresponds closely to the position of the amino terminus of the P. shermanii MCM sequences (111). This suggests that the mitochondrial sequence did not evolve by differentiation of amino acids present at the amino terminal end of a prokaryotic protein, but rather by extension of sequences at the 5' end of the reading frame. However, target sequences may also emerge by point mutations or rearrangement within the 5' untranslated region as has been observed with the yeast cytochrome oxidase subunit IV precursor where it has been demonstrated experimentally that randomly juxtaposed sequences can generate mitochondrial targeting sequences under selective pressure (110). This hypothesis is further supported by the lack of any evidence for exon-delimited targeting domains suggesting that the mitochondrial targeting sequence arose from adjacent sequences rather than by exon recruitment.

5.2.3 MCM Homology Among Species

94% homology is observed between human and murine MCM, with the divergence being at the mitochondrial leader sequence, where only 69% of the residues are identical (107).

Comparison of mammalian MCM sequences to the *P. shermanii* bacterial MCM sequences revealed that mammalian MCM (human, murine) exhibits 22%-26%

homology and 57%-60% homology to the Mut A and Mut B sequences from *P. shermanii* respectively (107). In addition, the mut A gene of *S. cinnamonensis* shares 27% and 43% identity to the Mut B and Mut A genes of *P. shermanii*, respectively, 27% identity to human MCM, and 25% identity to murine MCM. The mut B gene of *S. cinnamonensis* shares 72% and 27% identity to the Mut B and Mut A genes of *P.shermanii*, respectively, 63% identity to human MCM, and 61% identity to murine MCM (95).

While there is considerable similarity between bacterial and mammalian sequences, there is also significant differences. In particular, none of the cysteines (8 in mammals, 2 in bacteria) are conserved; cysteine residues are generally the most strictly conserved amino acid.

Despite the evolutionary distance, and the fact that the bacterial MCM catalyses the reverse reaction of the mammalian MCM, the presence of profound sequence similarity between their sequences reflects the homologous evolutionary origin of these proteins and the preservation of critical structure-function determinants for common mechanism of action (111). In addition, the single MCM gene in mammals may have arisen through divergent evolution from its heterodimer bacterial homolog. Alternatively, it may have arisen by divergence from one bacterial gene, with duplication and divergence of the second bacterial copy subsequent to separation of bacterial and eukaryotic lines or bacterial and mitochondrial lines.

5.3 MCM APOENZYME DEFICIENCY (*mut*)

5.3.1 Classification into the *mut* Group

An inherited disorder affecting methylmalonyl CoA metabolism is suspected on the basis of methylmalonic aciduria (or acidemia) in the presence or absence of homocystinuria and megaloblastic anemia (see section 4.2.1) (84). Biochemical studies and cell cultures techniques are employed to precisely identify the disorder involved (64).

The uptake and intracellular distribution of vitamin B_{12} is determined by incubating the cells for 96 hrs in the presence of medium containing 25 pg/ml (18pM) [^{57}Co]-CN-Cbl bound to human serum as a source of TCII (82). The intracellular Cbls are then extracted into hot ethanol and separated by high performance liquid chromatography. Cbl-dependent enzyme activity can be indirectly and independently assayed in cell extracts grown in medium with and without added exogenous Cbl (82). MCM activity can be measured indirectly by measuring the incorporation of labelled propionate into acid precipitable material, while MS activity can be measured by measuring the incorporation of labelled MeTHF (84).

Cell complementation analysis is employed to further define the phenotype of a cell line (84). Equal numbers of cultured fibroblasts from different patients are co-incubated in the presence or absence of PEG, an agent which induces cell fusion. If cell fusion results in increased uptake of either propionate and/or MeTHF, then the cell lines belong to different complementation classes, implying mutations at distinct genetic loci.

MMA without homocystinuria is the clinical characteristic of MCM apoenzyme deficiency. In *mut* class, the cells demonstrate low [^{14}C]-propionate uptake (see Table 3).

[^{14}C]-MeTHF and [^{57}Co]-CNCbl uptake fall within the normal range, and there is adequate synthesis of AdoCbl and MeCbl, although occasionally AdoCbl may be relatively low.

Recently, it became feasible to distinguish the *mut* and *cbl* forms by DNA-mediated gene transfer which is a variation of the classical complementation procedure (112). MCM cDNA clone transferred into *mut* fibroblasts restored the activity of the methylmalonyl CoA (succinyl CoA) pathway measured by metabolism of [^{14}C] propionate in culture. Identical gene transfers into *cbl* fibroblasts did not result in an increase in propionate incorporation. The results of gene transfer correlated with those of classical somatic cell complementation and biochemical methods.

5.3.2 *mut* Subclasses

Mutase apoenzyme defect is classically sub-divided into two groups designated *mut*^{0} and *mut*$^{-}$ on the basis of residual mutase activity.

5.3.2.1 *mut*$^{-}$ cell lines

mut^{-} cell lines exhibit residual enzyme activity in cell extracts when assayed with high concentration of AdoCbl (113). In these extracts, the mutant apoenzyme retain maximally 0.5%-50% of control activity. Incubation of *mut*$^{-}$ cells in elevated concentrations of OH-Cbl has been shown to result in an increase in MCM activity as measured by [^{14}C]-propionate incorporation, although the level remains well below that in controls. *mut*$^{-}$ patients, however, do not respond clinically to Cbl therapy (113). Different levels of basal mutase activity have been observed among the *mut*$^{-}$ cells reflecting biochemical

heterogeneity. MCM from *mut*$^-$ fibroblasts has a Km for the cofactor AdoCbl that is 200-5000 times that of controls (113-115), but a normal Km for the substrate methylmalonyl CoA. These data suggest that the mutase apoenzyme is structurally abnormal leading to a reduced affinity for the cofactor. In addition, MCM from *mut*$^-$ cells exhibit increased thermolability relative to control enzyme. Using radioimmunoassay, the amount of cross reacting material (CRM) detected ranged from 20%-100% of control (116). All *mut*$^-$ cells exhibit normal mRNA levels (117).

5.3.2.2 *mut*^{0} cell lines

The *mut*^{0} subclass constitutes about 2/3 of the *mut* complementation group. Mutase activity in extracts of cultured fibroblasts is undetectable (<0.1% of control) even when assayed in the presence of AdoCbl concentrations greatly in excess of that normally required to saturate the enzyme (113). In addition, intact *mut*^{0} cells do not respond to OH-Cbl supplementation (113). Northern blot analysis revealed that some *mut*^{0} cell lines have decreased levels of MCM mRNA, suggesting that the primary defect involves transcription, processing or stability of mRNA (117). It is estimated that in Caucasian and African-American patients at least 25% of mutations in the *mut*^{0} class express this low message phenotype. Ogasawara et al (118) recently reported that undetectable mRNA levels is present in 13 of 16 mutant alleles (81%) of Japanese patients. Radioimmunoassay revealed no immunologically cross reactive mutase protein in the extracts of some *mut*^{0} cell lines, while others demonstrated CRM levels ranging from 3%-40% of controls (116). *mut*^{0} cells were further pulse labelled to determine how amounts of newly synthesized mutase protein

detected by specific immunoprecipitation compared with the CRM values (119). All of the *mut*^{0} cell lines that displayed CRM had detectable newly synthesized mutase. Of the CRM negative *mut*^{0} lines, 50% showed no detectable amounts of MCM; the other 50% had amounts of newly synthesizes mutase ranging from barely detectable to nearly half of that seen in controls, suggesting mutations which lead to the synthesis of unstable mutase protein rapidly degraded intracellularly. This reflects the considerable phenotypic heterogeneity within the *mut*^{0} subclass. Thus, the absence of enzyme activity in *mut*^{0} cells can be accounted for by the absence of protein synthesis, the presence of an abnormal or unstable protein, or by the presence of an apparently normal immunoreactive protein that is inactive because of a mutation.

In addition to the heterogeneity observed at the molecular level within the *mut* subclasses, phenotypic pleomorphism in *mut*^{0} and *mut*$^-$ is prevalent. *mut*$^-$ patients present with onset of illness later in infancy or childhood than *mut*^{0} patients and symptoms of intermittent severity (120). Phenotypic variability is clinically evident in this biochemical subclass, with patients exhibiting normal to severe neurological dysfunction, with or without episodic acidosis. The level of enzyme activity within this subclass was not found to be directly predictive of clinical outcome (120). In contrast, *mut*^{0} patients present with profound neonatal illness and have poor prognosis with high mortality. The survivors have significant growth and mental retardation (120). The observed neurological dysfunction in *mut*$^-$ and *mut*^{0} patients is thought to be caused by the accumulation of methylmalonic acid, which is a potential toxin, or secondary acidosis, ketosis, hyperammonemia, and hypoglycaemia (71).

Because pairwise crosses between *mut*^{0} and *mut*$^-$ generally yield noncomplementing heterokaryons and because of the observed codominant expression of *mut*^{0} and *mut*$^-$ alleles (121), it is accepted that both mutant types (*mut*^{0} and *mut*$^-$) reflect abnormalities of the locus coding for the mutase structural gene (113). The identification of mutations within the mutase gene that lead to the absent (*mut*^{0}) or abnormal enzyme kinetics (*mut*$^-$) have firmly established that these phenotypes are allelic mutations at the MUT locus (113).

Southern blot analysis using MCM cDNA as a probe revealed HindIII and TaqI polymorphisms at the MUT locus in *mut*^{0} and *mut*$^-$ lines (117). However, no distinct relationship to *mut* phenotypes could be established because of the small sample size studied.

5.3.3 Mutations at the MUT Locus

The *mut* class is characterized by mutations at the MUT locus, resulting in defects of the MCM apoenzyme (121). Molecular cloning of MCM permitted genetic analysis of mutations that underlie *mut* MMA. Southern blot analysis has failed to identify any gross abnormalities at the MUT locus, indicating that the majority of the mutations are point mutations, or small deletions or insertions (122). Since the majority of *mut*^{0} cells and all *mut*$^-$ cells express normal mRNA, most of the defects are assumed to be mutations within the open reading frame. Eighteen distinct mutations underlying the *mut* phenotype have been identified, all of which are point mutations (Table 1).

TABLE 1 LIST OF MUTATIONS IN HUMAN MCM. AA= amino acid; HMZ-DNA= homozygous mutation detected at the DNA (genomic) level; HTZcDNA= heterozygous mutation detected in cDNA; REF= references; PM= DNA polymorphism; percom= personal communication with Dr. Wayne Fenton (Yale University); X= stop codon; FrSh= frameshift.

TABLE 1 LIST OF MUTATIONS IN HUMAN MCM

AA CHANGE	BASE CHANGE	EXON	CELL LINE	*mut*$^{0/-}$	HMZ/HTZ	REF
Q13X	C_{128}->T	II	FB 552	*mut*^{0}	HTZ-DNA	123
E84X	G_{326}->T	II	-------	*mut*^{0}	-------	118
R93H	G_{354}->A	II	WG 1130	*mut*^{0}	HMZ-DNA	1
G94V	G_{357}->T	II	515	*mut*$^{-}$	HTZcDNA	percom
W105R	T_{389}->C	II	WG 1607	*mut*^{0}	HTZcDNA	124
E117X	G_{425}->T	II	347	*mut*^{0}	HMZ-DNA	118
Y231N	T_{767}->A	III	WG 1600	*mut*$^{-}$	HMZcDNA	percom
$FrSh_{231}$->X_{508}	Delete CA_{769}	III	359	*mut*^{0}	HTZ-DNA	118
R369H	G_{1182}->A	VI	WG 1599	*mut*$^{-}$	HTZcDNA	percom
A377E	C_{1206}->A	VI	WG 1607	*mut*^{0}	HTZcDNA	124
G623R	G_{1943}->A	XI	WG 1681	*mut*^{0}	HTZcDNA	126
G626C	G_{1952}->A	XI	STI	*mut*$^{-}$	HTZ-DNA	127
G630E	G_{1965}->A	XI	WG 1609	*mut*^{0}	HMZ-DNA	127
G648D	G_{2019}->A	XI	CHO	*mut*$^{-}$	HTZ-DNA	127
H678R	A_{2109}->G	XII	WG 1511	*mut*$^{-}$	HMZcDNA	percom
R694W	C_{2156}->T	XII	MM 87	*mut*$^{-}$	HMZ-DNA	127
G703R	G_{2183}->C	XII	WG 1681	*mut*^{0}	HTZcDNA	126
G717V	G_{2226}->T	XIII	WG 1610 WG 1611 WG 1613	*mut*$^{-}$ *mut*$^{-}$ *mut*$^{-}$	HMZ-DNA HTZ-DNA HMZ-DNA	125 125 125
H532R (PM)	A_{1671}->G	IX	WG 1511 WG 1599 WG 1610 WG 1611 WG 1613 WG 1681 CHO MM 87	*mut*$^{-}$ *mut*$^{-}$ *mut*$^{-}$ *mut*$^{-}$ *mut*$^{-}$ *mut*^{0} *mut*$^{-}$ *mut*$^{-}$	HMZcDNA HTZcDNA HMZ-DNA HMZ-DNA HMZ-DNA HMZcDNA HTZ-DNA HMZ-DNA	percom percom 125 125 125 126 127 127
V671I (PM)	G_{2087}->A	XII	WG 1610 WG 1611 WG 1613 WG 1681 WG 1511 WG 1599 CHO MM 87	*mut*$^{-}$ *mut*$^{-}$ *mut*$^{-}$ *mut*^{0} *mut*$^{-}$ *mut*$^{-}$ *mut*$^{-}$ *mut*$^{-}$	HMZ-DNA HMZ-DNA HMZ-DNA HMZcDNA HMZcDNA HTZcDNA HTZ-DNA HMZ-DNA	125 125 125 126 percom percom 127 127

Figure 6 describes the position of these mutations. The effect of each of these mutations on the activity of the enzyme has been assayed by gene transfer of expression vectors bearing single mutations into MCM-deficient fibroblasts, or overexpression of the mutant enzyme in *S. cerevisiae*. *S.cerevisiae* does not have endogenous MCM and does not produce AdoCbl, so that the recombinant MCM produced in this organism is entirely apoenzyme.

An amber mutation (C_{128}->T), identified in cDNA from the FB552 *mut*^{0} cell line, prematurely terminates translation at codon 18 within the mitochondrial leader sequence. This yields an abbreviated and unstable gene product that can not be targeted to the mitochondria, hence the *mut*^{0} phenotype (123). The immunoreactive protein produced by these cells reflects translation from an internal initiation codon downstream from the termination codon created by the mutation, and therefore lacks a mitochondrial leader peptide. Although only one cDNA species was cloned from this cell line, analysis of genomic DNA indicates that this cell line is heterozygous for the C_{128} mutation and a polymorphic HindIII site, suggesting that the heterologous allele is not represented in the mRNA.

Compound heterozygous mutations were identified in the cDNA from a *mut*^{0} fibroblast cell line, WG 1607, and the pathogenicity of the observed changes was confirmed by DNA-mediated gene transfer (124). The first mutation results in a change from the non-polar tryptophan to the basic arginine at amino acid position 105 (W105R). The second mutation, which results in a A377E change, falls within a strongly hydrophobic segment and inserts the positively charged glutamine in place of hydrophobic alanine, thus altering

FIG. 6 **MUTATIONS IDENTIFIED IN *mut* MMA.** The positions of mutations identified are shown along the protein. Letters represent amino acid change. Mutations causing *mut*^{0} phenotype are represented above the line, while those causing *mut*$^{-}$ phenotype are represented below the line. FR=frameshift; X=stop codon. The figure is not drawn to scale.

MUTATIONS OF HUMAN MCM

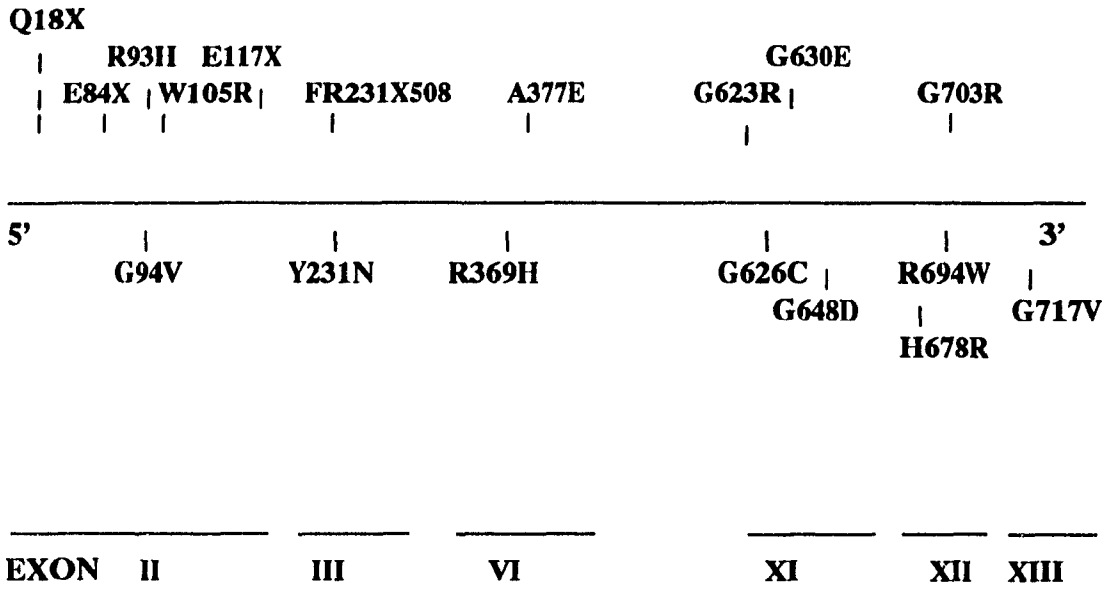

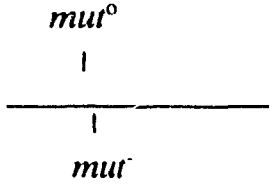

secondary and tertiary structures of the segment. Both mutations alter evolutionary conserved amino acid.

A mutation which substitutes valine for glycine at amino acid position 717 (G717V) is present in 4 *mut*$^-$ cell lines, three of which (WG 1610, WG 1611, WG 1613) are derived from unrelated patients of African-American origin (125). All three patients exhibited similar clinical course, which was intermediate between the fulminant and the benign forms of MMA, suggesting that this phenotype is the specific consequence of the G717V mutation (phenotype-genotype relationship). WG 1610 and WG 1613 patients are homozygous for the G717V mutation, while WG 1611 is heterozygous for the same mutation and an allele that does not produce detectable mRNA. In addition, two additional homozygous changes (H532R and V671I), characterized as polymorphisms by expression studies, were identified in these three patients. G717V alters an amino acid conserved between mammalian and bacterial MCM, and the change is assumed to disrupt protein folding by introducing an additional alpha-helix rotation in the carboxy terminus of the protein (125).

A R93H mutation was identified in a *mut*^{0} cell line, WG 1130, which participates extensively in interallelic complementation (1). For more details, refer to section 5.3.4.

Recently, cDNA from a *mut*^{0} fibroblast cell line, WG 1681, from an African-American male infant, was cloned and sequenced in Dr. D.S. Rosenblatt's laboratory at

McGill University (126). Compound heterozygosity was demonstrated for two novel changes at highly conserved sites: G623R and G703R. Expression studies demonstrated that the two heterozygous changes are pathogenic *mut*^{0} mutations. In addition, two homozygous polymorphisms (H532R and V671I), previously described in three unrelated African-American patients (125), were found. The G623R and G703R changes result in the substitution of large basic residues for small hydrophobic amino acids near the carboxy terminus of the MCM polypeptide.

Very recently, Crane and Ledley reported cloning and sequencing DNA from four *mut* cell lines (127). STI and CHO, two *mut*$^{-}$ cell lines, were found to be heterozygous for G626C and G648D respectively. The second allele in both lines is not expressed. WG 1609 (REG), a *mut*^{0} line, and MM87, a *mut*$^{-}$ line, were found to be homozygous for G630E and R694W respectively.

Ogasawara et al (118) identified two novel mutations in MCM in cells from two *mut*^{0} Japanese patients assumed to cause the low mRNA phenotype observed in those cells. The first patient (#347) has the homozygous E117X mutation, and the second patient (#359) has the heterozygous E117X and a frameshift mutation at amino acid 231 causing a premature termination at codon 508. Both mutation would produce truncated non-functional polypeptides. Moreover, the E117X mutation was identified in six of sixteen Japanese patients, suggesting a relatively high incidence of the mutation among Japanese patients (118).

The rest of the mutations described here have been conveyed through personal communication with Dr. Wayne Fenton (Yale University) and have not been published. All of them give rise to *mut*$^-$ phenotype and have been identified only at the cDNA level. H678R identified in WG 1511 and Y231N in WG 1600 are homozygous mutations, while G94V, identified in cell line 515, and R369H, in WG 1599, are heterozygous changes. The mutations in the second alleles have not been identified.

5.3.4 Interallelic Complementation in *mut* MMA

My research project is based on the observation that WG 1130 cell line from a patient with *mut*^{0} MMA exhibited unusual complementation phenotype when cell fusion complementation analysis were performed with WG 1130 and a series of cultured fibroblast lines representing the *cbl*A, *cbl*B and *mut* complementation classes (1). As expected 1130 complemented with *cbl*A and *cbl*B cell lines. However, complementation was also observed with three of nine *mut*^{0} cell lines and four of five *mut*$^-$ cell lines. Since there is a single locus for the gene encoding mutase, constitution of the activity in the heterokaryons must occur by means of interallelic (intragenic) complementation. Interallelic complementation involves the interaction of differently altered polypeptide chains in the same multimeric protein to produce a functional hybrid protein molecule. The mechanism of such complementation was discussed by Crick and Orgel who suggested that restoration of function might be due to the correction of defect in one monomer by some unaltered part of the other (128). The MCM

cDNA from WG 1130 was cloned and sequenced and was found to contain a homozygous G_{354}->A (R93H) mutation, which was later confirmed to be homozygous at the genomic level (129). Expression vectors carrying MCM with the R93H change expressed no enzymatic activity when introduced into cells with low mRNA phenotype, compared to transfection with wild type MCM vector which restored the activity. These expression studies confirmed that R93H is the pathogenic mutation (129). Cotransfection studies in which clones bearing the R93H change are introduced into cells together with vectors expressing mutations identified in *mut*^{0} or *mut*$^-$ cells that complemented with WG 1130 demonstrated that complementation between R93H and these mutations occurred at the molecular level. These results point to further heterogeneity within both *mut*^{0} and *mut*$^-$ and enable identification of mutations affecting discrete components of apoenzyme function. So far, WG 1130 is found to complement 5 of 15 *mut*^{0} lines and 7 of 9 *mut*$^-$ lines (Table 2).

My research plan was to conduct fusions among the *mut* cell lines available to me to look for somatic cell complementation, and screen for mutations using PCR-SSCP analysis. Because of the large number of *mut* cells available to me, I concentrated on 13 cell lines, in seven of which mutations are already characterized, in order to correlate the position of mutations and the ability to complement other mutations with the structure of the protein.

The overall purpose of these experiments is to provide a pattern for grouping the mutations according to the complementation data in defined domains in order to get a

clearer understanding of the important structural domains of MCM, and be able to make correlation between genotype and phenotype.

TABLE 2 COMPLEMENTATION PATTERN OF *mut* CELL LINES WITH WG 1130. + = the cell lines complement each other;

- = the cell lines do not complement each other.

TABLE 2

COMPLEMENTATION PATTERNS OF *mut*$^-$ CELL LINES WITH WG 1130

mut$^-$ cell lines	
WG 1511	+
WG 1562	+
WG 1610	+
WG 1611	+
WG 1613	+
WG 1738	+
WG 1919	+
WG 1599	-
WG 1618	-

COMPLEMENTATION PATTERN OF *mut*^{o} CELL LINES WITH WG 1130

mut^o cell lines	
WG 1517	+
WG 1601	+
WG 1609	+
WG 1681	+
WG 1713	+
WG 1510	-
WG 1512	-
WG 1602	-
WG 1607	-
WG 1608	-
WG 1612	-
WG 1727	-
WG 1864	-
WG 2041	-
WG 2077	-

CHAPTER 6

MATERIALS AND METHODS

6.1 CLINICAL HISTORY OF *mut* PATIENTS

The classification of cell lines from patients in a particular group (*cbl*A-G, *mut*) is based initially on clinical presentation (84). Measurements of cellular Cbl uptake, cofactor distribution, and uptake of labelled propionate and labelled MeTHF in cultured fibroblasts provide confirmation of the defect (64). A definite diagnosis is then made by complementation analysis studies using a panel of cells with known disorders (84).

If a cell line falls in the *mut* complementation group, then the propionate incorporation assay is used to further subdivide it into the *mut*$^-$ or *mut*^{0} class. This is done by assaying propionate incorporation in cultured cells in the presence of increasing amounts of exogenous OH-Cbl (113). *mut*$^-$ cells exhibit decreased activity in the presence of added Cbl (Table 4); *mut*^{0} cells exhibit no change in activity with added Cbl (Table 3).

6.1.1 *mut*^{0} Patients

The fibroblast cell line WG 1130 is from a French Canadian female who was diagnosed with MMA in the first week of life (1). She had recurrent vomiting, dehydration, metabolic episodes, and died at 5 months of age. Because of the unresponsiveness to OH-Cbl in the culture medium, she was classified in the *mut*^{0} subclass (Table 3).

TABLE 3 PROPIONATE UPTAKE OF muto CELL LINES. Growing cells were incubated in [1-^{14}C] propionate containing-media for 18 hours with and without PEG. Cellular macromolecules were precipitated with 5% trichloroacetic acid, and cells were dissolved in 0.2N NAOH. Propionate incorporation was determined from levels of radioactivity and related to total cellular protein determined by the Lowry method (130).

TABLE 3 PROPIONATE UPTAKE OF *mut*^{0} CELL LINES

CELL LINE	[^{14}C]PROPIONATE UPTAKE (nmole/mg protein/18h)	
	without OH-Cbl	with OH-Cbl
MCH 24 (Control)	18.0	18.0
WG 1130	0.57	0.40
WG 1681	1.1	0.85
WG 1713	1.4	1.6
WG 1727	1.5	1.3
WG 2041	2.0	2.0

WG 1607 was diagnosed with MMA following his readmission to the hospital at 36 hours of age with respiratory distress (124). He exhibited organic acidemia, hyperammonemia, and neutropenia. The patient died at one and a half years of age during a recurrent episode of metabolic acidosis. The cell line has been shown to express the *mut*^{0} phenotype.

The fibroblast cell line WG 1609 is from a Danish female who was diagnosed with MMA in the first week of life. She died at age one and a half years. Cultured cells from WG 1609 were defined to have a *mut*^{0} phenotype.

WG 1681 is a well characterized *mut*^{0} cell line from a male infant of African-American origin with no family history of MMA (Table 3) (126). He was diagnosed with MMA in the first week of life after showing symptoms of lethargy, hyperammonemia, and acidosis. He had several readmissions due to acidosis, and at 3 1/2 years of age he had an approximate 6 months delay in his verbal and fine motor development.

WG 1713 is *mut*^{0} cell line from a male Hispanic patient who was extremely sick at 10 days with acidosis, lethargy, vomiting, high blood ammonia, and seizure (Table 3). He was shown to have MMA, microcephaly, cerebral edema, global retardation, and severe developmental delay with slow progress.

WG 1727 developed a duodenal ulcer at the age of 6 years, and underwent

a partial gastrectomy. From age 8 on, he continued to have intermittent episodes of elevated levels of methylmalonic acid. Fibroblasts from WG 1727 fall into the *mut*^{0} class (Table 3).

WG 2041 fibroblasts are from a Hispanic patient with MMA who presented in the first week of life with acidosis, neonatal coma, hyperammonemia, and very high levels of methylmalonic acid in the urine. WG 2041 was defined to have a *mut*^{0} phenotype (Table 3).

6.1.2 *mut*$^-$ Patients

Complementation analysis and assay of propionate incorporation in WG 1599 and WG 1511 cultured cells with increasing amounts of OH-Cbl demonstrated that these patients fall into the *mut*$^-$ class. No clinical information is available for these two cell lines.

WG 1610 is a well characterized *mut*$^-$ cell line from a black patient who was diagnosed with MMA at the age of 3 years (125). On evaluation, he had metabolic acidosis and hyperammonemia. He has had several readmissions for episodes of metabolic imbalance.

WG 1618 is a caucasian female who presented at the age of 4 years with ketoacidosis and hyperammonemia (131). She was diagnosed with MMA, though her presentation was not very characteristic. The majority of children with MMA are identified at a younger age then WG 1618 when they present in metabolic crisis, and their urine MMA

level is usually higher than this patient's. This patient has an unusually mild *mut*$^-$ defect, and the cells show a higher propionate uptake level than other *mut* patients (Table 4).

WG 1738 is an Irish/Italian patient who presented at 5 years with MMA excretion in the urine and an atypical clinical finding in that he never had an acidotic episode. He is mentally retarded and has autistic behaviour. His fibroblasts fall into the *mut*$^-$ class (Table 4).

The patient WG 1919 is a white female who had basal ganglia stroke at 10 months and was diagnosed with MMA. She recovered well and was found to be developmentally normal. This patient is classified into the *mut*$^-$ category (Table 4).

6.2 CELL CULTURE

Control (MCH 24) and patient skin fibroblasts were obtained from the Repository for Mutant Human Cells at the Montreal Children's Hospital (Montreal, Que.), and were determined to be free from mycoplasma contamination. Cultures were grown as a monolayer in 175 cm^2 flasks (Falcon, Oxnard, CA) and maintained in 30 ml of Eagles' minimum essential medium (MEM) with Earle's salts, L-glutamine, and non-essential amino acids (Flow Laboratories, Mississuaga, Ont.), supplemented with 10% (v/v) fetal bovine serum (FBS) (Gibco Laboratories, Grand Island, N.Y.). The cell cultures were kept in incubators at 37°C in an atmosphere of 5% CO_2, 95% O_2, and 86% humidity.

TABLE 4 PROPIONATE UPTAKE OF *mut*$^-$ CELL LINES. Growing cells were incubated in [1-^{14}C] propionate-containing media for 18 hours with and without PEG. Cellular macromolecules were precipitated with 5% trichloroacetic acid and cells were dissolved in 0.2N NAOH. Propionate incorporation was determined from levels of radioactivity and related to total cellular protein determined by the Lowry method (130).

TABLE 4 PROPIONATE UPTAKE OF *mut*⁻ CELL LINES

CELL LINE	[^{14}C]PROPIONATE UPTAKE (nmole/mg protein/18h)	
	without OH-Cbl	with OH-Cbl
MCH 24 (Control)	18.0	18.0
WG 1618	2.9	6.8
WG 1738	2.8	7.0
WG 1919	0.72	1.3

6.3 CELL FUSION COMPLEMENTATION ANALYSIS

Fibroblasts cultured from the thirteen unrelated patients (6 *mut*$^-$, 7 *mut*^{0}) were fused in all possible pairwise combinations and MCM activity was assayed in the heterokaryons by measuring the incorporation of ^{14}C from [1-^{14}C] propionate (New England Nuclear; Boston, MA) into high molecular weight acid precipitable material. This provides an indirect measure of MCM activity in intact cells. [^{14}C]-propionate is incorporated into protein following its conversion to succinyl CoA by MCM and to amino acids via the TCA cycle.

Cells to be tested were seeded into 35mm Falcon tissue culture dishes at a density of 400,000 cells per dish. Mixed cultures consisted of 200,000 cells from each of two cell lines. 24 hours after the cultures had been plated, 1 ml of a 40% solution of polyethylene glycol-1000 (PEG) (J.T. Baker Chemical Co.; Phillipsburg, NJ) in phosphate-buffered saline (pH 7.4) (PBS) was applied for 60 seconds to the cellular monolayer in the plates to be fused to induce cell fusion. The PEG was removed and the cultures extensively washed with serum-free MEM, then incubated with MEM supplemented with 10% FBS. The following day, the ability of cultures to incorporate label from [1-^{14}C]-propionate into acid precipitable material was assayed. Medium was replaced with Puck's F medium supplemented with 15% fetal bovine serum and 100μM [1-^{14}C]-propionate (diluted with 0.01 M unlabelled propionate to give a specific activity of 10μCi/μmol), and cultures were incubated for 18 hours. At the end of this time, the medium was removed, and the cultures were rinsed three times with cold PBS. Cold 5% trichloroacetic acid (TCA) was then added to precipitate macromolecules, and the plates were incubated for 15 min. at 4°C. After two

additional washes with 5% TCA, the precipitate was dissolved in 1 ml of 0.2N NAOH overnight. Radioactivity of an aliquot (700 μl) was determined by liquid scintillation counting in a Beckman 5801 liquid scintillation counter (Mississauga,Ont.), and related to total cell protein determined by Lowry method (130). The uptake was expressed as nmol propionate incorporation/mg protein/ 18 hours. All values were the means of triplicate determinations.

The mean of propionate uptake of the fused and unfused groups was compared. If a stimulation of [^{14}C]-propionate incorporation has occurred in the PEG treated group (as compared to the parallel cultures that had not been exposed to PEG), intragenic complementation was assumed to have occurred. If there was no increase in propionate incorporation, no intragenic complementation was assumed to have occurred. It has been shown previously that the exposure of unmixed cultures of each individual cell line to PEG for 60 seconds does not cause stimulation of propionate uptake (132).

The fusion of *mut* cell lines with fibroblasts from other complementation groups known to be defective in other genes (*cblA* or *cblB*) served as positive controls in the experiments; the propionate uptake of a control cell line (MCH 24) was also recorded. A set of triplicate blank dishes (no cells) were included in each experiment.

6.3.1 Statistical Analysis of Complementation

All data of crossed *mut* pairs were statistically evaluated using student's *t* test analysis. All *p* values are one-tailed and compare fused with unfused combinations of cell lines. Complementation is indicated by an increase in propionate uptake in mixed fused cultures relative to mixed unfused cultures ($p<0.05$). Variation is expressed as the standard

deviation of the mean.

6.4 MUTATION DETECTION

6.4.1 DNA Extraction

Fibroblasts from the control (MCH 24) and 37 *mut* patients, of which approximately two thirds are *mut*^{0} and one third *mut*$^-$, were harvested from 175 cm^2 tissue cultures flasks by trypsinization, and washed and centrifuged three times at 1500 rpm for 10 min. at room temperature in an IEC HN-S centrifuge (Needham, Mass.) for collection. Between each centrifugation, the pellet was resuspended in PBS buffer. The cell pellet was resuspended in 500μl PBS and centrifuged at 14,000 rpm for 5 min. at 4°C in a Brinkmann 5415 Eppendrof centrifuge (Westbury, N.Y.). The pellet was then gently resuspended in 350μl of solution A (1mM Tris pH 8, 1mM EDTA, 1mM NaCl), and 350μl of solution B (solution A, 2% SDS), and proteinase K (0.25 mg/μl) were sequentially added. The cellular solution was incubated for 3 hours at 37°C. DNA was then extracted once with equal volumes of Tris-phenol (Maniatis, et al., 1989), once with phenol:chloroform (1:1), and once with TE:chloroform (1:1). 1/25 volume of 5M NaCl and 2 volumes of cold absolute ethanol were added to precipitate the DNA, which was then resuspended overnight in sterile water. Concentration of the DNA solution was determined by measuring the absorbance at 260nm in a Beckmann DU-64 spectrophotometer (Fullerton, CA.), and DNA quality was assessed by the 260nm/280nm ratio.

6.4.2 Genomic Polymerase Chain Reaction (PCR)

Primers within the flanking introns were designed using OLIGO Primer Analysis Software (National BioSciences) (Table 5). Genomic DNA was amplified using oligonucleotides specific for exons 9 (262 bp), exon 11 (318 bp), and exon 12 (274 bp). The reaction mixture of 50μl consisted of 0.5μg DNA, 1μM of each 5' and 3' primers, 200μM of each dNTP (dATP, dGTP, dCTP, dTTP), 1X Perkin Elmer Cetus reaction buffer (10mM Tris-HCl pH 8.3, 50mM KCL, 1.5mM $MgCl_2$, 0.01% w/v gelatin), and 2U Taq polymerase (Pharmacia) or 2U Amplitaq (Perkin Elmer Cetus). Samples overlaid with 50μl mineral oil were amplified in a Diamed Coy thermal cycler (Missisuaga, Ont.). Following incubation at 94°C for 4 min., each amplification consisted of 30 cycles of denaturation at 94°C for 1 minute, annealing temperature for 1.5 minutes, and extension at 72°C for 1.5 minutes. A final extension was performed at 72°C for 10 min. The primer sequences and annealing temperatures are described in Table 4. Because of the non-specific bands in exon 9, the amplification was modified according to Yap and McGee (133). 10 cycles of amplification were performed as described above, followed by an additional 30 cycles using a denaturation temperature of 88°C for 1 minute. Amplification was confirmed by electrophoresing 5μl of PCR product on a 1% agarose gel in 1X TAE buffer and 0.1μg/ml ethidium bromide. The amplified fragments were confirmed to be of the correct size by their position compared to the DNA Lambda HindIII marker fragment (0.1 μg/μl).

TABLE 5 SEQUENCES OF PRIMERS USED FOR GENOMIC PCR AND DIRECT SEQUENCING.

TABLE 5 GENOMIC PCR AND DIRECT SEQUENCING PRIMERS

EXON	PRIMER#	SEQUENCE	ANNEAL TEMP.
9	9-1	5'CCTTTCCTTGACTTTTTC 3'	51°C
	9-2*	5'TGCCATTACCCTCTTTTG 3'	
11	11-1	5'ACTTGAAGATTTGCTGTG 3'	48°C
	11-2*	5'TGCTGTCATCATTTTACTAC 3'	
12	12-1	5'CAGGGTTTTTATAGTCATTA 3'	50°C
	12-2*	5'CAAGATTCCCATCACAGT 3'	

* denotes antisense primer

6.4.3 PCR-based Single Stranded Conformation Polymorphism (PCR-SSCP) Analysis

Gene mutations of PCR amplified exons 9, 11, and 12 were detected using PCR-SSCP analysis (134). These 3 exons were targeted for SSCP analysis because each contained known mutations or polymorphisms. PCR reactions and PCR-SSCP analysis were performed in association with two summer students, Brian Hershenfield and Adrian Chan. The protocol followed involved denaturing 10-20μl of PCR product with 0.5M NaOH/10mM Na_2EDTA (pH 8) solution (1 vol:10 vol). The mixture was heated at 42°C for 5 min. then placed on wet ice. Prior to loading, 98% deionized formamide/0.025% bromophenol blue/0.025% xylene cyanol/10 mM Na_2EDTA (1 vol:11 vol) was added to the mixture. The formamide was deionized using ion-exchange Sephadex AG-501-X8D mixed- bed resin (BioRad). Denatured samples were loaded onto a Bio-Rad Protean II 0.75mm x 20cm x 20cm gel of 7.5% polyacrylamide [30% acrylamide (29:1)], 5% glycerol, and 0.5X TBE. Electrophoresis was performed at room temperature with internal cold water circulation in 0.5X TBE running buffer at maximum power and current for 4,800 Volts-Hour (Bio-Rad 500/200 and Fisher Scientific FB703). Gels were stained for 45 minutes in 500 ml of 0.5X TBE running buffer containing 750μl of 1mg/ml ethidium bromide (0.5-1.5μg/ml), and photographed under UV illumination.

CHAPTER 7

RESULTS

7.1 SOMATIC CELLS COMPLEMENTATION ANALYSIS

Complementation analysis was performed on 13 *mut* cell lines. The design of each experiment was to test each MCM-deficient line in 2 different fusions:

1. fusions between *mut* strains in all possible pairwise combinations.

2. fusions of *mut* strains with fibroblasts from patients with a genetically distinct disorder (*cblA* or *CblB*) with which all the mut lines are expected to complement (intergenic complementation). These fusions act as a positive control to assure that the procedures were working properly. In addition, such positive control fusions run in parallel with the test fusions provide a measure of the upper limit of the incorporation that could be expected of complementing MCM mutants.

The criterion for complementation in each experiment was that complementation between a pair of *mut* strains was tentatively inferred if the propionate incorporation of mixed fused fibroblast cultures was greater than the propionate incorporation of untreated, but otherwise identical mixtures of mutant cells. Two strains were said to complement definitively if the statistical analysis of the data showed propionate incorporation in the fused to be significantly greater than the unfused ($p<0.05$).

Complementation experiments were generally done only once unless propionate uptake value of the mixing of two cell lines without fusion was more then 25% higher or lower then the value expected from a 1:1 mixing without fusion.

Figure 7 summarizes the data of the fusions in a complementation panel. Extensive intragenic complementation was observed in fusions involving twelve of the thirteen *mut* strains crossed. Among seventy-eight different pairwise crosses, twenty-two showed intragenic complementation. Complementation analysis data between the *mut* lines are presented in Table 6. Numbers indicate the mean of propionate incorporation of triplicate determinations ± standard deviation. The results were reproducible. Thus, if the same two cell lines are fused on seperate days, the values are reproducible.

Each mutant strain incorporated low amounts of radioactivity compared to control strain MCH 24 (Table 7). For example, the range of propionate incorporated in the mutant strains ranged from 0.64 nmoles/mg protein/18 hrs to 3.21, while the control strain (MCH 24) incorporated 15 nmoles propionate/mg protein/18 hrs. The range of baseline incorporation of [^{14}C]-propionate varied between *mut*^{o} and *mut*$^{-}$ cell lines (Table 8). The range of baseline or residual incorporation of propionate in nmoles propionate/mg protein/18hrs was 0.51-1.71 (mean 0.94±0.40) in *mut*^{o} cells, and 0.55-3.21 (mean 1.28±0.99) in *mut*$^{-}$ cells. One-tailed *t* test comparison between *mut*^{o} and *mut*$^{-}$ baseline propionate incorporation values revealed that the difference between the two values was not statistically significant ($p=0.2061$). Mixing of different mutants in the absence of fusion failed to stimulate [1-^{14}C]- propionate incorporation (Table 7). Thus, complementation required cell fusion and could not be accounted for by cross-feeding of mixed cells. Activity was not restored when homokaryons were produced by self-fusion (Table 6, Table 7). For example, WG 1713 without fusion incorporated 0.87±0.08 nmoles propionate/mg protein/18 hrs, and with fusion it incorporated 0.77±0.19 nmoles propionate/mg protein/18 hrs.

FIG. 7 COMPLEMENTATION GRID SUMMARIZING COMPLEMENTATION ANALYSIS BETWEEN *mut* CELL LINES. **+** represents complementation between pairs of mutants; **-** represents the absence of complementation between pairs of mutants; HMZ= homozygous mutation in the DNA; HTZ= compound heterozygous mutation in the DNA; HMZcDNA= homozygous mutation in the cDNA; HTZcDNA= heterozygous mutation in cDNA.

mut COMPLEMENTATION GRID

***mut* Cell Lines (Mutation)**	1511	1610	1618	1713	1727	1738	1919	2041	1130	1681	1599	1607	1609
WG 1511 *mut*$^-$ (H678R) HMZcDNA		+	-	-	-	-	-	+	+	-	-	-	-
WG 1610 *mut*$^-$ (G717V) HMZ			+	-	-	+	-	-	+	-	-	-	-
WG 1618 *mut*$^-$ (Unknown)				-	+	+	+	-	-	+	-	-	+
WG 1713 *mut*^{o} (Unknown)					+	+	+	+	+	-	-	-	-
WG 1727 *mut*^{o} (Unknown)						-	-	-	-	-	-	-	+
WG 1738 *mut*$^-$ (Unknown)							-	-	+	-	-	+	-
WG 1919 *mut*$^-$ (Unknown)								-	+	-	-	-	-
WG 2041 *mut*^{o} (Unknown)									-	-	-	-	-
WG 1130 *mut*^{o} (R93H) HMZ										+	-	-	+
WG 1681 *mut*^{o} (G623R,G703R) HTZ											-	-	-
WG 1599 *mut*$^-$ (R369H) HTZcDNA												-	-
WG 1607 *mut*^{o} (W105R,A377E) HTZ													-
WG 1609 *mut*^{o} (G630E) HMZ													

\- Do not complement

\+ Do complement

TABLE 6 GENETIC COMPLEMENTATION ANALYSIS IN PEG-INDUCED HETEROKARYONS IN HUMAN SKIN FIBROBLASTS DEFICIENT IN MCM ACTIVITY. Numbers indicate the mean of triplicate determinations of [1-^{14}C] propionate incorporation (nmoles propionate/ mg protein/ 18 hours) ± standard deviation. Activities in fused cells are displayed under those of unfused cells (i.e. unfused/fused).

[1] Activity expressed in units of [illegible] generated per mg protein per 18 hours ± sd. Activities in fused cell sets multiplied under the curve, cell size unfused / fused

[2] change with fusion significant at $p < 0.01$

[3] change with fusion significant at $p <$

[4] change with fusion significant at $p <$

TABLE 7 PEG-MEDIATED CELL FUSION COMPLEMENTATION ANALYSIS AMONG *mut* CELL LINES. Unmixed represents the uptake value of the cell line by itself without fusion. Mixed fibroblast cultures were fused by 60 seconds exposure to polyethylene glycol (PEG). Mixed unfused cultures (without PEG) and unmixed cultures served as controls. Complementation (COMP) is indicated by an increase in propionate uptake in fused cultures relative to unfused cultures. + = the cell lines complement each other; - = the cell lines do not complement each other.

TABLE 7 INTRAGENIC COMPLEMENTATION ANALYSIS

[^{14}C] PROPIONATE UPTAKE
(nmoles/mg protein/18 Hrs)

		MIXED WITH WG 1713		
Cell Line	Unmixed (no PEG)	Without PEG	With PEG	COMP
WG 1713 (*mut*^{o})		0.87±0.08	0.77±0.19	-
WG 1130 (*mut*^{o})	0.88±0.17	0.80±0.10	1.10±0.10	+
WG 1738 (*mut*$^{-}$)	1.41±0.11	1.20±0.10	3.10±0.20	+
WG 1618 (*mut*$^{-}$)	3.21±0.16	2.12±0.29	2.0±0.12	-
WG 1681 (*mut*^{o})	0.64±0.02	0.71±0.11	0.63±0.0	-
WG 1943 (*cblA*)	1.50±0.20	1.10±0.10	6.30±0.20	+
MCH 24 (control)	15.0±1.0			

TABLE 8 BASELINE [^{14}C]-PROPIONATE INCORPORATION IN *mut* X CELLS. Baseline incorporation of [^{14}C]-propionate into *mut*$^-$ and *mut*^{0} cells expressed in nmoles propionate incorporated/ mg protein/ 18 hours ± standard deviation. The value for each cell line represents the mean of triplicate determinations.

TABLE 8 BASELINE [^{14}C]-PROPIONATE INCORPORATION IN *mut* CELLS

BASELINE [^{14}C]-PROPIONATE INCORPORATION IN *mut* CELLS

(nmoles propionate incorporated/mg protein/18 hrs ± standard deviation)

mut^{0} cells		*mut*$^{-}$ cells	
WG 1609	0.51±0.06	WG 1599	0.55±0.06
WG 1681	0.64±0.02	WG 1511	0.73±0.03
WG 1727	0.79±0.11	WG 1919	0.79±0.04
WG 1713	0.87±0.08	WG 1610	1.0±0.1
WG 1130	0.88±0.17	WG 1738	1.41±0.11
WG 2041	1.15±0.07	WG 1681	3.21±0.16
WG 1607	1.71±0.23		
MEAN:	0.94±0.40	MEAN:	1.28±0.99
RANGE:	0.51-1.71	RANGE:	0.55-3.21

One-tailed *t* test comparison between *mut*^{0} and *mut*$^{-}$ propionate incorporation values p=0.2061 "not significant"

In the 22 complementing crosses, the mean increase in propionate uptake in mixed fused cultures compared to mixed unfused cultures was statistically significant ($p<0.05$) (Table 6). The percentage increase in propionate incorporation after fusion in the twenty-two complementing pairs grouped according to their *mut* phenotype is shown in table 9. The degree of complementation observed varied from a six-fold increase in propionate incorporation (Table 9, WG 1511 x WG 1130) to an increase of approximately 20% (Table 9, WG 1609 x WG 1618). Statistical comparision (one-tailed *t* test) of percentage increase in propionate incorporation in *mut*$^-$ X *mut*$^-$ pairs versus *mut*^{0} X *mut*^{0} pairs, in *mut*$^-$ X *mut*$^-$ pairs versus *mut*$^-$ X *mut*^{0} pairs, and in *mut*^{0} X *mut*^{0} pairs versus *mut*$^-$ X *mut*^{0} pairs did not reveal any statistically significant difference between the pairs ($p=0.4225$, $p=0.3260$, and $p=0.3734$ respectively) (Table 9). Thus, there does not seem to be any pattern for the magnitude of correction of MCM defect by complementation. In *cbl*A or *cbl*B / *mut* heterokaryons, propionate incorporation after fusion (intergenic complementation) was intermediate between that in normal controls and patients cells (Table 7). For example, when WG 1943 (*cbl*A) was fused with WG 1713, propionate incorporation was 6.30±0.0 nmoles propionate/mg protein/18 hrs which is intermediate between the normal incorporation level (15.0±1.0 in MCH 24) and that which *mut* strains incorporated when they complemented (intragenic complementation) (1.10±0.10 in the fusion of WG 1713 with WG 1130). The statistical significance of the correction of defect in intergenic complementation was constantly extremely significant ($p<0.0001$ one-tailed *t* test).

Cells-free blanks, which reflect the relative level of background activity, gave propionate uptake values of 0.001% of the normal control MCH 24 (0.015±0.01 nmoles/mg

TABLE 9 PERCENTAGE INCREASE IN PROPIONATE INCORPORATION AFTER FUSION IN THE TWENTY-TWO COMPLEMENTING PAIRS. The twenty-two complementing pairs are grouped according to their *mut* phenotype.

TABLE 9 THE TWENTY-TWO COMPLEMENTING COMBINATIONS

mut$^-$ x *mut*$^-$	Mean of Percentage Increase in Propionate Incorporation of Triplicates After Fusion (%)	Statistical Comparision of Propionate Incorporation in Triplicate Unfused versus Fused (One-tailed *t* test)
WG1511xWG1610 (H678RxG717V)	143 (150,109,170)	p<0 005
WG1919xWG1618	95 (105,100,79)	p<0 0001
WG1618xWG1610	74 (79,90,52)	p<0 005
WG1738xWG1618	68 (54,63,88)	p<0 05
WG1738xWG1610	52 (67,27,62)	p<0 005
	Mean 86 4±35 2 Range 52-143	

mut^0 x *mut*^{0}	Mean of Percentage Increase in Propionate Incorporation of triplicates After Fusion (%)	Statistical Comparision of Propionate Incorporation in Triplicate Unfused versus Fused (One-tailed *t* test)
WG1130xWG1681 (R93HxG623R,G703R)	221 (236,224,204)	p<0 0001
WG1130xWG1609 (R93HxG630E)	127 (114,86,180)	p<0 005
' 1727xWG1713	93 (75,89,114)	p<0 005
WG1727xWG1609	54 (67,14,80)	p<0 05
WG1130xWG1713	39 (25,71,22)	p<0 05
WG2041xWG1713	30 (50,33,8)	p<0 05
	Mean 94 0±72 0 Range.30-221	

mut^0 x *mut*$^-$	Mean of Percentage Increase in Propionate Incorporation of Triplicates After Fusion (%)	Statistical Comparision of Propionate Incorporation in Triplicate Unfused versus Fused (One-tailed *t* test)
WG1130xWG1511 (R93HxH678R)	471 (533,605,275)	p<0 005
WG1713xWG1738	160 (158,200,123)	p<0 0001
WG1713xWG1919	95 (75,143,67)	p<0 005
WG1727xWG1618	94 (85,114,83)	p<0 005
WG1130xWG1919	82 (63,89,114)	p<0 005
WG1130xWG1610 (R93HxG717V)	80 (62,112,67)	p<0 005
WG2041xWG1511	75 (67,82)	p<0 005
WG1607xWG1738	74 (67,93,62)	p<0 0001
WG1130xWG1738	59 (73,33,70)	p<0 005
WG1681xWG1618	34 (26,37,39)	p<0 005
WG1609xWG1618	18 (12,25,17)	p<0 05
	Mean 113 5±124 0 Range 18-471	

Statistical comparision of percentage increase in propionate incorporation (one-tailed *t* test):

***mut*$^-$ X *mut*$^-$ vs *mut*^{0} X *mut*^{0} p=0.4225 "not significant"**

***mut*^{0} X *mut*^{0} vs *mut*$^-$ X *mut*^{0} p=0.3734 "not significant"**

***mut*$^-$ X *mut*$^-$ vs *mut*$^-$ X *mut*^{0} p=0.3260 "not significant"**

protein/18 hrs (range 0.01-0.03) compared to 15.0±1.0 (range 14-16)). In addition, activities of fused homokaryons and of non complementing fused heterokaryons showed some decrease relative to unfused cellular mixtures (Table 6, Table 7). For example, WG 1713 x WG 1681 without fusion incorporated 0.71±0.11 nmoles propionate/mg protein/18 hrs, and when fused they incorporated 0.63±0.0 nmoles propionate/mg protein/18 hrs. This mild decrease may result from the toxic effects of PEG on cell metabolism.

7.2 COMPLEMENTATION MAP

The complementation data in table 6 can be summarized in a complementation map (Fig.8). Mutants can be placed in distinct classes such that all mutants within a class fail to complement with each other, but can complement mutants in other classes. Mutants, or classes of mutants, are said to overlap if they do not complement with each other, and they do not overlap if they do complement with each other. The simplest arrangement of classes is in a unique linear order.

As a result of 78 different pairwise combinations, a linear complementation map of the MCM locus containing 3 different segments representing 3 major complementation groups has been constructed. Since it was not possible to construct a simple map with all 13 cell lines, four mutants could not be accommodated on this map, and therefore their complementation patterns were not considered. These are WG 1511 (H678R), WG 1713, WG 1727, and WG 1738 (mutations unknown in all 3 cell lines). Mutants grouped together above a line belong to the same subgroup, thus they do not complement each other but behave identically with respect to their ability to complement

FIG. 8 **HUMAN MCM COMPLEMENTATION MAP.** Map of *mut* cell lines showing 3 groups and 2 intervals. The numbers identify individual strains. Mutants grouped together above a line belong to the same subgroup. Cell lines placed in different groups above non-overlapping lines complement each other. Fusions between lines in the same group or between groups represented by overlapping lines do not complement each other.

mut COMPLEMENTATION MAP

WG 1610 (*mut*$^{-}$, G717V)
WG 1919 (*mut*$^{-}$, unknown)
WG 1130 (*mut*^{o}, R93H)
WG 1609 (*mut*^{o}, G630E)
WG 1618 (*mut*$^{-}$, unknown)
WG 1681 (*mut*^{o}, G623R, G703R)

WG 1599 (*mut*$^{-}$, R369H)
WG 2041 (*mut*^{o}, unknown)
WG 1607 (*mut*^{o}, W105R, A377E)

---

other specific mutants. For example, WG 1130 and WG 1618 fall in the same subgroup, thus they do not complement each other. However, both cell lines complement all the strains in the class comprised of WG 1609, WG 1610, WG 1681, and WG 1919. The subgroup whose line overlaps all the others is defined by three cell lines (WG 1599, WG 1607, and WG 2041) who were incapable of complementing with any of the other strains.

7.3 PCR-SSCP ANALYSIS

PCR-SSCP analysis was performed on PCR amplified fragments of exons 9, 11, and 12 from 30 *mut* patients and 8 normal controls. These 3 exons were targeted for SSCP analysis because each harboured known mutations or polymorphisms. The normal controls showed 2 different band migration pattern (3 and 4 band pattern) (Fig.9, lane 1 and 2).

The two exon 12 and six exon 9 positive control DNA (from cell lines with known mutations or polymorphisms in the exon) failed to demonstrate any altered migration, while the 2 exon 11 positive controls showed a different band pattern compared to normal controls.

Analysis of exon 9 of the 30 *mut* lines revealed 1 mobility shift in WG 1727 with respect to either normal control pattern. Altered band patterns compared to normal controls were found in three patients (WG 1713, WG 1919, WG 2041) in exon 12 (Fig.9, lane 6 and 8 for WG 1919 and WG 2041, respectively), and in one patient (WG 1738) in exon 11.

FIG. 9 **PCR-SSCP ANALYSIS OF EXON XII FROM mut CELL LINES.**

This panel represents the electrophoresis patterns obtained from the SSCP analysis of exon XII PCR products of *mut* genomic DNA. The detection of DNA species was by ethidium bromide staining. The lane M is HaeIII DNA marker, lane ND represents non-denatured PCR product of exon XII. Lanes 1 to 10 are AW3, AC, WG 1130, WG 1510, WG 1800, WG 1919, WG 1958, WG 2041, WG 2046, and WG 2077. AW3 and EC are two normal control cell lines.

PCR-SSCP ANALYSIS OF EXON XII FROM *mut* CELL LINES

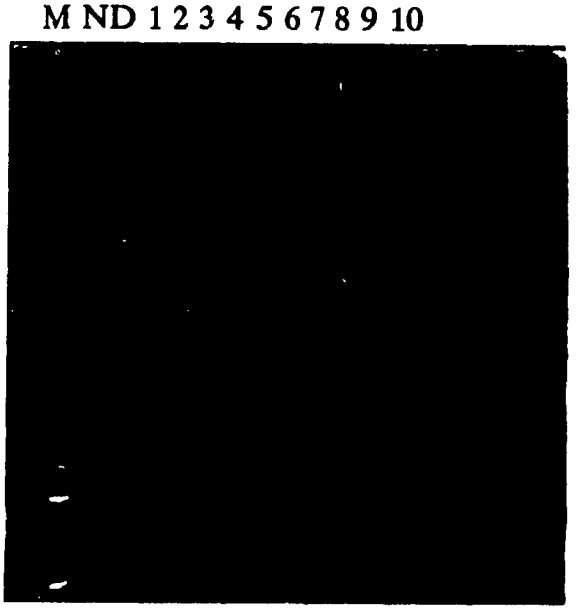

The rest of the cell lines showed band patterns that resembled either of the normal control patterns.

CHAPTER 8

DISCUSSION

I have studied interallelic (intragenic) complementation in functional methylmalonyl CoA mutase (MCM) activity, in cultures of PEG-induced heterokaryons of pairwise combinations of 13 *mut* mutants. Complementation was examined in all possible pairwise fusions by measuring MCM activity indirectly by [1-^{14}C] propionate utilization in intact cells (Fig.7).

Interallelic complementation can be defined as the phenomenon by which a biological function, which has been lost or altered by a mutation, may be restored through a mutual compensation provided by a mutant in the same function but defective differently (135). Interallelic complementation experiments were first performed in vivo with the early findings of Fincham (1959) that introduction of glutamic dehydrogenase gene carrying different mutations into am mutants of *Neurospora crassa* restored enzyme activity (136). Complementation experiments have also been performed in vitro. The earliest observation was that of Woodward (1959) who obtained adenylosuccinase activity by mixing cell free extracts of two different ad-4 locus mutants of *Neurospora crassa* (136). Complementation was employed as a criterion for establishing nonallelism among mutants. Since then, interallelic complementation has been described in proteins with multiple subunits (136) such as the heterotetrameric propionyl CoA carboxylase (PCC) (137), the homodimeric alkaline phosphatase (138), the homotetrameric b-galactosidase (139), the homotetrameric

argininosuccinate lyase (140), the homohexameric glutamate dehydrogenase (141), the heterodimeric tryptophan synthetase (136), and recently the homodimeric methylmalonyl CoA mutase (MCM) (1).

Interallelic complementation between mutations of the homodimeric MCM apoenzyme was first described in the *mut*^{o} cell line WG 1130 (1) (see section 5.3.4). I have shown that extensive intragenic complementation characterizes human MCM. Among 13 cell lines tested against each other, 22 out of the 78 combinations were complementary (Fig.7). All but one of the strains complemented at least once (Fig.7). Of the 12 complementing strains, 2 cell lines (WG 1130 and WG 1618) were remarkable because they participated in the most positive complementation tests (WG 1130 complemented with 7 of the 12 lines crossed with, WG 1618 complemented with 6 of the 12 lines crossed with) (Fig.7). A complementation grid with only the *mut* cell lines with known mutations is shown in figure 9. All of these results were obtained with heterogenous populations of PEG-treated cells, containing in any given experiment heterokaryons of undefined composition, homokaryons, and unfused parental cells. The increase in propionate uptake reflects partial restoration of MCM activity in heterokaryons, although this increase was less than that observed in crosses of *mut* cells with *cblA* or *cblB* cells (intergenic complementation) (Table 7). The level of MCM activity restored in the complementary combinations of *mut* lines varied (Table 6, Table 9). The fact that some crosses resulted in a six fold increase in propionate incorporation (WG1130xWG1511) while with others the increase was only 20% (WG1609xWG1618) is interesting (Table 9). The difference in degree of complementation

FIG. 10 COMPLEMENTATION GRID OF *mut* CELL LINES WITH KNOWN MUTATIONS. + represents complementation between pairs of mutants; - represents the absence of complementation between pairs of mutants; HMZ= homozygous mutation in the DNA; HTZ= compound heterozygous mutation in the DNA; HMZcDNA= homozygous mutation in the cDNA.

COMPLEMENTATION GRID OF *mut* CELL LINES WITH KNOWN MUTATION

mut CELL LINE	R93H HMZ *mut*^{o} WG1130	W105R,A377E HTZcDNA *mut*^{o} WG1607	G623R,G703R HTZ *mut*^{o} WG1681	G630E HMZ *mut*^{o} WG1609	H678R HMZcDNA *mut*$^{-}$ WG1511	G717V HMZ *mut*$^{-}$ WG1610
1130		-	+	+	+	+
1607			-	-	-	-
1681				-	-	-
1609					-	-
1511						+
1610						

\- DO NOT COMPLEMENT

\+ DO COMPLEMENT

may result if both alleles of a cell line participate in complementation versus only one allele in another cell line. The fusion of WG 1130 and WG 1511 resulted in the six fold increase in propionate uptake (Table 9). Each cell line harbours a homozygous mutation, R93H (*mut*^{0}) in WG 1130 (1) and H678R (*mut*$^{-}$) in WG 1511 (personnal communication with Dr. Wayne Fenton, Yale University). This high increase in propionate incorporation may be due to the fact that R93H and H678R complement each other, and since there are 2 alleles of each mutation, the degree of complementation is doubled. For the cell lines which exhibited only 20% increase in propionate uptake (Table 9, WG 1609xWG 1618, the contribution of each allele to the correction of the defect may be not very significant. Since the mutations in WG 1618 are not known yet, no prediction can be made. Table 10 describes the percentage increase in propionate incorporation after fusion according to location of mutations in the complementing pairs.

Interallelic complementation was demonstrated between *mut*^{0} mutations (i.e. WG 1713 and WG 1130), between *mut*$^{-}$ mutations (i.e. WG 1618 and WG 1511), and between *mut*^{0} and *mut*$^{-}$ mutations (i.e. WG 1607 and WG 1738) (Table 9). However, there exist a subset of *mut*^{0} and *mut*$^{-}$ alleles (WG 1607 and WG 1599) that complement neither 1130 nor each other. Thus, the ability to complement was not predicted by the *mut*^{0}/*mut*$^{-}$ phenotype of the cell. In addition, statistical comparision of propionate incorporation increase after fusion in complementing pairs according to their *mut*^{0}/*mut*$^{-}$ phenotype (Table 9) failed to detect any statistically significant difference between *mut*$^{-}$ x *mut*$^{-}$ complementing pairs versus *mut*^{0} x *mut*^{0} complementing pairs, *mut*^{0} x *mut*^{0} versus *mut*$^{-}$ x *mut*^{0}, and *mut*$^{-}$ x

TABLE 10 PERCENTAGE INCREASE IN PROPIONATE INCORPORATION AFTER FUSION IN *mut* CELL LINES ACCORDING TO LOCATION OF MUTATION.

TABLE 10 STATISTICAL ANALYSIS OF COMPLEMENTING PAIRS ACCORDING TO LOCATION OF MUTATIONS

Complementating Pairs with Mutations in Different Putative Domains		Mean of Percentage Increase in Propionate Incorporation of Triplicates After Fusion (%)	Statistical Comparision of Propionate Incorporation in Triplicate Unfused versus Fused (One-tailed *t* test)
R93HxH678R	*mut*^{0} x *mut*$^-$	471 (533,605,275)	$p<0.005$
R93HxG623R,G703R	*mut*^{0} x *mut*^{0}	221 (236,224,204)	$p<0.0001$
R93HxG630E	*mut*^{0} x *mut*^{0}	127 (114,86,180)	$p<0.005$
R93HxG717V	*mut*^{0} x *mut*$^-$	80 (62,112,67)	$p<0.005$

Complementing Pair with Mutation in Same Putative Domain		Mean of Percentage Increase in Propionate Incorporation of Triplicates After Fusion (%)	Statistical Comparision of Propionate Incorporation in Triplicate Unfused versus Fused (One-tailed *t* test)
H678RxG717V	*mut*$^-$ x *mut*$^-$	143 (150,109,170)	$p<0.005$

mut^{-} versus *mut*$^{-}$ x *mut*^{0} (one-tailed *t* test p values were 0.4225, 0.3734, 0.3260 respectively).

To account for interallelic complementation, a general theory of complementation was first proposed by Crick and Orgel in 1964 (128). They considered several possible ways in which interaction between polypeptides could lead to complementation. The first and most plausible theory involves homologous correction (142). It is postulated that the close juxtaposition of a defective region in one monomer with a correct homologous region of another monomer can result in the correction of the defect. In this case, active sites, cofactor binding sites, and subunit dimerization sites of multimeric proteins are the most likely regions involved in interallelic complementation (136). Thus, an amino acid change that compromises one of these important sites may be compensated for through the interaction with another polypeptide with an amino acid change in another site. In the case where the active sites are shared between 2 monomers, in a homogeneous aggregate all sites are defective, but in a hybrid aggregate some sites are functional (142).

The second theoretical model proposed is the conformational-correction hypothesis (143). It is assumed that the defects responsible for loss of activity in mutant forms of enzymes need not always involve the active sites themselves and could involve parts of the peptide chain associated with conformational change (144). Thus, some mutations may produce a localized deformity or misfolding in the polypeptide, the effect of which may be corrected by interaction with another subunit (143). Therefore, subunit interaction may lead to important conformational changes that produce a functional enzyme (135).

A third model for interallelic complementation postulates that it is the

formation of a hybrid protein that leads to restoration of function of the protein (135,143). Polypeptides which have been altered at different molecular sites interact to form a hybrid or heteromeric protein which is functional (143). The most convincing evidence in support of this theory comes from experiments with *E.coli* mutants of alkaline phosphatase where ^{35}S was used to label subunits from the various mutants (145). The different heterodimers formed were able to restore alkaline phosphatase activity. In addition, hybrids formed from different mutant subunits had different specific enzymic activities. In mammalian cells, Shapiro et al. (146) described interallelic complementation among mutants of the HPRT gene in chinese hamster ovary cells. They demonstrated the hybrid nature of the complementing enzyme as the basis for correction of the defect.

A crucial test of all of these hypotheses requires more information about the configuration of enzymes. For now, the exact manner of the polypeptide-polypeptide interaction is not yet known in any of the systems studied. However, it is important to note that the mechanism underlying complementation may not be the same in all systems.

Since there is no information available concerning the subunit structure of MCM enzyme, one must speculate about the nature of the mutations in certain cell lines on the basis of the complementation results. Different mechanisms can be envisioned. Mutations that occur in different functional or structural domains on different *mut* chains can complement in dimeric enzyme because a normal counterpart of the mutated domain is available in each chain. It is possible that WG 1130 and WG 1618 (the 2 most frequent complementers) have abnormalities that impair the active site of the protein while affecting

to a lesser extent its capacity to aggregate or to correct other mutants conformationally, as has been reported for the glutamate dehydrogenase mutant *am*[1], an active-site mutant that remains highly competent in its interaction with other monomers (147). However, extensive complementation might result without the need for homologous correction. Mutations may disrupt the conformation of the protein and by consequence the integrity of its active sites. Altered subunits, when formed as hybrids, may result in the proper conformation or infer stability of the protein (143) as with *E. coli* alkaline phosphatase, where affinities between subunits were a function of the particular structural alteration involved (136). In addition, by stabilizing or conformationally correcting the multimer during interallelic complementation, the active site of another polypeptide may become available (143).

The observed complementation with *mut*^{o} mutations and *mut*$^{-}$ mutations suggests that the heterodimers formed between mutant subunits are either able to compensate for an important site, or stabilize protein structure.

Interallelic complementation in MCM and the consequent effect on the tertiary structure folding and stability may also occur because of alteration in the net surface charge of the enzyme. For example, Qureshi et al (126) proposed that in WG 1681, which is a compound heterozygous for G623R and G703R, the substitution of a positively-charged arginine for glycine may change the net surface charge of each encoded subunit, and thus inactivate MCM. Upon formation of heterodimers with R93H of WG 1130, the proper surface charge may be restored, and consequently the enzyme is active. This is supported by examples from the glutamate dehydrogenase homohexameric enzyme in *Neurospora crassa*

(147). The am^{19} mutation results in a substitution of lysine for methionine leading to an abnormal electrophoretic mobility because of an alteration in the net surface charge. However, the normal electrophoretic mobility was restored to normal when am^{19} formed hybrids with am^{1} mutation which affected the enzyme active site. Enzyme activity was thereby restored due to the normal net surface charge restored by the interallelic complementation between the mutants (147).

The amino acid position of a mutation may determine the *mut* phenotype and interallelic complementation patterns. At the primary amino acid level, *mut*$^-$ mutations appear to cluster at the C-terminus and *mut*^{o} mutations at the N-terminus (Fig.6). However, certain *mut*^{o} and *mut*$^-$ mutations do not fall into their putative regions. For example, the R93H mutation results in a *mut*^{o} phenotype while a G94V change results in a *mut*$^-$ phenotype (Table 1). In addition, three *mut*^{o} mutations (G623R, G703R, and G630E) fall within the *mut*$^-$ cluster at the C-terminus. With respect to intragenic complementation and the distribution of mutations, WG 1511 (H678R) cell line complement the G717V mutation of cell lines WG 1610, WG 1611 and WG 1613 (129). However, WG 1511 (H678R) does not complement with WG 1681 (G623R, G703R). Thus, the primary amino acid position cannot determine *mut*^{o}/*mut*$^-$ phenotypes, nor can it predict interallelic complementation patterns.

Complementation between *mut*^{o} and *mut*$^-$ lines may not only depend on the location of the mutations, but also the specific residues changed may be important in determining whether or not complementation will occur. The specific amino acid alterations

in the tryptophan-binding pocket of the dimeric tryptophan repressor protein in *E.coli* determined whether or not the mutations would exhibit interallelic complementation (148). A T44M mutation was able to complement G85R, G85W, and G85K mutations in the binding pocket, but was unable to complement a G85E mutation. A positive charge or indole ring appeared to be required for the observed intragenic complementation (148). These results suggest a type of site-specific intragenic complementation where only certain alterations at an amino acid position complement another. However, among the *mut* mutations identified, there does not seem to be any correlation between the interallelic complementation and the specific amino acid substituted. For example, R93**H** complements with G717**V**, G623**R**, G630**E**, but it does not complement with W105**R**, and A377**E**. In addition , **R369H** does not complement with any cell line.

Thus, no specific pattern of charge or amino acid structure or distribution along the protein appear to be essential for the intragenic complementation observed within the *mut* class. In fact, Crick and Orgel point out that the complex nature of the folding of polypeptide chains precludes any way of interpreting complementation data in term of how subunits interact (128).

The important factor in the complementation may not be the CRM status of the complementing cell. In several complementation combinations one of the partners does not produce any detectable CRM (136,138). This does not exclude the possibility that it does produce some protein which is not recognized immunologically. Combination of low CRM mutants yielded unexpectedly high enzyme activity in *E.coli* alkaline phosphatase (138). This

means that the mutant proteins suffer from some instability but may be rescued by complementation. In addition, although mutant *am*^{14} of the glutamate dehydrogenase from *Neurospora crassa* produces no active enzyme and a very low level of immunological cross-reactivity because of its defective conformation (136), it can complement with several other *am* mutants. Moreover, in MCM, WG 1130, which participates in the largest number of complementations, demonstrated in Western blot analysis a band intensity that was 10% relative to the *mut*$^-$ cell line WG 1599 which has normal levels of CRM and protein) (119). It is interesting that WG 1599 does not complement any *mut* cell line. The R93H mutation which may affect protein stability or turnover is compensated for upon formation of hybrids with other *mut* mutations (G623R, G703R, G717V).

Ledley et al. (117) studied mRNA levels from certain *mut* cell lines. Both WG 1607 (W105R, A377E) and WG 1609 (G630E) had normal levels of MCM mRNA. It is interesting that WG 1607 does not complement WG 1130 (normal mRNA levels, R93H), while WG 1609 does (Fig.7). Thus, as of yet mRNA levels do not appear to be a criterion for complementation, although it is probable that cell lines with decreased mRNA levels would not participate in complementation. WG 1612 (unknown mutation) which has low levels of mRNA and does not complement WG 1130 lends support to this suggestion.

The level of residual or baseline propionate incorporation does not seem to correlate with the clinical classification. For example, two *mut*^{0} patients (WG 1607 and WG 1609) had similar clinical presentations and both died at one and half years of age. Their respective baseline [^{14}C]-propionate incorporation in nmoles/mg protein/18 hours are 1.71±0.23 and 0.51±0.06 (three fold difference between the two) (Table 8). Moreover, WG

1610, a *mut*$^-$ cell line from a patient with only intermediate complications, has baseline propionate incorporation of 1.0±0.1 (less than that of WG 1609). Only the baseline propionate incorporation of WG 1618 which is the highest (3.2±0.16) seems to correlate with its clinical phenotype (benign *mut*$^-$ MMA). These data suggest that the clinical heterogeneity of this disease does not derive from variation in the baseline propionate incorporation in different patients.

Genetic heterogeneity with respect to interallelic complementation also does not appear to correlate with clinical heterogeneity. WG 1130 cells, which are from a *mut*^{0} patient who died in infancy because of severe MMA, complement most *mut* cell lines. Surprisingly, WG 1618 which is from a mild, benign *mut*$^-$ patient, complements with many *mut* cell lines but not as many as WG 1130. Thus, no striking correlation was found between the severity of clinical expression and the complementation behaviour of a strain. It is probable then that the clinical heterogeneity observed represents the expression of different alleles within the individuals.

There does not seem to be any correlation between the baseline level of propionate incorporation (nmoles/mg protein/18 hrs) and the interallelic complementation pattern. WG 1607 (W105E,A377E) incorporated the highest *mut*^{0} baseline propionate level (1.71±0.23), and it only complements with one cell line, WG 1738 (*mut*$^-$, mutation unknown) which incorporated 1.41±0.11 nmoles propionate/mg protein/18 hrs (Table 8). In contrast, WG 1130 (*mut*^{0},R93H) which only incorporated 0.88±0.17 nmoles propionate/mg protein/ 18 hrs complemented with seven cell lines (Fig.7) (Table 8). WG1618 (unknown mutation) incorporated the highest *mut*$^-$ propionate baseline level (3.21±0.16), and complemented with

six cell lines (Fig.7) (Table 8).

Of the thirteen strains analyzed for intragenic complementation, mutations have been identified in six. Four have a homozygous mutation [WG 1130 (R93H) (1), WG 1511 (H678R) (personal communication, Dr. Wayne Fenton, Yale University), WG 1610 (G717V) (125), WG 1609 (G630E) (127)]. Two cell lines are compound heterozygous [WG 1681 (G623R and G703R) (126), WG 1607 (W105R and A377G) (124)]. WG 1511 is homozygous for H678R at the cDNA level (personal communication, Dr. Wayne Fenton). WG 1599 has a heterozygous substitution (R369H), the second allele is not characterized (personal communication, Dr. Wayne Fenton). The remaining cell lines (WG 1713, WG 1727, WG 1738, WG 1919, and WG 2041) crossed were chosen because they showed an altered migration pattern on PCR-SSCP gels. Although WG 1618 does not have any known mutation or altered migration pattern, it was included in the crosses because, as suggested by experiments performed in this laboratory, it exhibited an interesting complementation pattern.

Because neither the tertiary and quaternary structures of MCM nor the substrate and coenzyme binding sites are known, only speculation can be made as to the nature of the mutations. The mutations identified alter amino acid sequences conserved in human, and murine MCM, and in *P.shermanii* MUTB, which strongly suggests that these sites may be essential to MCM structure and function (127). Different models have been devised to predict secondary structures of proteins, and thus provide possible explanations

for the relative importance of the preserved sites (149). Ledley et al (125) and Qureshi et al (126) analyzed MCM structure in the regions around the G717V, and G623R and G703R mutations to look for disruption of putative alpha-helical or beta-sheet structures caused by the mutations. Using the model of Chou and Fasman (149) which predicts secondary structures of proteins, Ledley et al and Qureshi at al showed that normally in a secondary structure, glycine stabilizes beta-turns and disrupts alpha-helix structure. Thus, one way in which each of these three mutations inactivate MCM function may be due to the absence of the helix terminating glycine which may enable an adjacent alpha helix to extend further towards the carboxy terminus and disrupt the tertiary assembly or structure by introducing additional rotation. Alternatively, Qureshi et al proposed that the absence of the ß-turn stabilizing glycine at position 703 may disrupt ß-sheet formation, and that because charged residues are not usually present at the C-terminal of ß-strands (150), the positively charged arginine instead of the uncharged glycine at position 703 may be involved in altering the ß-strand interaction. Ledley et al also suggested that the valine introduced at position 717 may initiate beta-sheet formation, thereby disrupting proper protein folding (125). Other possible effects of the mutations may be due to the replacement of a small uncharged aa (glycine) with a larger aa (valine) in G717V (125) or with a very large hydrophilic residues (Arginine) in G623R and G703R (126) which itself may alter catalytic, binding or dimerization determinants.

Correlation of mutations to the interallelic complementation patterns may be helpful in examining the structure-function relationships of the protein. Interallelic

complementation has been used as a tool in prokaryotes and lower eukaryotes to define functional or structural domains (136). Intragenic complementation was observed between specific amino(N)-terminal mutants and carboxy(C)-terminal mutants of the bacteriophage T4 DNA polymerase lacking DNA polymerase polymerizing functions (151). The positive complementation results provided genetic evidence for a discrete N-terminal domain which, based on protein sequence similarities studies with *E.coli* DNA pol I, has been suggested to encode a 5'->3'exonuclease or RNase H-type activity. In addition, interallelic (intracistronic) complementation has recently revealed a novel activity of the DNA-binding domain in SV40 T antigen (17). Mutations in two different functions of T antigen were able to complement each other to restore the growth stimulatory activity. A S189N mutation in the DNA-binding domain complemented a E107K mutation in the Rb-binding domain. It was proposed that the DNA-binding domain harbours an unknown and novel activity, which is abolished by the S189N mutation, involved in growth stimulation (17). This new function cooperates with retinoblastoma-suppressor protein binding and tumour suppressor p53 binding to stimulate cellular proliferation in quiescent cells, thereby abolishing the growth-arresting properties of these proteins. Other ways of intragenic complementation have been described in which gene mutations can be corrected by additional alterations in the gene itself (i.e. reversion, suppression, recombination). These are fruitful approaches in order to identify amino acid replacements compatible with the function of the enzyme. One type of second-site suppression mutation is illustrated by genetic engineering in alpha1-antitrypsin deficiency (152). The Z form of the disease is caused by a E342K substitution. Using crystallography data, glutamic acid 342 was found to be positioned adjacent to lysine 290 in the wild type

protein and was assumed to form a salt bridge with it. The Z mutation which changes the charge at position 342 eliminates the salt bridge and results in misfolding of the molecule. Brantly et al. (152) corrected the defect by mutating lysine 290 to glutamic acid, thereby creating the opposite charge relationship of the original one that would restore the salt bridge. This illustrates how intrachain complementation could correct a defect.

Thus, intragenic complementation has major significance as a probe of the structure/function of a gene. Numerous *mut* mutations that participate in interallelic complementation are already identified. These intragenically complementing alleles likely identify functionally or structurally independent domains in the protein.

The clustering of mutations which eliminate enzyme activity at the amino terminal of the protein (natural mutations (R93H and W105R) (1,124) and non-natural mutation (L153V) (153)) suggests the presence of a critical functional domain in this region in which even subtle changes in structure, such as that produced by a valine to leucine substitution (L153V) have significant effects on enzyme activity (127). The function of this domain and the mechanism by which R93H but not W105R engage in interallelic complementation is not known. Predictive analysis of secondary structure (150) in that region did not indicate any specific conformational changes caused by these mutations. The mutation in WG 1130, which replaces arginine at position 93 with a histidine giving rise to *mut*^{0} phenotype, falls in an interesting region of the gene very rich in arginine and proline residues. The fact that alleles with the R93H mutation complement with alleles having mutations in the Cbl binding domain supports the suggestion that the region surrounding

R93H has a distinct function (129).

One of the mutations in WG 1607 (*mut*°), W105R, substitutes an evolutionary conserved tryptophan residue with an arginine residue (124). It has been observed in human and mouse MCM proteins that tryptophan residues, along with tyrosine and proline residues, are non-randomly distributed in the amino half of the molecule. The significance of this asymmetry is not clear. However, it is suggested that such residues may be more resistant to attacks by free radicals formed during the rearrangement of methylmalonyl CoA (124). This suggests that the amino terminal may harbour the substrate binding domain.

The fact that the residues altered by each of the mutations identified are conserved evolutionary among human, mouse, and the MutB gene of *P.shermanii*, and that fact that each substitution interferes with the enzymatic activity suggests that these residues occur in regions critical for enzyme structure or function (127) (Fig.11). The *mut*⁻ mutations cluster within a 90 amino acid segment region of the enzyme between residues 626 and 717 near the carboxyl terminus. Thus, the Cbl binding domain is putatively localized to that region (127). This was confirmed by Marsh and Holloway (154) who cloned and determined the nucleotide sequence of the gene encoding the small subunit, component S, of the AdoCbl-dependent glutamate mutase of *Clostridium tetanomorphum* (mutS). The deduced amino acid sequences of mutS showed homology with the C-terminal portion of MCM from human, mouse, and MuT B from *P.shermanii*, and from a region of *E.coli*'s methionine synthase which has been shown to bind Cbl (71) (Fig.11) These results were surprising since component S does not bind Cbl on its own. In addition, two short regions of highly

FIG. 11 **AMINO ACID SEQUENCES OF COBALAMIN-DEPENDENT ENZYMES FROM DIFFERENT SPECIES ALIGNED.** mutB-Hum, mutB-Mou, and mutB-Psh represent residues 610-650 of human, 608-748 of mouse, and 593-728 of *P.shermanii* methylmalonyl CoA mutase, respectively. mutS represents residues 1-137 of glutamate mutase component S, and metH represents residues 741-883 of *E.coli* methionine synthase. Conserved residues are marked by * and shown in bold type. Conservatively substituted residues are marked by +.

```
                1       +++ + -   * *    *  ++          +++    + ++    ++ 50
metB_Hum   REGRRPRLLV AKMGQDGHDR GAKVIATGFA DLGFDVDIGP LFQTPREVAQ
metB_Mou   REGRRLGLLV AKMGKDGHDR GAKVIATGFA DLGFDVDIGP LFQTPREVAH
metB_Psh   AEGRRPRILL AKMGQDGHDR GQKVIATAYA DLGFDVDVGP LFQTPEETAR
     metS  ..MEKKTIVL GVIGSDCHAV GHKILDHSFT NAGFNVVNIG VLSSQEDFIH
     metH  QGKTNGKMVI ATVKGDVHDI GKNIVGVVLQ CNNYEIVDLG VMVPAEKILR

             51* +       + ++*+  +          + ++     *   *++ + **   100
metB_Hum   QAVDADVHAV GVSTLAAGHK TLVPELIKEL NSLGRPDILV MCGGVIPPQD
metB_Mou   DAVDADVHAV GVSTHAAGHK TLVPELIKEL TALGRPDILV MCGGVIPPQD
metB_Psh   QAVEADVHVV GVSSLAGGHL TLVPALRKEL DKLGRPDILI TVGGVIPEQD
     metS  AAIETKADLI CVSSLYGQGE IDCKGLREKC DEAGLKGIKL FVGGNIVVGK
     metH  TAKEVNADLI GLSGLITPSL DEMVHVAKEM ERQGF.TIPL LIGGATTSKA

           101         +         ++          ++   +                150
metB_Hum   YEF......L FEVGVSNVFG PGTRIPKAAV QVLDDIEKCL EKKQQSV*..
metB_Mou   YEF......L YEVGVSNVFG PGTRIPRAAV QVLDDIEKCL AEKQQSV*..
metB_Psh   FDE......L RKDGAVEIYT PGTVIPESAI SLVKKLRASL DA*.......
     metS  QNWPDVEQRF KAMGFDRVYP PGTS.PETTI ADMKEVLGVE *.........
     metH  HTAVKIEQNY SGPT...VYV QNAS.R..TV GVVAALLSDT QRDDFVARTR
```

conserved sequences identified by the motifs, DXHXXG, and GXXXIXXXXGG, were invariant in all the proteins aligned (Fig.11). Interestingly, two *mut*^{0} mutations, G630E and G703R, fall in the region where most *mut*$^{-}$ mutations cluster. It may be proposed that these two mutations result in the *mut*^{0} phenotype because they completely disrupt the Cbl binding region. In fact, G630E and G703R each alter a putative consensus amino acid, the last glycine of the first and second motif, respectively. The mutations which produce a *mut*$^{-}$ phenotype in this region, such as H678R and G638D, affect other residues. Interestingly, the cell lines with *mut*^{0} mutations in that region (WG 1609 (G630E) and WG 1681 (G703R)) do not complement with each other nor with cell lines with *mut*$^{-}$ mutations in that region (WG 1610 (G717V) and WG 1511 (H678R)) (Fig.10). Again, this may be due to the fact that the *mut*^{0} mutations in that region disrupt consensus amino acids part of the two motifs, and thus completely disrupt the Cbl binding domain rendering the polypeptide unable to complement with any polypeptide harbouring a mutation in that region.

It is interesting that there is little sequence homology between MutA and MutB in the regions surrounding this presumed Cbl binding domain, since the *P.shermanii* MCM binds only one mole of cofactor per heterodimer (127). Because the nonconservative H523R substitution has no effect on enzyme activity, and substantial insertion/deletion is present within residues 546-547 among mammalian and bacterial MCM sequences, the Cbl binding domain is presumed to be bound by the region between residues 523 and 626 (127). Regions of insertions/deletions between species are assumed to represent spacers between functional domains in the protein. The most important structural requirement for Cbl binding to MCM of different organisms may be the tertiary structure (24). This is supported

by the observation that Cbl binding to human TCII and TCI, rat intrinsic factor, and porcine haptocorrin (all of which are Cbl binding proteins) is destroyed in the presence of urea and guanidine-HCl, which are well known to denature hydrogen bonds (24).

Although six of the seven mutations identified in the putative Cbl binding region involve replacement of glycine residues, these residues are probably not directly associated with the binding of Cbl but rather they may alter the secondary structure of the protein, thereby disrupting the interaction between the enzyme and the cofactor (127). Nevertheless, the fact that each of these mutations (*mut*$^-$ or *mut*^{0}) complements R93H suggests that they are associated with similar functional defects in the enzyme activity.

The significance of discrete regions of sequence similarities of MCM between different species depends upon understanding the relative functions of the alpha and beta chains of *P.shermanii*. If both the α and ß chains independently possess the complete function of the human protein, then all the structural determinants for enzyme activity may be included among these discrete homologies (111). If however different aspects of enzyme function have been sorted between the α and ß chains, then the determinants for their respective functions may be identified by analysis of the differential preservation of homologous residues (111). An observation in support of this is the presence only in the alpha subunit of a sequence which is significantly homologous to a portion of the sequence of the methylmalonyl CoA binding subunit of transcarboxylase from *P.shermaii* (100).

Assuming that the alpha and beta polypeptides of *P.shermanii* each harbours different domains of MCM enzyme, Ledley and Crane (127) suggested that since the prokaryotic MCM enzyme is encoded by two homologous genes while the mammalian MCM is encoded by a single gene, then the heteromeric prokaryotic MCM may provide a model for the observed interallelic complementation within the human MCM locus. The fact that interallelic complementation occurs when heterodimers are formed between the mutant clones carrying the R93H mutation and the clones with a mutation in the Cbl binding domain suggests that the heterodimers formed are like the prokaryotic enzyme in that they possess a single asymmetrical reactive centre as opposed to the homodimeric mammalian enzyme with its two symmetrical reactive centres. The subunits with the R93H mutation would contribute the Cbl binding domain, while the subunits with defects in Cbl binding would contribute a domain complementary to the one altered by R93H (127).

Interestingly, the *mut*$^-$ cell line WG1618 (mutation unknown) (Fig.7), which is the second most frequently complementing cell line (complements with 3 *mut*^{0} and 3 *mut*$^-$), does not complement WG 1130 which is the most frequent complementer. WG 1618 is an atypical *mut*$^-$ cell line (131). Biochemical analysis revealed that activity of MCM was essentially undetectable by in vitro assay of the cultured cells extracts. However, in the presence of excess OH-Cbl propionate uptake was significantly higher (2.5 fold) than in other *mut*$^-$ fibroblasts. These findings suggest that this patient has an unusually mild *mut* defect. Thus, WG 1618 may have an indirectly affected Cbl-binding domain, and could be easily stabilized during heterodimer formation. Therefore, heterodimers formed between WG

1618 and other *mut*$^-$ cell lines such as WG 1511 and WG 1610 may restore proper Cbl-binding. WG 1618 may harbour another mutation in the amino terminal resulting in its inability to complement WG 1130. Thus, heterodimers between WG 1130 monomers and WG 1618 fail to complement.

Complementation maps have been widely used to represent complementation data and to form the basis of some theories of complementation (155). Complementation maps consist of an arrangement of segments in which each segment represents one or a group of mutations. None of the mutants within the same group complemented one another in heterokaryons but they complemented all of the other mutants. Members of overlapping groups do not complement, whereas members of non-overlapping groups do complement (Fig.8). Complementation maps tend to be collinear with the genetic map. However, an examination of published complementation maps has revealed that in some cases strict collinearity with the genetic map does not prevail, and also that complementation maps are often circular or must even be represented as spirals (135). A genetic map uniquely defines the position of each mutational site. A complementation map on the other hand defines a certain number of segments. It has been reported that there are cell lines which are not consistent with a simple complementation map, and the segments fall into lines only when the exceptions are ignored to simplify the complexity (155). To obtain an interallelic complementation map that is informative about the MUT locus, I had to ignore four cell lines (WG 1511 (H678R), WG 1738, WG 1727, and WG 1713).The data could then be summarized as a linear complementation map, (which is the simplest 2-dimensional shape

that can represent the data), the mutants being distributed among three subgroups in a simple pattern. The *mut* complementation map I constructed may have structural meaning relative to the enzyme. The map of MCM thus consists of 3 segments which define 2 intervals. This type of ordering is found to correspond in a somewhat collinear fashion to the site of mutations in the gene. Mutations were found to cluster within 2 distinct mutable domains, one towards the N-terminus and the other near the C-terminus. Speculations can be made about interallelic complementation in regions of the polypeptide (amino terminus and carboxy terminus) which pair with a homologous region in the multimer (like with like). The defect in one region (N terminus) of a *mut* monomer may be corrected with the normal homologous region of another monomer in a hybrid molecule with defects in different regions (C terminus). If mutations fall in same region such as G630E and G717V (both in the C terminus) of the polypeptide no complementation is observed. This theory seems to account for the observed correlation between the complementation and the genetic map. However, WG 1511, which was one of the four cell lines omitted from the complementation map to simplify the pattern, contradicts the theory of mutation clustering. WG 1511 has a mutation in the carboxy terminus (H678R), thus theoretically it would be placed with the group comprised of WG 1610, WG 1919, WG 1681, WG 1609. However, placing it in that group would imply that it does not complement with any of the 4 cell lines in that group. This is contradicted by the fact that WG 1511 complements with WG 1610. Since the mutations in the other three cell lines not included on the map (WG 1713, WG 1727, WG 1738) are not known, no speculation can be made for now. Three strains constituted a subgroup that produced no increase in MCM activity in any fusion. The group of non

complementers is comprised of the cell lines WG 2041, WG 1599, and WG 1607. It is interesting that both WG 1599 and WG 1607 harbour mutations in exon 6 (R369H and A377E respectively), suggesting that important determinants for function may be present in exon 6. Overlapping segments in a complementation map have been interpreted to reflect an overlapping defect across regions of polypeptides which interact in a multimer.

A complementation map representing the complementation pattern of the cell lines with known *mut* mutations is shown in figure 12. Again, WG 1511 (H678R) was not placed on the map because it complements with WG 1610 (G717V).

Since the majority of the mutants studied are genetic compounds (only WG 1130, WG 1609, and WG 1610 harbour homozygous mutations (Table 1)), a complementation map of such mutants cannot be interpreted as simply as the maps of homozygous individuals or microorganisms where only two alleles are present in the cells tested for complementation. As many as 4 allelic polypeptides may be present in the heterokaryons formed between 2 heterozygous fibroblasts (155). The frequency of complementation is thus likely to be greater, resulting in an increasing number of segments in the maps. A mutant with 2 different alleles is more likely to complement any other allele than is a mutant with only one type of allele. However, because some maps in microorganisms are very complex, the complexity of the map does not necessarily derive from the compound nature of the human mutants. In addition, a complementation map of nonconsanguinous human mutants is only a minimal representation of all the complementation that may be occurring. The map is the same whether the complementation occurs with only one or all 4 of the possible combinations of alleles in a heterokaryon of 2

FIG. 12 **COMPLEMENTATION MAP OF *mut* CELL LINES WITH KNOWN MUTATIONS.** Mutations placed on non-overlapping lines complement each other. Mutations placed on overlapping lines do not complement each other.

COMPLEMENTATION MAP WITH KNOWN MUTATION FROM *mut* CELL LINES

R93H (WG 1130, *mut*^{o})

G717V (WG 1610, *mut*$^{-}$)
G630E (WG 1609, *mut*^{o})
G623R,G703R (WG 1681, *mut*^{o})

W105R,A377E (WG 1607, *mut*^{o})

---

genetic compounds. Crick and Orgel suggest that multimeric proteins are likely to be symmetrical (128). Mutations affecting the same region near a symmetry axis will be close together on the genetic map and the complementation map would tend to be collinear with the genetic map. For example, G717V in WG 1610, G630E in WG 1609, and G623R and G703R in WG 1681 may all be near an axis of symmetry. They also suggested that the length of the segment in a complementation map would reflect the extent to which misfolding spreads along the chain. Thus, according to this hypothesis, since the segment comprised of WG 1599 (R369H), WG 1607 (W105R, A377E), and WG 2041 (mutation unknown) is the longest, it implies that the mutations in these cell lines cause misfolding which is long spread. This is supported by the fact that the cell lines in this segment do not complement with any other cell line.

The present significance of the map is that it summarizes the complementation data giving significance to certain mutants that neither enzymatic studies nor clinical assessment would confer. Classification of *mut* mutants into the 3 complementation groups did not correlate with pattern of clinical heterogeneity or mut^0/mut^- classification (Fig.8). One complementation group is comprised of patient WG 1609 (mut^0) who died at 18 months of age and of patient WG 1610 (mut^-) who remains with good prognosis at four years of age.

Through the characterization of mutations participating in intragenic complementation, and understanding the biochemical defects of the mutation and basis of complementation, one can provide a pattern for grouping the mutations according to the complementation data in defined structural or functional domains. Once domains are

identified, site-directed mutagenesis could specifically test particular residues to refine the boundaries of the domains or to further interpret the final structure. Knowledge of structure and function relationship in MCM may contribute to treatment of MMA by induction of enzyme activity or somatic gene therapy.

SUMMARY

In this study, I have examined interallelic (intragenic) complementation between mutants of the structural gene locus encoding MCM (*mut* mutants). Complementation experiments were conducted by fusing in all pairwise combinations thirteen fibroblast cell lines derived from patients with the *mut* form of MMA. Complementation was indicated by the increase in [1-^{14}C]-propionate incorporation into trichloroacetic acid precipitable material in multinucleated cells produced by fusion in the presence of PEG, compared to [1-^{14}C]-propionate incorporation in parallel but unfused cultures. Intragenic complementation was demonstrated in 22 of the 78 pairwise fusions, indicating that complementation at the MUT locus is extensive. Further studies of *mut* mutations participating in interallelic complementation will be helpful in determining relationship between structure and function of MCM.

CLAIMS TO ORIGINALITY

1. This thesis describes the occurrence of extensive interallelic complementation in *mut* MMA. Interallelic complementation was demonstrated in 22 of the 78 pairwise fusions between 13 mutants of the structural gene encoding MCM (*mut* mutants).

PUBLICATIONS

ABSTRACTS AND ACKNOWLEDGEMENT

1- Farah R., and Rosenblatt D.S.: Extensive intragenic complementation in *mut* methylmalonic aciduria (MMA). To be presented in poster session at the Annual Meeting of the Royal College of Physicians and Surgeons of Canada in Toronto, Ontario. Sept. 14-19, 1994.

I won a 1994 Canadian Society For Clinical Investigation trainee award.

2- Farah R., and Rosenblatt D.S.: Methylmalonic Aciduria: Intragenic complementation in the *mut* complementation group. To be presented in poster session at the Annual Meeting of the American Society of Human Genetics in Montreal, Quebec. Oct. 19-23, 1994.

Acknowledgement given in **Journal of Clinical Investigation 93(4):1812-1819, 1994.** Qureshi A.A., Crane A.M., Matiaszuk N.V., Rezvani I., Ledley F.D., and Rosenblatt D.S. Cloning and expression of mutations demonstrating intragenic complementation in *mut*^{0} methylmalonic aciduria.

REFERENCES

1. Raff, M.L., Crane, A.M., Jansen, R., Ledley, F.D., and Rosenblatt, D.S. 1991. Genetic characterization of a MUT locus mutation discriminating heterogeneity in *mut*^{o} and *mut*$^{-}$ methylmalonic aciduria by interallelic complementation. *J. Clin. Invest.* 87:203-207.

2. Mellman, I.S., Youngdahl-Turner, P., Willard, H.F., Rosenberg, L.E. 1977. Intracellular binding of radioactive hydroxocobalamin to cobalamin-dependent aponenzymes in rat liver. *Proc. Natl. Acad. Sci USA.* 74:916-920.

3. Glusker, J.P. 1982. X-Ray crystallography of B_{12} and cobaloximes. In B_{12}. D. Dolphin, editor. Wiley InterScience, Toronto. 23-106.

4. Pezacka E., Green, R., Jacobsen, D.W. 1990. Glutathionylcobalamin as an intermediate in the formation of cobalamin coenzyme. *Biochem. Biophys. Res. Commun.* 169:443-450.

5. Fenton, W. and Rosenberg, L.E. 1989. Inherited disorders of cobalamin transport and metabolism. In The Metabolic Basis of Inherited Disease. C.R. Scriver, A.L. Beaudet, W.S. Sly, and D. Valle, editors. McGraw-Hill Press, New York. 2065-2082.

6. Fenton, W.A. and Rosenberg, L.E. 1978. Genetic and biochemical analysis of human

cobalamin mutants in cell culture. *Annu. Rev. Genet.* 12:223-248.

7. Beck, W.S. 1982. Biological and medical aspects of vitamin B_{12}. In B_{12}. D. Dolphin, editor. Wiley InterScience, Toronto. 1-30.

8. Battersby, A.R. 1994. How nature builds the pigments of life: the conquest of vitamin B_{12}. *Science*. 264:1551-1557.

9. Herbert, V. 1988. Vitamin B_{12}: plant sources, requirements, and assay. *Am. J. Clin. Nutr.* 48:862-858.

10. Cooper, B.A., Rosenblatt, D.S. 1987. Inherited defects of vitamin B_{12} metabolism. *Annu. Rev. Nutr.* 7:291-320.

11. Retey, J. 1982. Methylmalonyl CoA mutase. In B_{12}. D. Dolphin, editor. Wiley InterScience, Toronto. 357-380.

12. Cooper, B.A. 1983. The assay of cobalamin-dependent enzymes: their utilization for evaluation of cobalamin metabolism. In The Cobalamins. C. Hall, editor. Ed., Churchill Livinstone.

13. Bradbeer, C. 1982. Bacterial transport of cobalamin. In B_{12}: Biochemistry and Medicine

Vol.2. D. Dolphin, Ed., editor. John Wiley & Sons, New York.

14. Deveaux, L.C., Clevenson, D.S., Bradbeer, C., and Kadner, R. 1986. Identification of the BtuCED polypeptides and evidence for their role in vitamin B_{12} transport in Escherichia coli. *J. Bacteriol.* 167:920-927.

15. Seetharam, B., Alpers, D.H. 1985. Cellular uptake of cobalamin. *Nutr. Rev.* 43:97-102.

16. Cooper, B.A. and Rosenblatt, D.S. 1987. Inherited defects of vitamin B_{12} metabolism. *Annu. Rev. Nutr.* 7:291-320.

17. Dobbelstein, M., Arthur, A.K., Dehde, S., Van Zee, K., Dichmanns, A., and Fanning, E. 1992. Intracistronic complementation reveals a new function of SV40 T antigen that cooperates with Rb and p53 binding to stimulate DNA synthesis in quiescent. *Oncogene.* 7:837-847.

18. Allen, R.H., 1975. Human vitamin B_{12} tansport proteins. *Prog. Hematol.* 9:57-84.

19. Dieckgraefe, B.K., Seetharm, B., Banaszak, L., Leykam, J., and Alpers, D.H. 1988. Isolation and structural characterization of a cDNA clone encoding rat gastric intrinsic factor. *Proc. Natl. Acad. Sci USA.* 85:46.

20. Nexo, E. and Olesen H.. 1982. Intrinsic factor, Transcobalamin and Haptocorrin. In B B_{12}: Biochemistry and Medicine, vol 2. Dolphin D., editor. John Willey & Sons, New York. 57-85.

21. Seetharam, B., Presti, M., Frank, B., Tiruppathi, C., Alpers, D.H. 1985. Intestinal uptake and release of cobalamin complexed with rat intrinsic factor. *Am. Phys. Soc.* 85:326-331.

22. Eiberg, H., Moller, N., Mohr, J., and Nielsen, L.S. 1986. Linkage of transcobalamin II (TCII) to the P blood group system and assignment to chromosome 22. *Clin. Genet.* 29:354-359.

23. Li, N., Seetharam, S., Lindemans, J., Alpers, D.H., Arwert, F., and Seetharam, B. 1993. Isolation and sequence analysis of variant forms of human transcobalamin II. *Biochem. Biophys. Acta*. 1172:21-30.

24. Li, N., Seetharam, S., Lindemans, J., Alpers, D.H., Arwert, F., and Seetharam, B. 1993. Isolation and sequence analysis of variant forms of human transcobalamin II. *Biochem. Biophys. Acta*. 1172:21-30.

25. Youngdahl-Turner, P., Rosenberg, L.E. 1978. Binding and uptake of Transcobalamin II by human Fibroblasts. *J. Clin. Invest.* 61:133-141.

26. Finkler, A.E. and Hall, C.A. 1967. Nature of the relationship between vitamin B_{12} binding and cell uptake. *Arch. Biochem. Biophys.* 120:79-85.

27. Youngdahl-Turner, P., Mellman, I.S., Allen, R.H., Rosenberg, L.E. 1979. Protein mediated vitamin uptake. *Exp. Cell Res.* 118:127-134.

28. Berliner, N. and Rosenberg, L.E. 1981. Uptake and metabolism of free cyanocobalamin by cultured human fibroblasts from controls and a patient with transcobalamin II deficiency. *Metabolism.* 30:230-236.

29. Pezacka, E.H., and Rosenblatt, D.S. 1993. Intracellular metabolism of cobalamin. Altered activities of B-ligand transferase and microsomal cob(III)alamin reductase in *cblC* and *cblD* fibroblasts. In press.

30. Kolhouse, J.F., Allen, R.H. 1977. Recognition of two intracellular cobalamin binding proteins and their identification as methylmalonyl CoA mutase and methionine synthetase. *Proc. Natl. Acad. Sci.* 74 (3):921-925.

31. Fenton, W.A., Ambani, L.M., Rosenberg, L.E. 1976. Uptake of hydroxocobalamin by rat liver mitochondria. *J. Biol. Chem.* 251 (21):6616-6623.

32. Banerjee, R.V., Matthews, R.G. 1990. Cobalamin-dependent methionine synthase. *Faseb*

J. 4:1450-1458.

33. Flavin, M., Oritz, P.J., Ochoa, S. 1955. Metabolism of propionic acid in animal tissues. *Nature.* 176:823.

34. Cannata, J.J.B., Focesi, A., Mazumder, R., Warner, R.C., Ochoa, S. 1965. Metabolism of propionic acid in animal tissues: properties of mammalian methylmalonyl coenzyme A mutase. *J. Biol. Chem.* 240 (8):3249-3257.

36. Allen, E., Kellermeyer, R.W., Stjernholm, T.L., Wood, H.G. 1961. Purification and properties of enzymes involved in the propionic acid fermentation. *J. Bacteriol.* 87:171-185.

37. Leng, R.A., Steel, J.W., Luick, J.R. 1967. *Biochem. J.* 103:785-790.

38. Kellermeyer, R.W., Wood, H.G. 1962. Methylmalonyl isomerase: a study of the mechanism of isomerization. *Biochemistry* 1:1125-1131.

39. Phares, E.F., Long, M.V., Carson, S.F. 1962. An intramolecular rearrangement in the methylmalonyl isomerase reaction as demonstrated by positive and negative ion mass analysis of succinic acid. *Biochem. Biophys. Res. Commun.* 8:142-146.

40. Gurnani, S., Mistry, S.P., Johnson, B.C. 1960. Function of vitamin B_{12} in methylmalonate

metabolism: effect of a cofactor form of B_{12} on the activity of methylmalonyl CoA isomerase. *Biochim. Biophys. Acta*. 38:184-186.

41. Frenkel, E.P., Kitchens, R.L. 1975. Intracellular localization of hepatic propionyl CoA carboxylase and methylmalonyl CoA mutase in humans and normal and vitamin B_{12} deficient rats. *Br. J. Haematol.* 31:501-513.

42. Barker, H.A., Weissbach, H., Smyth, R.D. 1958. A coenzyme containing pseudovitamin B_{12}. *Proc. Natl. Acad. Sci.* 44:1093-1097.

43. Smith, R.M., Monty, K.J. 1959. Vitamin B_{12} and propionate metabolism. *Biochem. Biophys. Res. Commun.* 1:105-109.

44. Willard, H.F. and Rosenberg, L.E. 1980. Interaction of methylmalonyl CoA mutase from normal human fibroblasts with adenosylcobalamin and methylmalonyl CoA: evidence for non-equivalent sites. *Arch. Biochem. Biophys.* 200 (1):130-139.

45. Murakami, Y. 1992. Molecular design and catalytic function of a B_{12} enzyme mimetic. *Trends Biotech.* 10:170-177.

46. Vitols, E., Walker, G.A., Huennekens, F.M. 1966. Enzymatic conversion of vitamin B_{12} to a cobamide coenzyme, α-(5,6-Dimethylbenzimidazolyl)deoxy-adenosylcobamide

(Adenosyl-B_{12}). *J. Biol. Chem.* 241 (7):1455-1461.

47. Walker, G.A., Murphy, S., Huennekens, F.M. 1969. Enzymatic conversion of vitamin B_{12}a to adenosyl-B_{12}: evidence for the existence of two separate reducing systems. *Arch. Biochem. Biophys.* 134:95-102.

48. Kerwar, S.S., Spears, C., McAuslan, B., Weissbach, H. 1971. Studies on vitamin B_{12} metabolism in HeLa cells. *Arch. Biochem. Biophys.* 142:231-237.

49. Fenton, N. and Rosenberg, L.E. 1978. Mitochondrial metabolism of hydoxocobalamin: Synthesis of adenosylcobalamin by intact rat mitochondria. *Arch. Biochem. Biophys.* 189:441-447.

50. Utley, C.S., Marcell, P.D., Allen, R.H., Asok, C.A., and Kolhouse, J.F. 1985. Isolation and characterization of methionine synthetase from human placenta. *J. Biol. Chem.* 260:13656-13665.

51. Mellman, I.S., Lin, P.H., Ruddle, F.H., and Rosenberg, L.E. 1979. Genetic control of cobalamin binding in normal and mutant cells: Assignment of the gene for 5-methylenetetrahydrofolate: L-homocysteine S-methyltransferase to human chromosome 1. *Proc. Natl. Acad. Sci. USA* 76:405.

52. Rosenblatt, D.S. and Erbe, R.W. 1977. Methylenetetrahydrofolate reductase in cultured human cells: Growth and metabolic studies. *Ped. Res.* 11:1137-1141.

53. Mudd, S.H., Uhlendorf, B.W., Freeman, J.M., Finkelstein, J.D., and Shih, V.E. 1972. Homocystinuria associated with decreased methylenetetrahydrofolate reductase activity. *Biochem. Biophys. Res. Commun.* 46:905-912.

54. Poston, M., Stadtman, T.C. 1975. Cobamides as cofactors: Methylcobamides and the synthesis of methionine, methane and acetate. In Cobalamin : Biochemistry and Pathophysiology. M.D. Bernard M.Babior, editor. Wiley-Interscience, New York. 111-123.

55. Rosenblatt, D.S., Cooper, B.A., Pottier, A., Lue-Shing, H., Matiaszuk, N., and Grauer, K. 1984. Altered vitamin B_{12} metabolism in fibroblasts from a patient with megaloblastic anemia and homocystenuria due to a new defect in methionine biosynthesis. *J. Clin. Invest.* 74:2149-2156.

56. Rosenblatt, D.S. and Cooper, B.A. 1989. Selective deficiencies of methyl B_{12} (*cbl*E and *cbl*G). *Clin. Invest. Med.* 12:270-271.

57. Matthews, R.G., Jencks, D.A, Frasca, V., and Matthews, K.D. 1986. Methionine biosynthesis in chemistry and biology of pteridines. In Pteridines and Folic Acid Derivatives. B.A. Cooper and V.M. Whitehead, editors. de Gruyter, New York. 698.

58. Vanoni, M.A., Sungsook, L., Floss, H.G., and Matthews, R.G. 1990. Stereochemistry of reduction of methylenetetrahydrofolate to methyletetrahydrofolate catalyzed by pig liver methylenetetrahydrofolate reductase. *J. Am. Chem. Soc.* 112:3987-3992.

59. Levine, J.S. and Allen, R.H. 1985. Intrinsic factor within parietal cells of patients with juvenile pernicious anemia: a retrospective immunohistochemical study. *Gastroenterology* 88:1132-1136.

60. Katz, M., Mehlman, C.S., and Allen, R.H. 1974. Isolation and characterization of an abnormal intrinsic factor. *J. Clin. Invest* 53:1274-1283.

61. Yang, Y.-M., Ducos, R., Rosenberg, A.J., Catrou, P.G., Levine, J.S. 1985. Cobalamin malabsorption in three siblings due to abnormal intrinsic factor that is markedly susceptible to acid and proteolysis. *J. Clin. Invest.* 76:2057-2065.

62. Grasbeck, R. 1972. Familial selective vitamin B_{12} malabsorption. *N. Engl. J. Med.* 287:358-(letter).

63. Burman, J.F., Walker, W.J., Smith, J.A., Phillips, A.D., Sourial, N.A. 1985. Absent ileal uptake of IF-bound vitamin B_{12} in the Imerslund-Grasbeck syndrome (Familial vitamin B_{12} malabsorption with proteinuria). *GUT* 26:311-314.

64. Banerjee R.V., Johnston, N.L., Sobeski J.K., Datta, P., and Matthews, R.G. 1989. Cloning and sequence analysis of the *Escherichia coli* metH gene encoding cobalamin-dependent methionine synthase and isolation of a tryptic fragment containing the cobalamin-binding domain. *J. Biol. Chem.* 264:13888-13895.

65. Oberholzer, V.G., Levin, B., Burgess, E.A., and Young, W.F. 1967. Methylmalonic aciduria: An inborn error of metabolism leading to chronic metabolic acidosis. *Arch. Dis. Child.* 42:492-504.

66. Halvorsen, S., Stokke, O., and Eldjarn, L. 1970. Abnormal patterns of urine and serum amino acids in methylmalonic acidemia. *Acta. Paediatr. Scand.* 59:28-32.

67. Coulombe, J.T., Shih, V.E., and Levy, H.L. 1981. Massachusetts metabolic disorders screening program II. Methylmalonic aciduria. *Pediatrics.* 67:26-31.

68. Morrow, G., Barness, L.A., Cardinale, G.J., Abeles, R.H., and Flaks, J.G. 1969. Congenital methylmalonic acidemia: enzymatic evidence for two forms of the disease. *Proc. Natl. Acad. Sci. USA* 63:191-197.

69. Barness, L.A. and Morrow, G. 1968. Methylmalonic aciduria: A newly discovered inborn error. *Ann. Intern. Med.* 69:633-635.

70. Matsui, S.M., Mahoney, M.J., and Rosenberg, L.E. 1983. The natural history of the inherited methylmalonic acidemias. *N. Engl. J. Med.* 308:857-861.

71. Ledley, F.D. 1990. Perspectives on methylmalonic acidemia resulting from molecular cloning of methylmalonyl CoA mutase. *Bioessay* 12, No. 7:335-340.

72. Matsui, S.M., Mahoney, M.J., and Rosenberg, L.E. 1983. The natural history of the inherited methylmalonic acidemias. *N. Engl. J. Med.* 308:857-861.

73. Gravel, R.A., Mahoney, M.J., Ruddle, F.H., and Rosenberg, L.E. 1975. Genetic complementation in heterokaryons of human fibroblasts defective in cobalamin metabolism. *Proc. Natl. Acad. Sci. USA* 72:3181-3185.

74. Willard, H.F., Mellman, I.S., and Rosenberg, L.E. 1978. Genetic complementation among inherited deficiencies of methylmalonyl-CoA mutase activity: evidence for a new class of human cobalamin mutant. *Am. J. Hum. Genet.* 30:1-13.

75. Rosenblatt, D.S. and Cooper, B.A. 1987. Inherited disorders of vitamin B_{12} metabolism. *Blood Reviews* 1:177-182.

76. Batshaw, M.L., Thomas, G.H, Cohen, S.R. 1984. Treatment of the *cblB* form of methylmalonic acidemia with adenosylcobalamin. *J. Inher. Metab. Dis.* 7:65-68.

77. Mahoney, M.J., Hart, A.C., Steen, V.D., and Rosenberg, L.E. 1975. Methylmalonicacidemia: biochemical heterogeneity in defects of 5'- deoxyadenosylcobalamin synthesis. *Proc. Natl. Acad. Sci. USA* 72:2799-2803.

78. Fenton, W.A. and Rosenberg, L.E. 1981. The defect in the *cbl*B class of human methylmalonic acidemia: deficiency of cob(I)alamin adenosyltransferase activity in extracts of cultured fibroblasts. *Biochem. Biophys. Res. Commun.* 98:283-289.

79. Cooper, B.A., Rosenblatt, D.S., and Watkins, D. 1990. Methylmalonic aciduria due to a new defect in adenosylcobalamin accumulation by cells. *Am J. Hematol.* 34:115-120.

80. Rosenberg, L.E., Paterl, L., Lilljeqvist, A. 1975. Absence of an intracellular cobalamin-binding protein in cultured fibroblasts form patients with defective synthesis of 5'-deoxyadenosylcobalamin and mehtylcobalamin. *Proc. Natl. Acad. Sci USA.* 72:4617-4621.

81. Aspler, A.L., Shevell, M.I., and Rosenblatt, D.S. 1993. Combined methylmalonic aciduria and homocystinuria: phenotype classification and outcomes in *cbl*C disease. *Am. J. Hum. Genet.* 53(2):396.(Abstr.)

82. Mellman, I., Willard, H.F., and Rosenberg, L.E. 1978. Cobalamin binding and cobalamin-dependent enzyme activity in normal and mutant human fibroblasts. *J. Clin. Invest.* 63:952-960.

83. Byck, S. and Rosenblatt, D.S. 1991. Metabolic cooperation among cell lines from patients with inborn errors of vitamin B_{12} metabolism: differential response of *cbl*C and cblD. *Clin. Invest. Med.* 14:153-159.

84. Rosenblatt, D.S. 1993. Inherited errors of cobalamin metabolism: an overview. *International Symposium in London.*

85. Sillaots, S., and Rosenblatt,D.S. 1992. Lysosomal transport of other metabolites: Lysosomal cobalamin transport. In Pathophysiology of Lysosomal Transport. M.D. Jess G.Thoene, editor. CRC Press, Boca Raton. 201-230.

86. Tuchman, M., Kelly, P, Watkins, D., and Rosenblatt, D.S. 1988. Vitamin B_{12}-responsive megaloblastic anemia, homocystinuria, and transient methylmalonic aciduria in *cbl*E disease. *J. Pediatr.* 113:1052-1056.

87. Rosenblatt, D.S. 1992. Vitamin B_{12} (Cbl)-responsive disorders. *Symposium on Inborn errors (Japan).* 593-596.

88. Hall, C.A. 1990. Function of vitamin B_{12} in the central nervous system as revealed by congenital defects. *Am J. Hematol.* 34:121-127.

89. Christensen, B., Rosenblatt, D.S., Chu, R.C., and Ueland, P.M. 1994. Effect of

methionine and nitrous oxide on homocysteine export and remethylation in fibroblasts from cystathionine synthase deficient, *cbl*G and *cbl*E patients. *Pediatr. Res.* In press

90. Hall, C.A., Lindenbaum, R.H., Arenson, E., Begley, J.A., and Chu, R.C. 1989. The nature of the defect in cobalamin G mutation. *Clin. Invest. Med.* 12:262-269.

91. Sillaots, S.L., Hall, C.A., Hurteloup, V., Rosenblatt, D.S. 1992. Heterogeneity in *cbl*G: differential retention of cobalamin on methionine synthase. *Biochem. Med. Metab. Biol.* 47:242-249.

92. Kolhouse, F.J., Utley,C., Allen, R.H. 1980. Isolation and characterization of methylmalonyl CoA mutase from human placenta. *J Biol. Chem* 255:2708-2712.

93. Han, Y.S., Bratt, J.M., Hogenkamp, P.C. 1984. Purification and characterization of methylmalonyl CoA mutase from acaris lumbricoides. *Comp. Biochem. Physiol.* 78B (1):41-45.

94. Murthy, V.V., Jones, E., Cole, T.W., Johnson, J. 1977. Purification of methylmalonic CoA mutase from *Propionibacterium shermanii* using affinity chromatography. *Biochem. Biophys. Acta* 483:487-491.

95. Birch, A., Leiser, A., and Robinson, J.A. 1993. Cloning, sequencing, and expression of the gene encoding methylmalonyl coenzyme A mutase from *Streptomyces cinnamonensis. J.*

Bacteriol. 175:3511-3519.

96. Fenton, W.A., Hack, A.M., Huntington, W., Gertler, A., Rosenberg, L.E. 1982. Purification and properties of methylmalonyl coenzyme A mutase from human liver. *Arch. Biochem. Biophys.* 214 (2):815-823.

97. Francalanci, F., Davis, N.K., Fuller, J.Q., Murfitt, D., Leadlay, P.F. 1986. The Subunit Structure of methylmalonyl CoA mutase from *Propionibacterium shermanii. Biochem J* 236:489-494.

98. Marsh, N., Harding, S.E., and Leadlay, P.F. 1989. Subunit interactions in *Propionibacterium shermanii* methylmalonyl CoA mutase studied by analytical ultracentrifugation. *Biochem J* 260:353-358.

99. Marsh, N., Leadlay, P.F., Evans, P.R. 1988. Crystallization and preliminary diffraction data for adensoylcobalamin-dependent methylmolaonyl CoA mutase from *Propionibacterium shermanii. J. Mol. Biol.* 200:421-422.

100. Marsh, N., McKie, N., Davis, N.K., Leadlay, P.F. 1989. Cloning and structural characterization of the genes coding for adenosylcobalamin-dependent methylmalonyl CoA mutase from *Propionibacterium shermanii. Biochem J* 260:345-352.

101. Ledley, F.D., Lumetta, M., Nguyen, P.N., Kolhouse, J.F., and Allen, R.H. 1988. Molecular cloning of L-methylmalonyl-CoA mutase: Gene transfer and analysis of mut cell lines. *Proc. Natl. Acad. Sci. USA* 85:3518-3521.

102. Jansen, R., Kalousek, F., Fenton, W.A., Rosenberg, L.E., and Ledley, F.D. 1989. Cloning of full-length methylmalonyl-CoA mutase from a cDNA library using the polymerase chain reaction. *Genomics* 4:198-205.

103. Ledley, F.D., Lumetta, M.R., Zoghbi, H.Y., VanTuinen, P., and Ledbetter, D.H. 1988. Mapping of human methylmalonyl CoA mutase (MUT) locus on chromosome 6. *Amer. J. Hum. Genet.* 42:839-846.

104. Zoghbi, H.Y., O'Brien, W.E., and Ledley, F.D. 1988. Linkage relationships of the human methylmalonyl-CoA mutase to the HLA and D6S4 loci on chromosome 6. *Genomics* 3:396-398.

105. Nham, S.U., Wilkemeyer, M.F., and Ledley, F.D. 1990. Structure of the human methylmalonyl CoA mutase (MUT) locus. *Genomics* 8:710-716.

106. Sertic, J., Vincek, V., Ledley, F.D., Figueroa, F., Klein, J. 1990. Mapping of the L-methylmalonyl CoA mutase gene to mouse chromosome 17. *Genomics* 6:560-563.

107. Wilemeyer, M.F., Crane, A.M., Ledley, F.D. 1990. Primary structure and activity of mouse methylmalonyl CoA mutase. *Biochem J* 271:449-455.

108. Fenton, W.A., Hack, A.M., Helfgott, D., and Rosenberg, L.E. 1984. Biogenesis of the mitochondrial enzyme methylmalonyl CoA mutase. *J Biol. Chem* 259:6616-6621.

109. Isaya, G., Kalousek, F., Fenton, W.A., and Rosenberg, L.E. 1991. Cleavage of precursors by the mitochondrial processing peptidase requires a compatible mature protein or an intermediate octapeptide. *J. Cell Biol.* 113 (1):65-76.

110. Bibus, C.R., Lemire, B.D., Suda, K., Schatz, G. 1988. Mutations restoring import of a yeast mitochondrial protein with a nonfunctional presequence. *J Biol. Chem* 263:13097-13102.

111. Leadlay, P.F., Ledley, F.D. 1990. Primary sequence homology between methylmalonyl CoA mutase from *Propionibacterium shermanii* and *Homo sapiens*. In Biomedicine and Physiology of Vitamin B_{12}. J.C.and Bhatt Linnell,H.R., editor. Children's Medical Charity, London. 341-352.

112. Wilkemeyer, M.F., Crane, A.M., and Ledley, F.D.. 1991. Differential diagnosis of *mut* and *cbl* methylmalonic aciduria by DNA-mediated gene transfer in primary fibroblasts. *J Clin. Invest* 87:915-918.

113. Willard, H.F. and Rosenberg, L.E. 1977. Inherited deficiencies of human methylmalonyl CoA mutase activity: reduced affinity of mutant apoenzyme for adenosylcobalamin. *Biochem. Biophys. Res. Commun.* 78:927-934.

114. Morrow, G., and Lebowitz, J. 1976. Studies of methylmalonyl-coenzyme A carbonylmutase activity in methylmalonic acidemia. II. In vitro binding kinetics with adenosylcobalamin. *Biochem. Med.* 15:241-245.

115. Morrow, G., Revsin, B., Clark, R., Lebowitz, J., and Whelen, D.T. 1978. A new variant of methylamlonic acidemia-defective coenzyme-apoenzyme binding in cultured fibroblasts. *Clin. Chem. Acta* 85:67-72.

116. Kolhouse, J.F., Utley, C., Fenton, W.A., and Rosenberg, L.E. 1981. Immunochemical studies on cultured fibroblasts from patients with inherited methylmalonic acidemia. *Proc. Natl. Acad. Sci. USA* 78:7737-7741.

117. Ledley, F.D., Crane, A.M., and Lumetta, M. 1990. Heterogeneous alleles and expression of methylmalonyl CoA mutase in *mut* methylmalonic acidemia. *Am. J. Hum. Genet.* 46:539-547.

118. Ogasawara, M., Matsubara, Y., Mikami, H., Narisawa, K. 1994. Identification of two novel mutations in the methylmalonyl-CoA mutase gene with decreased levels of mutant

mRNA in methylmalonic acidemia. *Hum. Mol. Genet.* 3 no. 6:867-872.

119. Fenton, W.A., Hack, A.M., Kraus, J.P., and Rosenberg, L.E. 1987. Immunochemical studies of fibroblasts from patients with methylmalonyl-CoA mutase apoenzyme deficiency: detection of a mutation interfering with mitochondrial import. *Proc. Natl. Acad. Sci. USA* 84:1421-1424.

120. Shevell, M.I., Matiaszuk, N., Ledley, F.D., Rosenblatt, D.S. 1993. Varying neurological phenotypes among *mut*^{0} and *mut*$^{-}$ patients with methylmalonyl CoA mutase deficiency. *Am. J. Med. Genet.* 45:619-624.

121. Willard, H.F. and Rosenberg, L.E. 1980. Inherited methylmalonyl CoA mutase apoenzyme deficiency in human fibroblasts. *J. Clin. Invest.* 65:690-698.

122. Burman, J.F., Mollin, D.L., Sourial, N.A., and Sladden, R.A,. 1979. Inherited lack of transcobalamin II in serum and megaloblastic anemia: a further patient. *Br. J. Haematol.* 43:27-38.

123. Ledley, F.D., Jansen, R., Nham, S.U., Fenton, W.A., and Rosenberg, L.E. 1990. Mutation eliminating mitochondrial leader sequence of methylmalonyl CoA mutase causes muto methylmalonic aciduria. *Proc. Natl. Acad. Sci USA.* 87:3147-3150.

124. Jansen, R. and Ledley, F.D. 1990. Heterozygous mutations at the MUT locus in fibroblasts with *mut*^{0} methylmalonic acidemia identified by PCR cDNA cloning. *American Journal of Human Genetics* 47:808-814.

125. Crane, A.M., Martin, L.S., Valle, D., and Ledley, F.D. 1992. Phenotype of disease in three patients with identical mutations in methylmalonyl CoA mutase. *Hum. Genet.* 89:259-264.

126. Qureshi, A.A., Crane, A.M., Matiaszuk, N.V., Rezvani, I., Ledley, F.D. and Rosenblatt, D.S. 1994. Cloning and expression of mutations demonstrating intragenic complementation in *mut*^{0} methylmalonic aciduria. *J. Clin. Invest.* 93(4):1812-1819.

127. Crane, A.M. and Ledley, F.D. 1994. Clustering of mutations in methylmalonyl CoA mutase associated with *mut*$^-$ methylmalonic acidemia. *Am. J. Hum. Genet.* 55:42-50.

128. Crick, F.H.C. and Orgel, L.E. 1964. The theory of interallelic complementation. *J. Mol. Biol.* 8:161-165.

129. Crane, A.M., Jansen, R. Andrews, R., and Ledley, F.D. 1992. Cloning and expression of a mutant methylmalonyl Coenzyme A mutase with altered cobalamin affinity that causes *mut*$^-$ methylmalonic aciduria. *J. Clin. Invest.* 89:385-391.

130. Lowry, O.H., Rosenbrough, N.J., Farr, A.L., Randall, R.L. 1951. Protein measurement with the folin phenol reagent. *J. Biol. Chem* 193:265-275.

131. Shapira, S.K., Ledley, F.D., Rosenblatt, D.S.,and Levy, H.L. 1991. Ketoacidosis crisis as a presentation of mild ("benign") methylmalonic acidemia. *J. Pediatr.* 119:80-84.

132. Watkins, D., and Rosenblatt, D.S. 1986. Failure of lysosomal release of vitamin B_{12}: A new complementation group causing methylmalonic aciduria (*cblF*). *Am. J. Hum. Genet.* 39:404-408.

133. Yap, E.P.H., and McGee, J.O.D. 1991. Short PCR product yields improved by lower denaturation temperatures. *Nucleic Acid Research* 19:1713.

134. Hayashi, K.S. 1991. PCR-SSCP: a simple and sensitive method for detection of mutations in genomic DNA. *PCR Methods and Applications* 1:34-38.

135. Schlesinger, M.J., and Levinthal C. 1965. Complementation at the molecular level of enzyme interaction. *Ann. Rev. Microbiol.* 19:267-284.

136. Zabin, I., and Villarejo, M.R. 1975. Protein Complementation. *Ann. Rev. Biochem.* 44:295-313.

137. Gravel, R.A., Lam, K.F., Scully, K.J., and Hsia, Y.E. 1977. Genetic complementation of Propionyl-CoA carboxylase deficiency in cultured human fibroblasts. *Am. J. Hum. Genet.* 29:378-388.

138. Garen, A., Garen, S., 1963. Complementation in vivo between structural mutants of alkaline phosphatase from *E.coli*. *J. Mol. Biol.* 7:13-22.

139. Perrin, D., 1963. Immunological studies with genetically altered B-galactosidase. *Ann. NY Acad. Sci.* 103:1058-66.

140. McInnes, R.R., Shih, V., and Chilton, S. 1984. Interallelic complementation in an inborn error of metabolism: Genetic heterogeneity in argininosuccinate lyase deficiency. *Proc. Natl. Acad. Sci USA.* 87:4480-4484.

141. Coddington, A., Fincham, J.R.S. 1965. Proof of hybrid enzyme formation in a case of interallelic complementation in *Neurospora crassa*. *J. Mol. Biol.* 12:152-161.

142. McGavin, S. 1968. Interallelic complementation and allostery. *J. Mol. Biol.* 37:239-242.

143. Fincham, J.R.S. 1989. Genetic complementation. W.A. Benjamin, Inc., New York.

144. Gavin, S. 1968. Interallelic complementation and allostery. *J. Mol. Biol.* 37:239-242.

145. Schlesinger, M.J., Torriani, A., Levinthal, C. 1963. Hybrid protein formation of E.coli alkaline phosphatase leading to in vitro complementation. *J. Mol. Biol.* 7:1-12.

146. Shapiro, N.I., Luss, E.V., Volkova, L.V., Moiseenko, H.V. 1985. Complementation analysis of locus for hypoxanthine guanine phosphoribosyltransferase in Chinese hamster cells. *Somat. Cell. Mol. Genet.* 11:135-147.

147. Coddington, A., Finchman, J.R.S., and Sundaram, T.K. 1966. Multiple acitve varieties of Neurospora glutamate dehydrogenase formed by hybridization between two inactive mutant proteins in vivo and in vitro. *J. Mol. Biol.* 17:503-512.

148. Stobakk, N., Oxender, D.L., and El Gewely, M.R. 1992. Intragenic complementation between *Escherchia coli* trp repressors with different defects in the tryptophan-binding pocket. *Gene* 117:23-29.

149. Liteplo, G.R., Hipwell, S.E., Rosenblatt, D.S., Sillaots, S., and Lue-Shing, S. 1991. Changes in cobalamin metabolism are associated with altered methionine auxotrophy of highly growth autonomous human melanoma cells. *J. Cell. Phys.* 149(2):332.

150. Chou, P.Y., and Fasman, G.D. 1974. Prediction of protein conformation. *Biochem.* 13:222-244.

151. Reha-krantz, L.J. 1990. Genetic evidence for two protein domains and a potential new activity in bacteriophage T4 DNA polymerase. *Genetics* 124:213-222.

152. Brantly, M., Courtney, M., Crystal, R.G. 1988. Repair of the secretion defect in the Z form of alpha 1-antitrypsin by addition of a second mutation. *Science* 242:1700-1701.

153. Andrews, E., Jansen, R., Crane, A.M., Wilkemeyer, M.F., MacDonall, D., and Ledley, F.D. 1993. Activity of a recombinant human methylmalonyl CoA mutase in primary fibroblasts and *Saccharomyces cerevisiae*. *Biochem. Med. Met. Biol.* in press:

154. Marsh, E.N.G., Holloway, D.E. 1992. Cloning and sequencing of glutamate mutase component S from Clostridium tetanomorphum. Homology with other cobalamin-dependent enzymes. *Febs* 310:167-170.

155. Siddiqi, O. 1965. Interallelic complementation in vivo and in vitro. *Brit. Med. Bull.* 21:249-253.